Decomposition of Rayleigh Fading Dispersive Channels

A thesis

submitted in fulfilment

of the requirements for the Degree of

Doctor of Philosophy

in Electrical and Electronic Engineering

at the

University of Canterbury

Nicholas J. Baas

March 30, 2001

Abstract

This thesis identifies, develops and applies methods for the decomposition of fading dispersive channels. Such channels arise in wireless communication as a result of multipath and relative motion of the transmitter, scatterers and receiver. The decompositions considered are the f-power series and Karhunen-Loève (KL) expansions. For the KL expansion generalisations to rapid time variation are possible with the separate options of single spread and double spread decomposition. The single spread decomposition involves a model of the instantaneous channel transfer function with time variation supported by sample spaced coefficients. The double spread decomposition employs a model of each received pulse and requires symbol spaced coefficients.

The decompositions are applied to pulse shaping, channel modelling for equalisation and the determination of performance limits for linear modulation over fading dispersive channels. The results on pulse shaping show that, with moderate bandwidth expansion and appropriate design, it is possible to significantly lower the complexity of a mobile receiver. The approach suggests a way to move complexity and power consumption away from the mobile unit and into the base station.

The effects of diversity on performance are investigated by assuming a single pulse from a linear modulation format. This removes the need to consider intersymbol interference and allows conclusions about the impact of fading and dispersion on the probability of error and the average mutual information.

Acknowledgements

I take this opportunity to express my gratitude to all those who have assisted me during the time I have spent writing this thesis. My supervisor Des Taylor has shown great patience and has provided valuable feedback on the written material. Thanks go to Anthony Griffin, Brian Hart, Wing Seng Leon, Peter Renaud and others for many useful discussions and presentations.

Hessel, Joan and Susan Baas have given me unfailing support and for this I am especially thankful. I also appreciate the help of Colin Berry, Greg Brackley, Matthew Kidson, Kelvin Maxwell, Kevin Taylor, Diane Walton and the Baas, Holmes, Percy, Nicholson and Sherlock families.

Contents

Glossary

Symbol	Page
AMI - average mutual information	110
AWGN - additive white Gaussian noise	11
BLAST - Bell Labs layered space-time architecture	104
BPSK - binary phase shift keying	28
CCI - co-channel interference	31
CIR - channel impulse response	18
CSI - channel state information	7
DPSK - differential phase shift keying	19
ISI - intersymbol interference	6
KL - Karhunen-Loève	7
LMS - least mean square	13
MCRB - modified Cramér-Rao bound	62
MFB - matched filter bound	93
ML - maximum likelihood	36
MLSE - maximum likelihood sequence estimation	12
MMSE - minimum mean square error	31
OFDM - orthogonal frequency division multiplexing	4
OSI - open systems interconnection	1
PAM - pulse amplitude modulation	4
PSD - power spectral density	19
PSK - phase shift keying	4
PSP - per-survivor processing	14
QAM - quadrature amplitude modulation	4
QPSK - quaternary phase shift keying	21
RMS - root mean square	25
TSC - time selective coefficient	45
WSSUS - wide sense stationary uncorrelated scattering	21
A_c - normalising constant in pulse optimisation	68
A_τ - constant in MCRB	71
$B(f)$ - transfer function of a basic Nyquist pulse	64
BER - bit error rate	34
BER_o - BER outage threshold	35
$C(f)$ - overall pulse amplitude spectrum	20

Symbol	Page
d_1 - maximum normalised delay spread	25
f - frequency	20
f_D - one-sided Doppler spread	24
$f_D T$ - fade rate	27
f_s - $1/2T$	20
$g(\xi, \nu)$ - delay Doppler spread function	22
$h(t, \xi)$ - channel impulse response	18
i - TSC index	45
k - sample index	19
l - symbol index	18
m - primarily the diversity thread index	30
n - primarily the index of co-channel interference sources	30
$p(e)$ - probability of bit error	28
r - samples per symbol	29
$s(t)$ - transmitted signal	18
$s_R(t)$ - received signal	19
$s_T(t)$ - transmitted signal incorporating pulse shaping filter	18
t - time	18
$u(t, \xi)$ - overall channel impulse response	18
$\widehat{u}(t, \xi)$ - approximation to the overall channel impulse response	36
$v_l(t)$ - single received pulse	52
$x_{P,i}(t)$ - tapped delay line TSC	45
$x_{Q,i}(t)$ - single spread KL TSC	47
$x_{R,i,l}$ - double spread KL TSC	54
$x_{S,i}(t)$ - f-power series TSC	55
y_k - received samples	32
$z_{Q,i}(t)$ - single spread KL basis function (time domain)	47
z - scale factor, a Gamma random variable	94
α - raised-cosine pulse rolloff factor	20
γ_i - double spread KL eigenvalue	53
$\eta(t)$ - receiver filtered white Gaussian noise	19
$\lambda_{Q,i}$ - single spread KL eigenvalue	46
ν - Doppler frequency	22
ξ - relative transmission delay	18
ξ_0 - RMS delay spread	25
$\rho(t - t')$ - time selective correlation function	22
$\psi_i(t)$ - double spread KL eigenfunction (time domain)	53
$\Phi_{Q,i}(f)$ - single spread KL eigenfunction	46
$\Psi_i(f)$ - double spread KL eigenfunction	53

Chapter 1

Introduction

Communication systems provide an environment for the transfer of information among two or more parties physically separated in space where links may be fixed line or wireless. In modern communication systems there is widespread and varied deployment with interconnectivity and any one connection can involve a chain of links and switches. Fixed line systems include copper pair, co-axial cable and fibre optic cable whereas wireless or radio systems afford transmission between antennas by electromagnetic signal propagation.

By its nature the process of communication is layered. The user of a system is concerned with the quality and cost of a connection rather than how it is established. By the same token a telecommunication service provider is largely unconcerned with the content of information transferred. The provider must put in place equipment to facilitate communication but this is usually transparent to the user. The open systems interconnection (OSI) model [32] which represents a formalisation of communication systems separates functions between physical at the lowest level to applications at the highest level. There are five intervening layers allowing a connection to be made and maintained. End-user

information is passed down the layers and transferred at the physical layer. The communications problem at this low level involves signalling over the given medium. This thesis is primarily concerned with low level design of digital wireless communication systems.

There has been a demand for the implementation of digital systems to replace existing analog ones as the inherent advantages of digital systems have been recognised. Digital communication has the property that once information is encoded it can be transferred largely error free under certain conditions. The effects of channel distortion and noise can be removed on long distance links by sufficiently closely spaced repeaters. Since there is a finite number of symbols in a representation the cumulative degradation of the signal associated with analog transmission can be avoided. Digital communication does have the disadvantage that during conversion of information from analog sources into a digital format there is some level of quantisation distortion. It is generally accepted that the benefits outweigh the drawbacks.

At switching nodes in a digital network information is routed at layer three of the OSI model. Data networks are typically packet switched whereas voice networks have until quite recently been purely circuit switched [80] with a user being assigned a continuous connection accross the entire network. By contrast packet switching or asynchronous transfer mode involves dividing up information into blocks or packets of data. This enables the network to efficiently control traffic, merging data from many connections, sending packets on a number of possible paths and reordering data for any one connection at the destination.

All these ideas are particularly relevant at this time because of the remarkable growth in the functionality and availability of computing systems over the last quarter century.

However, the basic concepts have been known and discussed in the literature for some time. Research falls into the categories of information theory and communication theory. Information theory has evolved over the last fifty years out of early work by Shannon [41]. It is based on the notion that source or channel coding can lead to performance gains in terms of the efficiency of representation or transfer of information. This is a mathematical field and includes compression and channel coding theory. A related field is that of communication theory involving problems to do with the basic requirement to send and receive over physical channels. An early work of great importance which addresses this requirement at a fundamental level is that of Nyquist [73] concerning the design of pulses for use in digital modulation.

The systems considered throughout this thesis are wireless ones composed of a transmitter, channel and receiver with transmission occuring between antennas attached to the transmitter and receiver. Geographical features, such as buildings or hills reflect, diffract and scatter the electromagnetic signal. Rays arrive at the receiver from different directions having travelled on paths with different propagation delays. This leads to dispersion. An additional complicating factor is introduced if the transmitter and receiver move relative to each other. This gives the channel a time varying property, generally referred to as fading [55]. Figure 1.1 illustrates the basic structure of a wireless communication system. Source and channel encoding is performed at the transmitter. The channel can be modelled at baseband as a time varying linear filter as defined by Bello [9]. Source and channel decoding is performed by the receiver.

Various forms of modulation can be implemented at the transmitter depending on the application of the system. The most simple form is linear modulation in which sym-

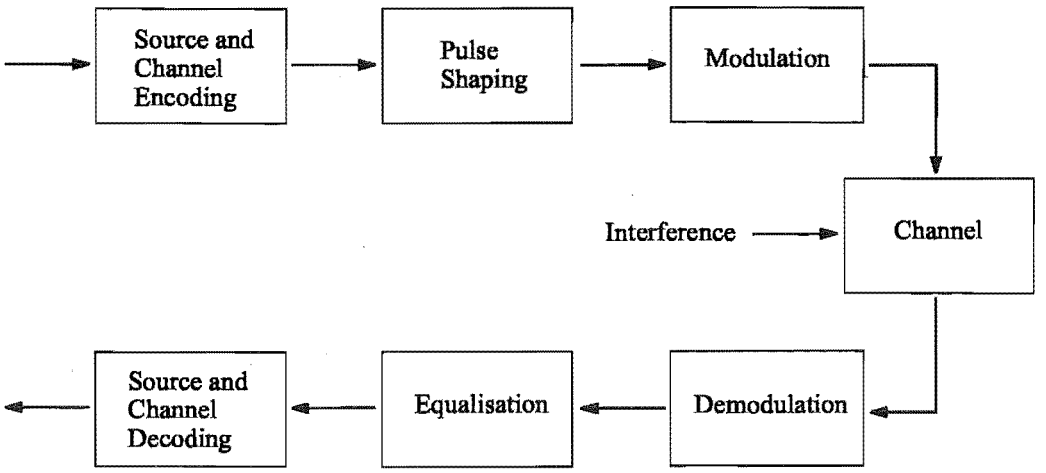

Figure 1.1: Basic structure of a communication system.

bols distributed in the amplitude-phase plane are convolved with a pulse shaping filter and modulated onto a carrier frequency. Some examples of linear modulation are pulse amplitude modulation (PAM), phase shift keying (PSK) and quadrature amplitude modulation (QAM). These are distinguished by their positioning of symbols in amplitude and phase called the constellation. Differential encoding/decoding is a means of removing the need for a channel and carrier phase reference. As already mentioned there are suitable bandlimited pulse shapes for modulation; such as the raised-cosine.

Another important class of modulation formats is continuous phase modulation which includes minimum shift keying. The idea here is that by sacrificing bandwidth efficiency it is possible to implement constant envelope modulation which lessens the need for amplifiers to have a wide linear range of operation.

The dispersive effects of the channel in the form of intersymbol interference can be controlled by signalling at a lower rate on a series of adjacent channels rather than at one high rate over the entire allocated band [15]. The overall approach is known as orthogonal frequency division multiplexing (OFDM). It is known however that the method

places demands on amplifiers in the form of increased peak to average power ratios. One solution that has been proposed for this problem is to appropriately code a transmitted OFDM signal [92].

A broad class of systems with relevance to the subject of modulation is spread spectrum [45, 76]. Direct sequence spread spectrum assigns each connection in the system a unique high rate code sequence. The information bearing signal is multiplied by the sequence in the transmitter and again at the receiver to recover it from the collection of other signals. Other users of the system appear as noise and an important feature of the system is that as more connections are made any single connection experiences a graceful degradation in performance. Frequency hopped spread spectrum is another form. Spread spectrum systems have inherent resistance to dispersion [45] since the effect of spreading and despreading is to narrow the received matched filter correlation. A direct approach to achieving this aim is presented in Chapter 4 of this thesis on pulse shaping.

In the analysis and design of wireless communication systems a critical component is the fading dispersive channel. Since the channel is unknown *a priori* it must be modelled and the relevant parameters in the model must be estimated. Generally a statistical characterisation of the channel is employed to allow for uncertainty. Fading dispersive channels can reasonably be assumed to have complex Gaussian statistics and be locally wide sense stationary uncorrelated scattering. Depending on the properties of the channel the statistical distributions can be Rayleigh or Rician. System and correlation functions are defined as in [9]. In this thesis the channel is assumed to be Rayleigh fading dispersive meaning that the statistics are zero mean complex Gaussian. General parameters for the channel are the delay and Doppler spreads corresponding to dispersive and time varying

properties of the channel. The use of the term dispersive in this thesis refers exclusively to time dispersion, delay spreading or frequency selective effect. The term fading is used to refer to frequency dispersion, Doppler spreading or time selective effect.

It is these effects that must be considered when designing a receiver. To compensate for intersymbol interference (ISI) and other forms of interference, equalisation is required. In addition to equalisation there are several other functions of a typical receiver. These include demodulation and sampling for signal detection. Associated with these are various synchronisation requirements consisting of carrier frequency offset estimation, carrier phase recovery and symbol timing recovery.

The availability or otherwise of diversity in communication systems also influences performance. In general terms diversity means the presence of more than one transmission path. For a wireless communication system there is a distinction between implicit and explicit diversity. Implicit diversity arises when there is multipath transmission through the surrounding physical environment. Explicit diversity is an introduced structure in the form of transmitter frequency diversity or receiver space diversity such as antenna arrays. Channel coding introduces redundancy and also represents a form of diversity. The nature and extent of diversity gains are investigated throughout this thesis.

1.1 Thesis Contributions

The starting point for the work that resulted in this thesis was to consider possible applications of wavelets [29] in communications and to develop enhancements to the design of equalisers. The study of wavelets is a recent development in the field of mathematics and

signal processing. A wavelet basis consists of functions or signals that are orthogonal with respect to time shifts but also under time scaling. At first glance possible applications of wavelets in communications include modulation, channel modelling and signal processing for receiver design [90].

The major departure from the starting point of the project, if there is one, lies in the realisation that it is functions other than wavelets that offer greater utility in wireless communication applications. Wavelet modulation is effectively a form of OFDM but has disadvantages relative to existing methods in frequency selective environments. The important property of fading dispersive channels is that they are essentially delay and Doppler frequency limited. This means that the channel can be modelled by expansions involving prolate spheroidal wave functions [82] or other related decompositions such as the Karhunen-Loève (KL) expansion. The thesis as it stands is primarily a development of models for fading dispersive channels with applications in the design of optimal systems and associated performance evaluation.

Equaliser design for communications involves developing algorithms for estimating channel state information (CSI) and for deconvolution which typically make use of known or estimated properties of the transmitted signal and channel. It is worthwhile to characterise the CSI in such a way that only a small number of parameters are required to be estimated. This has implications for the structure and complexity of equalisation algorithms.

Several decompositions of fading dispersive channels are developed as alternatives to the tapped delay line model usually used in practice. The alternative decompositions are generally more efficient than a tapped delay line. A single spread KL expansion is

based on an assumption that the time-frequency correlation function can be separated into a product of the delay power spectral density and the time selective correlation function. The resulting expansion has sample spaced coefficients. A double spread KL expansion involves a decomposition of an overall received pulse isolated from the rest of the received signal. The time varying and frequency selective aspects of the channel are jointly incorporated into an expansion with symbol spaced coefficients. The f-power series [9] is reasonably well known and is considered here for the sake of comparison with other decompositions.

The original contributions made in the thesis are predominantly the application of channel decompositions to the design or performance analysis of wireless systems and are:

1. development of a frequency domain form of the double spread KL expansion applicable to bandlimited modulation formats;

2. demonstration of the inherent immunity to ISI of powers of Nyquist pulses;

3. optimisation of pulse shaping filters in the sense of minimum mean peak-sample energy to mean residual ISI energy;

4. determination of the effects of CSI mismatch on the probability of error;

5. determination of matched filter bounds;

6. determination of average mutual information.

Three items have been submitted for publication [6, 4, 5]. The papers had been published [5] or accepted for publication [6, 4] at the time of final submission of this thesis.

Point 1 on the previous page describes an alternative to the time domain expression presented in [43] which also relies on a particular correlation property of the channel, namely that the channel correlation may be separated into a product of frequency and time selective correlation functions. In [25] the effect of utilising the successive eigenvalues of a flat fading channel for detection is investigated. In Chapter 3 of this thesis the double spread KL expansion is placed in the context of other decompositions such as the single spread KL expansion [30] and the f-power series expansion [9].

Point 2 appears in Chapter 4 and is a direct extension of the result in [56] for the slow fading linearly frequency selective channel. A squared Nyquist pulse applies to the linear channel and it is shown that higher powers apply to channels that have a polynomial channel transfer function of correspondingly higher order. This approach allows near ISI free transmission over dispersive channels. As the exponent of the pulse is increased the system can support larger delay spreads.

Point 3, also in Chapter 4, is also largely original. As with Point 2 it is assumed that the bandwidth of the pulse shaping filters can be progressively increased. An optimisation of the filters is performed over the channel delay profile and it is shown that for a fixed delay spread the signal to ISI ratio in dB is a linear function of allocated bandwidth. Other works take a similar approach [27, 52] but without consideration of excess bandwidth or optimisation over the channel model.

Point 4 represents a comparative study of the f-power series and single spread KL expansions for application to channel modelling in equalisation. In [31] the f-power series is studied in a similar way. In this thesis the underlying equaliser and its performance analysis is based on [44]. Point 5 on matched filter bounds is based on [20] and represents a

generalisation including possibly rapid channel time variation where the effects of Doppler spread introduce another form of implicit diversity. This extension is based on applying the analysis in [20] in combination with the double spread KL expansion. Point 6 is in the area of information theory and continues the matched filter bound assumption of an isolated pulse in order to draw conclusions about the average mutual information in systems for the fading dispersive channel.

Adaptivity of receivers is not considered in any detail and this is a logical next step for any extension of the material. In the area of pulse shaping the results in this thesis suggest a method whereby there may be no need for adaptive equalisation. In that case the work implies a more complete system than in the other chapters where results are obtained assuming rather than estimating CSI.

1.2 Literature Review

This thesis is concerned with system functions relating to the mitigation or removal of wireless channel impairments and with results on optimal performance. Background material and recent developments in the field are summarised in this section. These are mostly in the areas of equalisation and channel modelling.

A comprehensive early work on the overall topic of information theory is by Gallager [41]. This presents the fundamental theory of entropy, information and capacity and the related fields of source and channel coding. In source coding the entropy of a symbol in an alphabet represents the number of bits required for the representation of that symbol. The general idea is that a smaller number of bits can be used for frequently occuring symbols

and vice versa. This principle also forms the basis of methods for breaking ciphers [10].

In channel coding there is a tradeoff between the rate of information transfer and the probability that a symbol is received in error. The channel coding theorem states that there is a quantity C called the capacity of the channel. As long as the rate R of bits entering the encoder per second is less than C then the probability of error can be made arbitrarily low. This is achieved by introducing some form of redundancy during encoding. The converse to the coding theorem states that if the entropy of the source in bits per second is greater than C then it is impossible to achieve an arbitrarily low error probability [45].

Information theory now has many applications ranging from computer file compression to error control coding in communication systems. The communications viewpoint is presented in an early work by Wozencraft and Jacobs [91]. More recent work on the definition and determination of capacity in fading dispersive channels is found in [49, 67]. In slow, flat-fading channels the capacity is constant over long periods of time relative to the symbol spacing and the discrete time additive white Gaussian noise (AWGN) channel results are applicable [41]. In dispersive channels ISI must be taken into account. If the sequential nature of digital communications is ignored then the relevant result involves distribution of transmitted energy over compactly supported regions of frequency spectrum [41]. For fast fading channels the transfer function of the channel varies substantially over short periods of time and the concept of a limiting rate of information transfer must be redeveloped.

Basic works on the subject of digital communication include [63, 45, 76, 46]. These all describe linear modulation formats and evaluate performance for matched filter detection

in the AWGN channel. A detailed study of this problem is found in [3]. Fundamental results and techniques for synchronisation are developed in [68] where the treatment is directed towards maximum likelihood parameter estimation.

1.2.1 Modulation and Pulse Shaping

Basic references covering modulation include [45, 76]. There has been a great deal of emphasis in the literature on orthogonal frequency division multiplexing. The connection with the discrete Fourier transform is discussed in [88]. The work of Chang [15] defines an orthogonal set of adjacent and overlapping signals for data transmission. This definition is similar to multi-band wavelets and there has been speculation that some form of wavelet modulation may find application [61, 90]. In the mathematical field of wavelets the root raised-cosine pulse corresponds to the simplest Meyer scaling function [29]. Other general works on wavelets include [19, 89].

For this thesis the starting point is the raised-cosine pulse shaping filter. Pulse shaping is investigated in the context of ISI resulting from channel dispersion. The minimisation of ISI by pulse shaping is also considered in [27, 52].

1.2.2 Equalisation

There are various established methods of equalisation for fading dispersive channels. Three notable examples are linear equalisation, decision feedback equalisation and maximum likelihood sequence estimation (MLSE) [76]. Linear equalisation seeks to deconvolve the signal and channel with a simple transversal filter, the design of which goes back to Wiener [45]. Decision feedback equalisation is an extension of linear equalisation in

which previously detected symbols are weighted and subtracted from the incoming signal [71, 76]. MLSE considers all possible symbol sequences and selects the one most probably transmitted. In practice this is done using the Viterbi algorithm [39]. MLSE as a form of equalisation is described in [38, 83] and extended to fading dispersive channels with approximate CSI in [44]. The work in [66] considers the effect of residual ISI on the performance of MLSE when a truncated channel impulse response is assumed. Other works on the performance evaluation of MLSE include [14, 33].

A comprehensive survey of equalisation is found in [77]. Optimal linear receivers for the slow fading channel which jointly implement equalisation and diversity combining are described in [21, 47]. Various other works deal with the utilisation of the cyclostationary property of wireless signals for equalisation and blind equalisation [42, 74, 64].

A useful technique for performance evaluation of equalisers is Metzger's algorithm [70]. This offers a means of approximating the residual ISI probability density function which can then be used in the determination of the probability of bit error. Often a Gaussian model of ISI is sufficient for investigating the general performance of systems.

In the work of Cavers the effect of fading on conventional receivers is considered [12, 13]. Such receivers develop an error floor in fading because of ISI and degradation of the peak sample energy due to rapid variations in the channel over the interval of a few symbols. The combined structure of the channel and conventional receiver amounts to a form of mismatch.

Adaptive receivers estimate or predict the channel based on past estimates. In slow fading least mean square (LMS) tracking of the channel is sufficient [77]. In fast fading the channel effect must be estimated concurrently with equalisation. One method for

MLSE, which involves embedding the channel estimation within the Viterbi algorithm, is per-survivor processing (PSP) [78]. Thus, the receiver structure depends to a large extent on whether the fading is slow or fast. Adaptive MLSE receivers for fading dispersive channels are developed in [62, 26, 24, 17, 18, 79, 58, 57]. These are all based on some form of Viterbi algorithm. In particular, the approach in [24, 79, 58] involves the use of Kalman filtering to track rapid channel variations over time.

The calculation of matched filter bounds which offer a lower bound on performance for linear modulation in fading dispersive channels is developed in [65, 22, 36, 34]. The bound is obtained by assuming the transmission of an isolated pulse so that ISI need not be considered.

1.2.3 Channel Modelling

General references on wireless communication and channel modelling are [55, 51]. These include the isotropic scattering model of the fading channel. A method for the simulation of frequency-flat Rayleigh fading channels is described in [85]. A physical model of multi-path dispersive channels based on the assumption of no line-of-sight path and ellipses of scatterers is found to have roughly a one-sided exponential delay profile in [7].

Power series models of the fading dispersive channel are developed in [9]. The work in [56, 57, 58, 59] considers several applications of the f-power series. In [31] the precision of a truncated f-power series is considered. A double filtering receiver for flat-fading channels based on the t-power series is developed in [69, 87].

The KL expansion is described in [30]. It is primarily the works [21, 22, 23] that have been extended in this thesis. Those works identify the fact that a KL expansion in the

frequency domain is appropriate to bandlimited systems. Problems in which the channel is slow fading dispersive are considered.

Various other works on channel decomposition are [35, 8, 86]. References on spheroidal wave functions and their application in signal processing include [1, 37, 82, 53, 54].

Chapter 2

Wireless Communication

The fact that a wireless signal can be subject to fading and dispersion has implications for the design of wireless communication systems. In such cases a transmitted signal composed of a sequence of shift-orthogonal, overlapping pulses is distorted by the channel. Systems that experience frequency selectivity in the channel require equalisation in the receiver. Equalisation means the removal of distortion or the deconvolution of the channel response from the received signal.

This chapter defines a typical communication system in more detail including transmitter, channel and receiver. The transmitter implements linear modulation formats such as phase shift keying as opposed to non-linear ones such as constant envelope forms of continuous phase modulation. A statistical characterisation of the channel is developed as the basis for the channel decompositions considered in the next chapter. As far as the receiver is concerned, the implications of the channel are explained in the context of established design methods. The performance evaluation of the various systems is discussed.

2.1 Communication System

A mathematical description of communication systems is required to form the basis for design and analysis. In the simplest model the transmitted signal has a complex baseband representation defined as

$$s(t) = \sum_{l \in \mathbb{Z}} a_l \delta(t - lT), \tag{2.1}$$

or on incorporating a pulse shaping filter

$$s_T(t) = \sum_{l \in \mathbb{Z}} a_l c_T(t - lT), \tag{2.2}$$

where $\mathbb{Z}$ is the set of integers, a_l is an element from the complex symbol sequence, $c_T(t)$ is the transmitter pulse shape and T is the symbol spacing. The two-sided bandwidth of $c_T(t)$ is denoted W. The modulation format could be PAM, PSK or QAM.

The channel impulse response (CIR) as a function of time and delay is denoted $h(t, \xi)$. This impulse response incorporates both fading, time selective effects and dispersive, frequency selective effects. At a given time, t, the channel has the impulse response described as a function of delay, ξ.

The receiver is assumed to have a fixed front-end filter with impulse response $c_R(t)$. The impulse response of the overall pulse shape is given by

$$c(t) = c_T(t) \otimes c_R(t), \tag{2.3}$$

and the overall CIR is defined as

$$u(t, \xi) = c(\xi) \otimes h(t, \xi), \tag{2.4}$$

where $\otimes$ denotes convolution. The overall CIR with $\xi = t - lT$ and with the convolution explicitly shown, is expressed as

$$u(t, t - lT) = \int_{-\infty}^{\infty} c(t - lT - \tau)h(t, \tau)d\tau. \tag{2.5}$$

At the output of the front-end filter the received signal is given by

$$s_R(t) = \sum_{l \in \mathbb{Z}} a_l u(t, t - lT) + \eta(t), \tag{2.6}$$

where $\eta(t)$ is the filtered output due to additive white Gaussian noise (AWGN) with two-sided power spectral density (PSD) $N_0/2$.

2.1.1 Linear Modulation Formats

Phase shift keying (PSK) is obtained by uniformly distributing symbols around a circle in the amplitude-phase plane. For M_c-ary PSK the symbols are defined as $a_l \in \sqrt{E_s}e^{j2\pi(2i+1)/2M_c}$ for $i \in \{0, 1, \ldots, M_c\}$ where E_s is the symbol energy. If the energy per bit is denoted E_b then $E_s = \log_2(M_c)E_b$. Gray coding [45] is usually assumed so that a nearest neighbour symbol error introduces a single bit error. Furthermore, if a differentially encoded PSK signal (DPSK) is transmitted then there is no requirement for carrier phase recovery at the receiver. There is a penalty in terms of the probability of bit error for using differential decoding.

2.1.2 Pulse Shaping

A transmitter pulse shape $c_T(t)$ is said to be T-shift orthogonal if

$$c_T(t - lT) \otimes c_T^*(-t)\Big|_{t=kT} = \delta_{kl}. \tag{2.7}$$

The overall pulse shape is said to be Nyquist if the transmitter pulse shape is T-shift orthogonal and the receiver filter is matched to the transmitter pulse or more generally if

$$c((k-l)T) = \delta_{kl}. \tag{2.8}$$

A standard Nyquist overall pulse shape is the raised-cosine defined as

$$c(t) = \text{sinc}(t/T)\frac{\cos(\pi\alpha t/T)}{1-4\alpha^2 t^2/T^2} \tag{2.9}$$

with amplitude spectrum

$$C(f) = \begin{cases} T, & |f| \leq (1-\alpha)f_s \\ T\cos^2\left[\frac{\pi}{2}\frac{|f|-(1-\alpha)f_s}{2\alpha f_s}\right], & (1-\alpha)f_s < |f| \leq (1+\alpha)f_s \\ 0, & \text{otherwise} \end{cases} \tag{2.10}$$

where $f_s = 1/2T$ and α is the rolloff factor with $0 \leq \alpha \leq 1$. The sinc function is defined as

$$\text{sinc}(t) = \begin{cases} 1, & t = 0 \\ \frac{\sin(\pi t)}{\pi t}, & \text{otherwise} \end{cases} \tag{2.11}$$

A root raised-cosine pulse is T-shift orthogonal and is obtained by setting $C_T(f) = \sqrt{C(f)}$. This defines the relationship between time shift orthogonality and Nyquist properties. There are other ways to define Nyquist pulses such as the methods associated with generalised Meyer wavelet scaling functions [29].

Using Poisson's sum formula [46] the condition for the Nyquist pulse is expressed in the frequency domain as

$$\sum_{l\in\mathbb{Z}} C\left(f - \frac{l}{T}\right) = T. \tag{2.12}$$

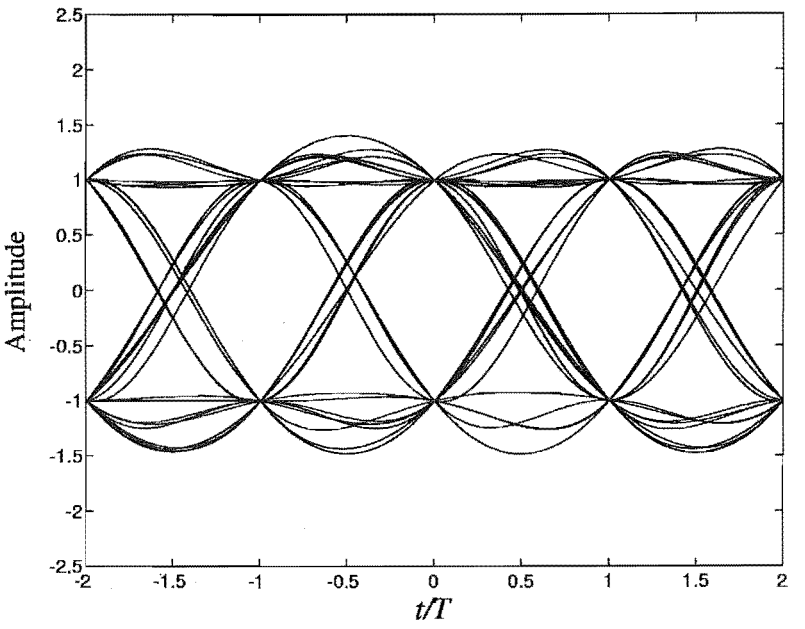

Figure 2.1: Eye diagram for raised-cosine pulse shaping with 50% excess bandwidth.

Figure 2.1 shows the eye diagram for a raised-cosine pulse shape with 50% excess bandwidth which is a standard setting. Figure 2.2 shows the amplitude and phase or in-phase/quadrature (IQ) plot of a quaternary phase shift keying (QPSK) signal for the same scenario.

2.2 Channel Modelling

Fading dispersive channels are characterised by system and correlation functions [76]. Here the channel is assumed to be wide sense stationary uncorrelated scattering (WSSUS) [9]. This means that correlations in time depend on time differences and correlations in frequency depend on frequency differences. The key system functions include the time varying CIR and the time varying channel transfer function. The Fourier transform relates the various system functions.

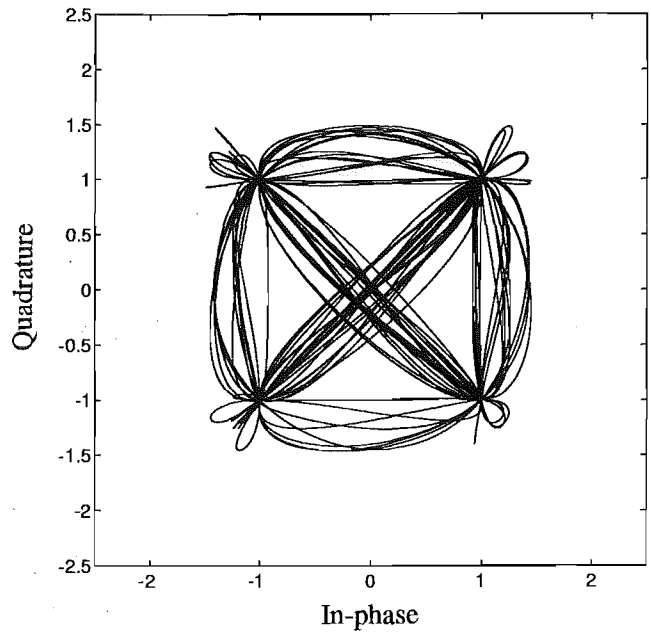

Figure 2.2: IQ plot of QPSK for raised-cosine pulse shaping with 50% excess bandwidth.

2.2.1 System Functions

The channel is described here by a time varying CIR, $h(t, \xi)$. As noted in [9] there are three other related system functions for describing the channel. These are the time varying channel transfer function, $H(f, t)$, the output Doppler spread function, $G(f, \nu)$, and the delay Doppler spread function, $g(\xi, \nu)$. As shown in Figure 2.3 these are related by the Fourier (downward) and inverse Fourier (upward) transforms [9].

2.2.2 Correlation Functions

Under the assumptions of WSSUS and a common time selective correlation function, ρ, across the delay profile it follows that

$$E\left[h(t, \xi)h^*(t', \xi')\right] = P_h(\xi)\rho(t - t')\delta(\xi - \xi'), \tag{2.13}$$

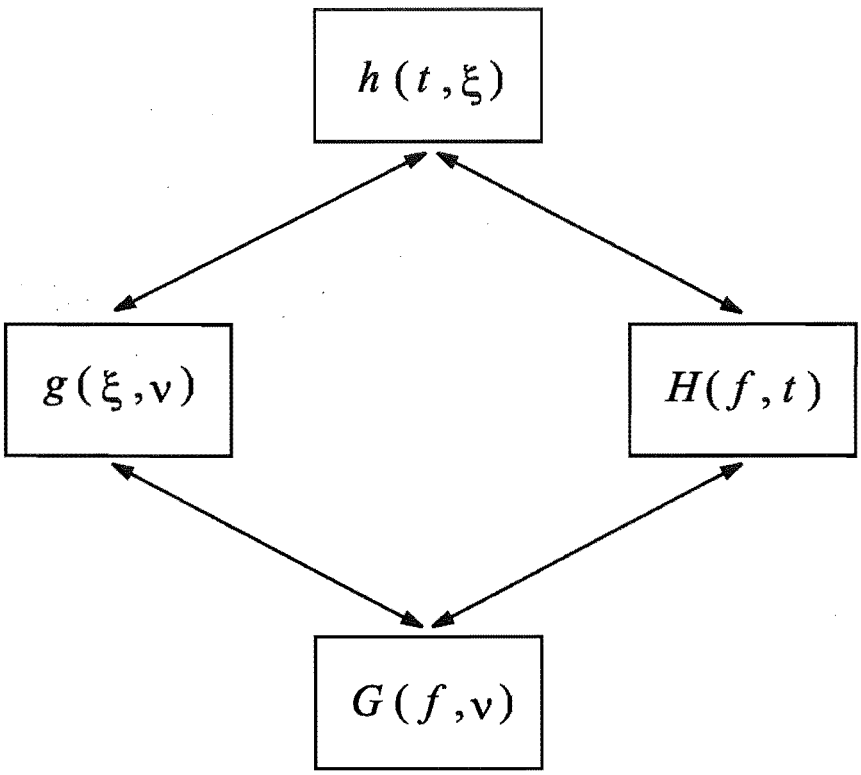

Figure 2.3: System functions for fading dispersive channels linked by Fourier and inverse Fourier transforms[9].

where $*$ denotes complex conjugation, P_h is the delay PSD and ρ is the time selective correlation function, normalised to unit power, that is $\rho(0) = 1$. The assumption on time selective correlation is a generalisation of standard assumptions used with tapped delay line models of the channel [55]. If the assumption is invalid in a given case then (2.13) can be modified appropriately. In this thesis a standard version of ρ is considered, derived under the assumption of isotropic scattering as [55]

$$\rho(t - t') = J_0(2\pi f_D(t - t')), \tag{2.14}$$

where f_D is the one-sided Doppler spread and J_0 denotes the zero order Bessel function of the first kind. Based on consideration of ellipses of scatterers for constant delay the scattering is only isotropic for large radius. However the Doppler spread is the same for all delays, ξ, so that (2.13) is representative of a practical situation. The function R_ρ, the Doppler PSD, is the Fourier transform of ρ in (2.14) and is given by [43]

$$R_\rho(\nu) = \begin{cases} \dfrac{1}{\pi\sqrt{f_D^2 - \nu^2}}, & |\nu| \leq f_D \\ 0, & \text{otherwise} \end{cases} \tag{2.15}$$

In the frequency domain the correlation is modelled as

$$E\left[H(f,t)H^*(f',t')\right] = R_H(f,f')\rho(t - t'), \tag{2.16}$$

where R_H is the frequency correlation function. R_H is the Fourier transform of P_h.

Consideration is given here to the following delay profiles.

$$P_h(\xi) = \begin{cases} \frac{1}{2}\left[\delta(\xi - \xi_0) + \delta(\xi + \xi_0)\right], & \text{two-ray} \\ \dfrac{1}{2\sqrt{3}\xi_0}\text{rect}\left(\dfrac{\xi}{2\sqrt{3}\xi_0}\right), & \text{uniform} \\ \dfrac{1}{\xi_0}\exp\left(\dfrac{\xi}{\xi_0}\right),\ \xi \geq 0, & \text{exponential} \end{cases} \tag{2.17}$$

where ξ_0 is the root mean square (RMS) delay spread and $d = \xi_0/T$ is the normalised RMS delay spread. For the uniform delay profile the maximum normalised delay spread is defined as $d_1 = 2\sqrt{3}d$. The rectangular function is defined as

$$\text{rect}(\xi) = \begin{cases} 1, & |\xi| \leq 1/2 \\ 0, & \text{otherwise} \end{cases} \tag{2.18}$$

Note that the two-ray and uniform delay profiles do not correspond to a causal channel filter response. However, upon bandlimiting of the CIR or convolution with the pulse shaping filter, the overall channel impulse filter response is capable of an eigen decomposition. This property is investigated in the next chapter. In addition the overall CIR is typically of finite energy and localised in time.

For the delay profiles considered it follows that

$$R_H(f, f') = \begin{cases} \cos(2\pi(f - f')\xi_0), & \text{two-ray} \\ \text{sinc}((f - f')2\sqrt{3}\xi_0), & \text{uniform} \\ \dfrac{1}{1 - j2\pi(f - f')\xi_0}, & \text{exponential} \end{cases} \tag{2.19}$$

The two-ray delay profile is easy to work with since decompositions can be obtained in closed form. The exponential profile is on balance the most realistic model and the uniform profile is of some theoretical interest since it is strictly delay limited.

The complex Gaussian distribution is an effective model of multipath channels. When the various components of the channel are combined the result is subject the central limit theorem. If a complex Gaussian variable x has zero mean and

$$E[|x|^2] = \sigma^2, \tag{2.20}$$

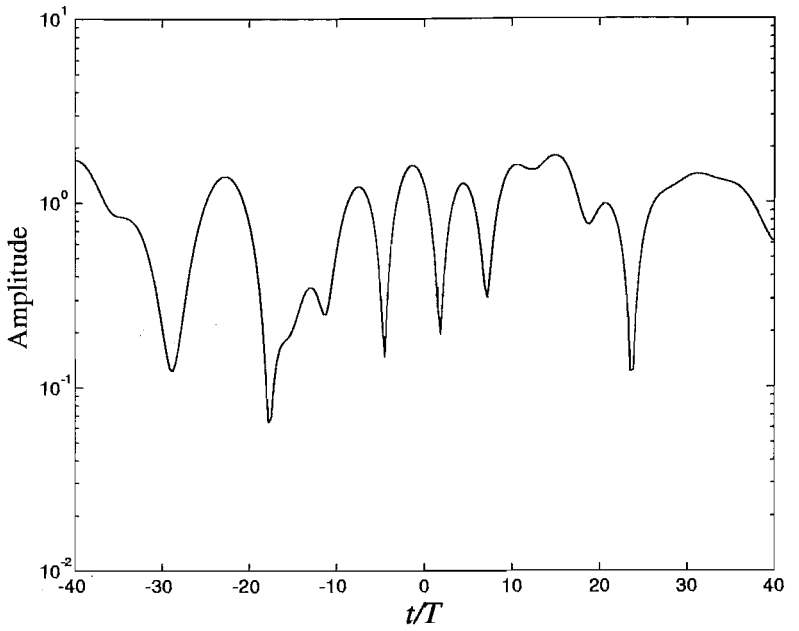

Figure 2.4: Amplitude of a Rayleigh fading process, $f_D T = 0.1$.

then the propbability density function (pdf) of x is given by

$$p_x(x) = \frac{1}{\pi\sigma} \exp\left(-\frac{|x|^2}{\sigma^2}\right). \tag{2.21}$$

The magnitude or envelope of x is denoted $|x|$ and has a Rayleigh pdf as

$$p_{|x|}(|x|) = \frac{2|x|}{\sigma^2} \exp\left(-\frac{|x|^2}{\sigma^2}\right). \tag{2.22}$$

The Rician distribution includes the Rayleigh distribution as one case as well as other cases which have non-zero means. Figure 2.4 shows the amplitude of a Rayleigh fading process and Figure 2.5, the phase.

The graphs are obtained using (2.14) and the method described in [85] for simulating a fading process. Windowing of the impulse response for the filter representing the fading process may in some situations be necessary when simulating adaptive receivers to create a more realisable and realistic model.

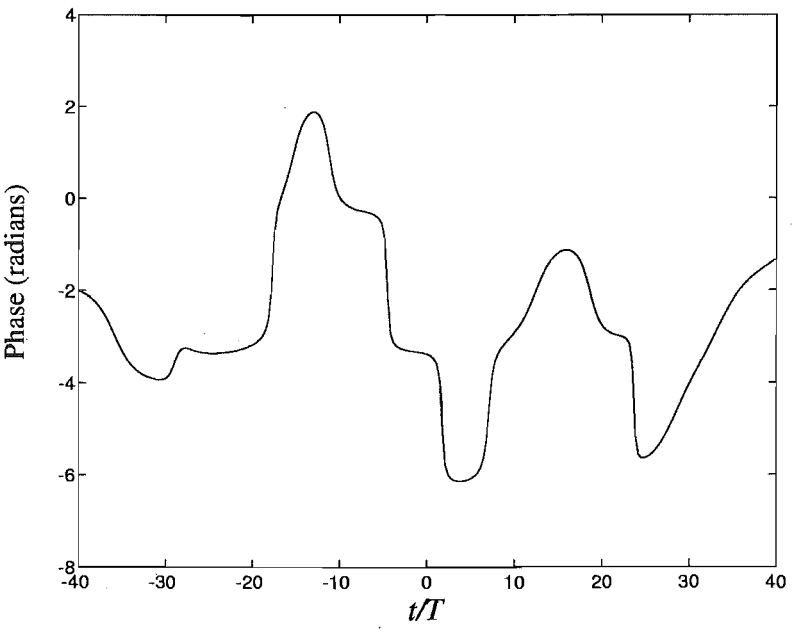

Figure 2.5: Phase of a Rayleigh fading process, $f_D T = 0.1$.

One of the fundamental difficulties in wireless communication is the deep fades or nulls in the channel amplitude. In slow fading the effective signal to noise ratio can be low for time periods of many symbols in duration. The figures show that rapid phase transitions tend to occur in deep fades. Depending on the receiver design these effects can result in sporadic events of many symbol errors. A critical tool in combatting periods of low signal to noise ratio is explicit diversity. However, the use of an optimal receiver and the exploitation of implicit diversity in the channel can also assist in minimising the effect of these impairments.

The product $f_D T$ is known as the fade rate. A value of 0.01 or less is generally taken to indicate slow fading; a value of 0.1 or greater respresents fast fading.

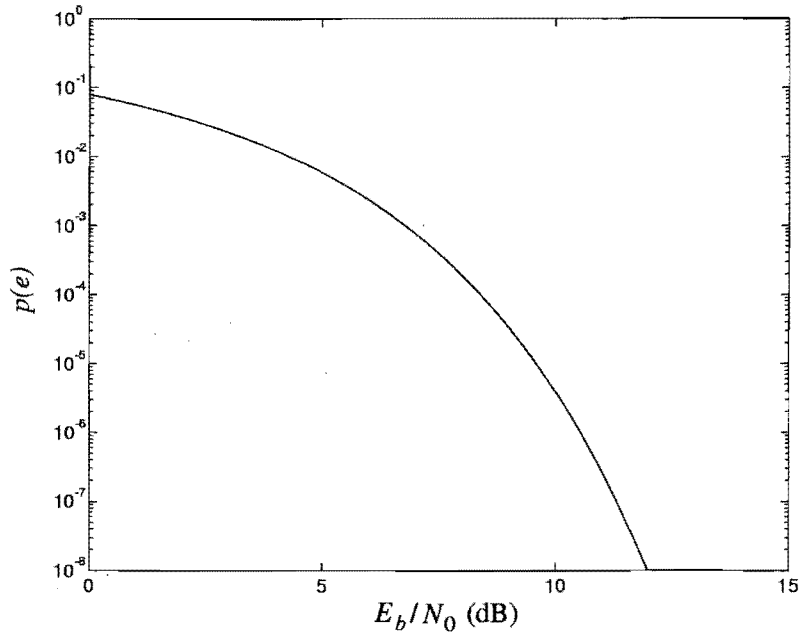

Figure 2.6: Probability of bit error, $p(e)$, vs E_b/N_0 for BPSK or QPSK over the AWGN channel.

2.3 Systems for the AWGN Channel

The probability of bit error, $p(e)$, for coherent binary PSK (BPSK) and QPSK (4-ary PSK) in AWGN is given by [3, 45]

$$p(e) = \frac{1}{2}\text{erfc}\left(\sqrt{\frac{E_b}{N_0}}\right), \tag{2.23}$$

where erfc is the complementary error function [45]. Figure 2.6 shows $p(e)$ versus E_b/N_0. The quantity E_b/N_0 arises frequently and represents the bit energy to noise energy ratio. It should be kept in mind that the performance of linear modulation formats in the ideal AWGN channel is a lower bound on the performance in fading channels.

2.4 Systems for Slow Fading Dispersive Channels

When the fading is slow the receiver design problem is a traditional one. The objective is to estimate CSI for equalisation and track slow variations. The receiver front-end filter can be matched to the transmitter filter rather than matched to the overall CIR up to the receiver. Thus $c_R(t)$ is typically set as in [12] as

$$c_R(t) = c_T^*(-t). \tag{2.24}$$

In this case the usual split of transmitter and receiver filter assuming that $C(f)$ is positive real and even for $|f| \leq W/2$, is defined by

$$C_T(f) = C_R(f) = \sqrt{C(f)}. \tag{2.25}$$

This ensures that if $c(t)$ is Nyquist then the impulse responses of the filters are T-shift orthogonal and $c_R(t)$ is the matched filter for $c_T(t)$. Furthermore, the symbol spaced sample output of $c_R(t)$ due to AWGN is a sequence of zero mean, mutually uncorrelated, Gaussian random variables.

Alternatively the receiver filter may be assumed to have an ideal low pass characteristic with two-sided bandwidth $1/T_r$ where $T_r = T/r$ is the sample spacing and r, the relative sample to symbol rate, is a positive integer, that is

$$C_R(f) = \begin{cases} 1, & |f| \leq \dfrac{1}{T_r} \\ 0, & \text{otherwise} \end{cases} \tag{2.26}$$

In this case c_T can optionally be set to be a full raised-cosine pulse shape with compensation of the symbol energy.

2.4.1 Co-Channel Interference and Diversity

To extend the system model a similar approach to that in [21] is adopted. When space diversity is available with sufficient antenna separation, there are M effectively uncorrelated channels carrying the same transmitted data. In addition, it is assumed here that there are N dominant co-channel interferers. Timing offsets are assumed for the interferers. However, for simplicity, all sources have the same coherent phase reference. That is, no consideration is given to carrier frequency offsets. The definitions in this section are based on [21].

The overall CIR for the nth interferer on the mth diversity thread is denoted $u_{n,m}(t,\xi)$ and is given by

$$u_{n,m}(t,\xi) = c(\xi - t_n) \otimes h_{n,m}(t,\xi), \tag{2.27}$$

where $n \in \{0,\ldots,N\}$, $n = 0$ is the desired information bearing signal, $m \in \{1,\ldots,M\}$, $h_{n,m}(t,\xi)$ is the corresponding CIR and t_n is the timing offset of the nth source or interferer relative to the timing of the desired signal, that is, $t_0 = 0$ and t_n for $n \geq 1$ is uniformly distributed over $[-T/2, T/2)$. The frequency correlation for the CIRs is defined as

$$E[H_{n,m}(f,t)H^*_{n',m'}(f',t')] = \frac{1}{\mathrm{SIR}_n} R_H(f,f')\rho(t-t')\delta_{nn'}\delta_{mm'}, \tag{2.28}$$

where SIR_n is the signal to interference ratio for the nth source and $\mathrm{SIR}_0 = 1$. For $n \geq 1$ and assuming an even distribution of energy over the dominant interferers we have [21]

$$\mathrm{SIR}_n = N\left(1 + \frac{1}{\mathrm{DWR}}\right)\mathrm{SIR}, \tag{2.29}$$

where SIR is the total signal to interference ratio and DWR is the dominant to weak interference ratio. The weak interference here is the output of the receiver filter due to

AWGN with constant power spectral density. This is different to the approach taken in [21] where the PSD of the weak interference is assumed to be due to other wireless signals with similar format, and therefore, is influenced by the shape of the transmitter filter. Hence, in the model of this section it is assumed that the weak interference is receiver front-end noise and all co-channel interference is cyclostationary. SIR_w is the signal to interference ratio for the weak interference and is given by

$$\mathrm{SIR}_w = (\mathrm{DWR} + 1)\mathrm{SIR}. \tag{2.30}$$

The SIRs are related as

$$\frac{1}{\mathrm{SIR}} = \sum_{n=1}^{N} \frac{1}{\mathrm{SIR}_n} + \frac{1}{\mathrm{SIR}_w}. \tag{2.31}$$

These SIRs are signal to interference ratios for separate diversity threads. The dominant co-channel interference (CCI) is correlated from thread to thread in contrast to the weak interference on different diversity threads which is uncorrelated. SIR_w is also referred to as the signal to noise ratio, denoted SNR.

2.4.2 Diversity Combining

Various approaches can be adopted for diversity combining and equalisation. In this section space diversity is assumed and memoryless combining is done with scalar antenna weights. Minimum mean square error (MMSE) diversity combining is assumed and developed as in [23]. Other forms relevant to this receiver structure are selection, fixed ratio and maximal ratio combining. Fixed ratio combining is also known as equal gain combining.

The following development is instructive in the sense that it describes how a system, including a linear receiver, is structured given a slow fading assumption. It also introduces the concept of minimum or least mean square error optimisation which is critical in many aspects of communication system design. In Chapter 4, a related optimisation process is used to design pulse shaping filters.

The kth sample at the output of the receiver filter is given by

$$y_k = \sum_{m=1}^{M} \sum_{n=0}^{N} \sum_{l \in \mathbb{Z}} a_{n,l} w_{m,k} u_{n,m}(kT, (k-l)T) + \sum_{m=1}^{M} w_{m,k} \eta_{m,k}, \tag{2.32}$$

where $w_{m,k}$ for $m \in \{1, .., M\}$ denotes the $\{m, k\}$th scalar antenna weight of the diversity combining scheme, $\eta_{m,k}$ is the $\{m, k\}$th sample due to the weak interference and $a_{n,l}$ is the symbol sequence of the nth dominant interferer. The desired component corresponds to $l = k$ and $n = 0$. A vector of antenna weights is defined as

$$\mathbf{w}_k = (w_{1,k}, w_{2,k}, .., w_{M,k})^{\dagger}. \tag{2.33}$$

where $\dagger$ denotes Hermitian transpose.

The following description of MMSE combining is based on [23]. The mean squared error, MSE, is defined as

$$\text{MSE} = E\left[|y_k - a_{0,k}|^2\right]. \tag{2.34}$$

Substituting from (2.32) and expanding (2.34) under the assumption of uncorrelated symbols the MSE can be written as

$$\text{MSE} = E_s\left[\mathbf{w}_k^{\dagger}\mathbf{A}_k\mathbf{w}_k - \mathbf{w}_k^{\dagger}\mathbf{b}_k - \mathbf{b}_k^{\dagger}\mathbf{w}_k - 1\right], \tag{2.35}$$

for BPSK and QPSK,

$$\mathbf{A}_k = \mathbf{F}_k + \mathbf{G}, \tag{2.36}$$

with

$$F_{mm'k} = \sum_{n=0}^{N} \sum_{l \in \mathbb{Z}} u_{n,m}(kT, (k-l)T) u^*_{n,m'}(kT, (k-l)T), \tag{2.37}$$

or, again using Poisson's sum formula,

$$F_{mm'k} = \sum_{n=0}^{N} \sum_{l \in \mathbb{Z}} \int_{-W/2}^{W/2} U_{n,m}(f, kT) U^*_{n,m'} \left(f - \frac{l}{T}, kT \right) df, \tag{2.38}$$

$$\mathbf{G} = \frac{\mathbf{I}}{\mathrm{SIR}_w}, \tag{2.39}$$

and

$$\mathbf{b}_k = (u_{0,1}(kT, 0), u_{0,2}(kT, 0), .., u_{0,M}(kT, 0))^T. \tag{2.40}$$

The MMSE occurs when

$$\mathbf{w}_k = \mathbf{A}_k^{-1} \mathbf{b}_k, \tag{2.41}$$

corresponding to

$$\mathrm{MMSE} = 1 - \mathbf{b}_k^\dagger \mathbf{A}_k^{-1} \mathbf{b}_k. \tag{2.42}$$

The usual approach to proving this result is to take the gradient [77] of the MSE. Since the MSE is not analytic an alternative proof is given here. A function g is defined as

$$g(\mathbf{w}_k) = \mathbf{w}_k^\dagger \mathbf{A}_k \mathbf{w}_k - \mathbf{w}_k^\dagger \mathbf{b}_k - \mathbf{b}_k^\dagger \mathbf{w}_k. \tag{2.43}$$

The matrix $\mathbf{A}_k$ is positive definite so that

$$0 \leq (\mathbf{w}_k - \mathbf{A}_k^{-1} \mathbf{b}_k)^\dagger \mathbf{A}_k (\mathbf{w}_k - \mathbf{A}_k^{-1} \mathbf{b}_k) = g(\mathbf{w}_k) - g(\mathbf{A}_k^{-1} \mathbf{b}_k). \tag{2.44}$$

Therefore $g(\mathbf{w}_k) \geq g(\mathbf{A}_k^{-1} \mathbf{b}_k) = \mathbf{b}_k^\dagger \mathbf{A}_k^{-1} \mathbf{b}_k$ and (2.42) follows.

The estimation of the overall CIR required to determine $\mathbf{A}_k$ and $\mathbf{b}_k$ can be done by assuming knowledge of the training sequence and, subsequently, the detected symbols. Again, standard minimum or least mean squares estimation is employed with the received samples as inputs. Having estimated $\mathbf{A}_k$ and $\mathbf{b}_k$ the method of steepest descent can be employed to find the required antenna weights. The update is given by

$$\mathbf{w}_{k+1} = (\mathbf{I} - \Delta\mathbf{A}_k)\mathbf{w}_k + \Delta\mathbf{b}_k, \tag{2.45}$$

where Δ is the step size parameter [77].

2.4.3 Equalisation and Diversity Combining

The approach described above for MMSE memoryless diversity combining can be generalised. An optimum linear receiver [21] implements both filtering and diversity combining. The receiver is based on matched filters. It is possible to achieve the same end with no matched filter but rather a transversal filter for each diversity thread. Using either approach the result is achieved by minimising a distortion spectrum. An implementation along these lines utilising finite-length filters is described in [47].

2.4.4 Performance Evaluation

Metzger's algorithm [70, 21] can be used to assess the performance of systems with residual ISI and CCI in terms of the bit error rate, BER, in a slow fading dispersive channel. The algorithm takes the real and imaginary components of the ISI and CCI and adopts a numerical procedure to obtain a model of the overall interference distribution. This process can be used to determine the bit error rate (BER) due to residual ISI in equalisation.

However, conclusions can often be drawn from a simple Gaussian model of interference.

Average BER results illustrate the level of error floors. Also useful is the BER distribution which expresses the outage probability, P_{out}, as a function of BER and a threshold value, BER_{o}. P_{out} is defined as [22, 60]

$$P_{\text{out}} = P\left[\text{BER} \geq \text{BER}_{\text{o}}\right], \tag{2.46}$$

where BER_{o} is a BER threshold. In many applications, such as voice communications, some errors are tolerable. P_{out} is the chance that the error rate exceeds the predefined threshold.

2.5 Systems for Fast Fading Dispersive Channels

When a wireless system is implemented in such a way that the fading can be considered fast, conventional receivers develop an error floor [12]. A conventional receiver in this context is partially matched in the sense that the receiver front end filter is matched to the transmitted pulse rather than the overall CIR. The error floor arises as a result of the ISI and the distortion of each received pulse introduced by fluctuations in the channel amplitude and phase over the interval of a symbol.

One approach to design in this situation is to raise the symbol rate thus reducing the fade rate and to use some form of diversity to allow for long deep fades. However, it is also possible to implement an equaliser that can compensate for time variation and remove error floors. The method developed in [44] extends the MLSE approach based on the Viterbi algorithm. The original method for time invariant dispersive channels is described in [38, 83]. For simplicity in this section the consideration of diversity is omitted.

The development is easily generalised to include diversity in the form of multiple threads. The material is based on [44] and is used only in Chapter 5 wherein conclusions can be made without considering diversity.

The origin of the term error floor is [16]. Throughout this thesis the term error floor describes the situation where the probability of error has a non-zero large signal to noise ratio asymptote. With this definition it is seen that different forms of mismatch lead to an error floor. For instance, the effect of fading is to produce a phase ambiguity for the detection of symbols in a conventional receiver leading to an error floor.

2.5.1 Maximum Likelihood Sequence Estimation

For MLSE the receiver implements a time varying matched filter, searches sequences and chooses the one with maximum likelihood (ML). A full derivation of the matched filter MLSE receiver is provided in [44]. The Viterbi algorithm is used to iteratively compute the metric and determine the ML sequence. Use of the branch metrics $|y_k - \hat{y}_k|^2$ without a matched filter delivers a receiver with equivalent performance characteristics under the assumption of AWGN. The quantity y_k is the received sample following filtering with the receiver filter implied by (2.26). The quantity $\hat{y}_k$ in a branch metric is the hypothesised received sample defined as

$$\hat{y}_k = \sum_{l \in \mathbb{Z}} \hat{a}_l \widehat{u}(kT_r, (k - lr)T_r), \tag{2.47}$$

where $\hat{a}_l$ is an hypothesised symbol in the sequence, $\widehat{u}(t, \xi)$ is an approximation to the overall CIR and $1/r$ is the sample rate relative to the symbol rate so that the sample spacing is given by $T_r = T/r$. Based on the use of these branch metrics, the total or path

metric for the hypothesised sequence $\hat{a} = \{\hat{a}_l\}$, $l \in \mathbb{Z}$, given $a = \{a_l\}$, $l \in \mathbb{Z}$ transmitted, is defined as

$$G(a, \hat{a}) = \sum_{k \in \mathbb{Z}} |y_k - \hat{y}_k|^2 \tag{2.48}$$

It is often assumed for the purposes of analysis that CSI is known *a priori*, to some degree of approximation. In practice an initial estimate of CSI is obtained by the use of a training sequence or some other procedure. Adaptive receivers for MLSE typically utilise per-survivor processing within the Viterbi algorithm [78] to maintain an estimate of CSI.

2.5.2 Performance Evaluation

The calculation of the probability of error for the MLSE receiver implied by (2.48) follows the development in [44] for MLSE with approximate CSI. The basis of the calculation is the pairwise probability of error, $P(a \to \hat{a})$, which is the probability that the transmitted sequence, $a = \{a_l\}$, $l \in \mathbb{Z}$, implies a greater total metric, $G(\cdot, \cdot)$, than an alternative sequence, $\hat{a} = \{\hat{a}_l\}$, $l \in \mathbb{Z}$. This probability is given by

$$P(a \to \hat{a}) = P(G(a, a) - G(a, \hat{a}) > 0). \tag{2.49}$$

In calculating the probability, the overall CIR in (2.47) is assumed to be of length L symbols where L is an odd integer. The models of the overall CIR developed in the preceding sections are bandlimited. Therefore the overall CIR is not time limited and, strictly speaking, its length, L, is infinite. However, it has been found that use of a small value of L with the metric in (2.48) leads to good approximations in the calculation of error probabilities. The fact that bandlimited signals are not time limited and vice versa is a manifestation of the uncertainty principle.

Further to the assumption of finite length, L, for the overall CIR it is assumed that consideration is limited to dominant short error events. Events begin at the symbol $l = 0$ and last $w + 1$ symbols where w is a small non-negative integer.

With these assumptions it is possible to fix the summation limits implicit in (2.49). Letting $k = mr + n$, $m \in \mathbb{Z}$, $n \in \{0, \ldots, r-1\}$, it follows that the range of k is defined by $m = -\frac{L-1}{2}, \ldots, w + \frac{L-1}{2}$. There are $w + L$ values of m and $(w + L)r$ values of k. For each value of k there are L values of l. The range of l is defined by $l = m - \frac{L+1}{2}, \ldots, m + \frac{L-1}{2}$.

The left hand side of the inequality in (2.49) is a complex Gaussian quadratic form. The pairwise probability of error is written as $P(\kappa > 0)$ where

$$\kappa = G(a, a) - G(a, \hat{a}) = \mathbf{x}^{\dagger}\mathbf{A}\mathbf{x}. \tag{2.50}$$

The column vector $\mathbf{x}$ is a concatenation of the subvectors $\mathbf{u}$, $\widehat{\mathbf{u}}$ and $\mathbf{n}$ as

$$\mathbf{x} = \left(\begin{array}{c} \mathbf{u} \\ \hline \widehat{\mathbf{u}} \\ \hline \mathbf{n} \end{array}\right) \tag{2.51}$$

The subvectors in turn contain the elements $u_{k,k-lr}$, $\widehat{u}_{k,k-lr}$ and η_k. Based on the above discussion the vectors $\mathbf{u}$ and $\widehat{\mathbf{u}}$ are of dimension $(w + L)Lr \times 1$ and the vector $\mathbf{n}$ is of dimension $(w + L)r \times 1$. A suitable index for the vectors $\mathbf{u}$ and $\widehat{\mathbf{u}}$ has a range of $\mathrm{ndx} = 1, \ldots, (w + L)Lr$ and is given by

$$\begin{aligned} \mathrm{ndx} &= \left(\left(m + \frac{L-1}{2}\right) r + n\right) L + l - m + \frac{L-1}{2} + 1 \\ &= m(rL - 1) + nL + l + \frac{L-1}{2} rL + \frac{L+1}{2}. \end{aligned}$$

Thus

$$m = \left\lfloor \frac{\mathrm{ndx} - 1}{Lr} \right\rfloor - \frac{L-1}{2},$$

$$n = \left\lfloor \frac{\text{ndx} - 1}{L} \right\rfloor \bmod r,$$

$$l = ((\text{ndx} - 1) \bmod L) + m - \frac{L-1}{2},$$

where the floor function $\lfloor \cdot \rfloor$ indicates rounding to nearest integer in the direction of minus infinity and mod is short for modulo.

The matrix $\mathbf{A}$ is defined from the following expression for the quadratic form,

$$\kappa = \sum_{k=-\frac{L-1}{2}r}^{(w+\frac{L+1}{2})r-1} \sum_{l=m-\frac{L-1}{2}}^{m+\frac{L-1}{2}} \left[\sum_{l'=m-\frac{L-1}{2}}^{m+\frac{L-1}{2}} \left[-2\text{Re}[u^*_{k,k-lr} a^*_l (a_{l'} - \hat{a}_{l'}) \widehat{u}_{k,k-l'r}] \right.\right. \\ \left.\left. + \widehat{u}^*_{k,k-lr} (a^*_l a_{l'} - \hat{a}^*_l \hat{a}_{l'}) \widehat{u}_{k,k-l'r} \right] - 2\text{Re}[\widehat{u}^*_{k,k-lr} (a^*_l - \hat{a}^*_l) \eta_k] \right]. \tag{2.52}$$

The probability density function of κ is denoted $p_\kappa(\kappa)$ and has a characteristic function, $P_\zeta(\zeta)$, given by [44]

$$P_\zeta(\zeta) = \int_{-\infty}^{\infty} p_\kappa(\kappa) \exp(j\zeta\kappa) d\kappa = \frac{1}{|\mathbf{I} - j\zeta \mathbf{R}_{\mathbf{xx}} \mathbf{A}|}, \tag{2.53}$$

where the covariance matrix is defined as

$$\mathbf{R}_{\mathbf{xx}} = E(\mathbf{x}\mathbf{x}^\dagger), \tag{2.54}$$

and is composed of nine submatrices as [44]

$$\mathbf{R}_{\mathbf{xx}} = \left(\begin{array}{c|c|c} \mathbf{R}_{\mathbf{uu}} & \mathbf{R}_{\mathbf{u\hat{u}}} & \mathbf{0} \\ \hline \mathbf{R}_{\mathbf{\hat{u}u}} & \mathbf{R}_{\mathbf{\hat{u}\hat{u}}} & \mathbf{0} \\ \hline \mathbf{0} & \mathbf{0} & \mathbf{R}_{\mathbf{nn}} \end{array} \right). \tag{2.55}$$

The pairwise probability of error is then calculated with residue theory [48] as

$$P(a \to \hat{a}) = - \sum_{i, \text{Im}[\text{pole}_i] < 0} \frac{\text{res}_i}{\text{pole}_i} \tag{2.56}$$

where pole_i is the ith pole of (2.53) and res_i is its residue.

The possible transmitted sequences are denoted $a^{w,x}$ so that a_l in (2.52) can be replaced by $a_l^{w,x}$. The index w enumerates the error events of length $w+1$. The index x identifies the transmitted sequences. The range of x is $x = 1, \ldots, {M_c}^{w+2L-1}$ where the quantity M_c is the number of symbols in the modulation format. For example, $M_c = 2$ for BPSK. The possible sequences chosen in error by the receiver are denoted by $a^{w,x,y}$ so that $\hat{a}_l$ in (2.52) can be replaced by $a_l^{w,x,y}$. The index y identifies different error events of length $w+1$. The Gaussian quadratic form κ can be replaced by $\kappa^{w,x,y}$ and $\mathbf{A}$ can be replaced by $\mathbf{A}^{w,x,y}$. An error event is signified by the quantity $\varepsilon^{w,x,y} = a^{w,x} - a^{w,x,y}$. A union bound on the probability of bit error is then given by [44]

$$p(e) \leq \sum_{w=0}^{\infty} \sum_{x=1}^{{M_c}^{w+2L-1}} \sum_{\varepsilon^{w,x,y}} \frac{P(a^{w,x})P(a^{w,x} \rightarrow a^{w,x,y})e(a^{w,x} \rightarrow a^{w,x,y})}{\log_2 M_c}. \tag{2.57}$$

The *a priori* transmission probability $P(a^{w,x}) = \frac{1}{{M_c}^{w+2L-1}}$, assuming all transmitted sequences are equally likely. The quantity $e(a^{w,x} \rightarrow a^{w,x,y})$ is the number of bit errors corresponding to an error event, $\varepsilon^{w,x,y}$, and $P(a^{w,x} \rightarrow a^{w,x,y})$ is the pairwise probability of error given by

$$P(a^{w,x} \rightarrow a^{w,x,y}) = P(\kappa^{w,x,y} > 0). \tag{2.58}$$

2.6 Summary

It is seen that there are well defined structures for the design and associated performance evaluation of communication systems with fading dispersive channels. In the next chapter the channel models are developed further. It is the extension and application of channel

decompositions that form the basis of this thesis. However, this is done in the context of existing models developed in this chapter. Two fundamentally different receiver structures have been presented for the separate cases of slow and fast fading channels. In slow fading it is fairly straightforward to implement diversity combining and to control the effects of interference in the sense of minimum mean square error. In fast fading the rapid variations of the channel over time are taken into account through extended application of the Viterbi algorithm for maximum likelihood sequence estimation.

Chapter 3

Channel Decomposition

This chapter identifies several options for the modelling of fading dispersive channels. As in the previous chapter, it is assumed that the channel can be modelled statistically and is WSSUS. With these assumptions it is possible to impose a structure which enables the channel to be locally specified over a symbol interval, with a small number of parameters. Having defined these structures the next four chapters demonstrate applications of both a theoretical and practical nature. The models are somewhat idealised and there are some approximations. Nevertheless the approach allows a study of fundamental issues arising in the field of wireless communication over fading dispersive channels.

From a theoretical standpoint the major contribution of this chapter is the extension of the Karhunen-Loève (KL) expansion [30] to certain models of fast fading dispersive channels. In practice the essentially delay and Doppler frequency limited property of wireless channels enables their decomposition. In addition, if it is assumed that the statistics are zero mean complex Gaussian then many quantitative assessments are greatly simplified. A zero mean complex Gaussian random process has a Rayleigh distributed

envelope and thus it makes sense to describe the channels as Rayleigh fading dispersive. The statistical modelling of wireless channels is designed to reflect the inherent uncertainty arising in practical systems. The Rayleigh fading dispersive channel incorporates the most detrimental effects such as time intervals of low effective signal to noise ratio and rapid phase transitions. Other models such as the Rician distribution introduce further considerations to the analysis.

To begin, the tapped delay line model of the channel is defined. The tapped delay line is the traditional model for fading dispersive channels and is based on the assumption that there are two or more distinct propagation delays for rays arriving at the receiver. Three alternative decompositions are presented as representations that are generally more efficient than a tapped delay line. A single spread KL expansion is based on the assumption that the time-frequency correlation function can be separated into a product of the delay PSD and the time selective correlation function. The resulting expansion has sample spaced coefficients. A double spread KL expansion involves a decomposition of an overall received pulse isolated from the rest of the received signal. The time varying and frequency selective aspects of the channel are jointly incorporated into an expansion with symbol spaced coefficients. The f-power series expansion [9] is reasonably well known and is considered here for the sake of comparison with other decompositions. In all cases the initial terms of the decomposition contain the majority of the channel energy and the decomposition can be truncated to give a model with finite dimension.

A numerical method analogous to the discrete Fourier transform is used to obtain the eigenvalues and eigenfunctions of the KL expansions and this represents sampling in frequency. In the case of a uniform delay profile with a single spread KL expansion

the eigenfunctions in frequency are spheroidal wave functions [82]. The theory associated with such functions offers another means of obtaining the basis for an expansion [37, 1]. The functions are orthogonal over two intervals of frequency, one finite and one infinite.

Coefficient covariances for the decompositions are obtained for use in later chapters. The mean squared error of approximation is a simple performance measure for investigating the impact of truncating higher order terms to make the dimension finite. Such truncation is a form of mismatch and is similar to the use of a conventional receiver for the fading channel. Some results illustrating the error of approximation for combinations of delay profile and decomposition are presented in this chapter. The issue of truncation is taken up again in Chapter 5. In practice the level of truncation is chosen so as the error of approximation has minimal impact on receiver performance.

3.1 Tapped Delay Line

The tapped delay line model of the channel is based on a discrete multipath structure such that the channel can be expressed as

$$u(t,\xi) = \sum_{i=0}^{N_\tau - 1} x_{P,i}(t) c(\xi - \tau_i), \tag{3.1}$$

where N_τ is the number of different delays and $x_{P,i}(t)$ is a complex valued time selective coefficient (TSC). For an equi-spaced delay of τ the tapped delay line model is shown in Figure 3.1. In general the number of delays and their values are chosen to match the type of channel being modelled in terms of multipath density and delay spread.

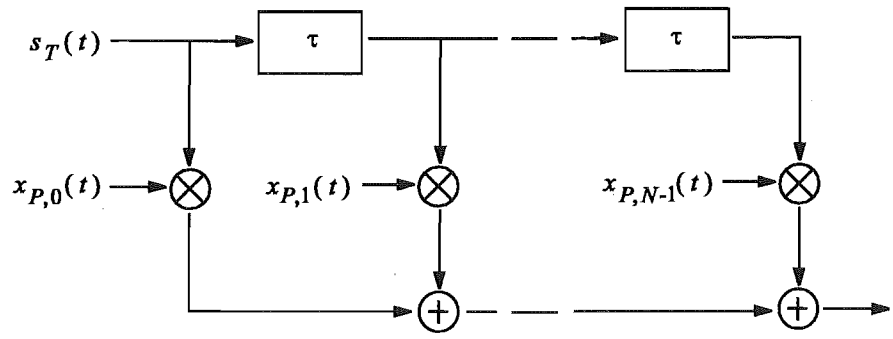

Figure 3.1: Tapped delay line channel model with equi-spaced delays.

3.2 Single Spread Karhunen-Loève Expansion

The single spread KL expansion can be defined in a number of ways. These are distinguished by whether the pulse shape is incorporated into the defining integral equation and whether there is mismatch between the expansion and the channel being modelled. In all cases there is a set of eigenvalues, $\{\lambda_{Q,i}\}$, and eigenfunctions, $\{\Phi_{Q,i}(f)\}$, for $i \in \{0, 1, \dots\}$, obtained as solutions of the integral equation [30]

$$\int_{-W/2}^{W/2} R_Q(f, f')\Phi_{Q,i}(f')df' = \lambda_{Q,i}\Phi_{Q,i}(f), \tag{3.2}$$

where Q determines the underlying structure of the model and has the following definitions

$$Q = \begin{cases} H, & \text{exact model of CIR} \\ U, & \text{exact model of overall CIR} \\ \widetilde{H}, & \text{mismatched 2nd order model of CIR} \\ \widetilde{U}, & \text{mismatched 2nd order model of overall CIR} \end{cases} \tag{3.3}$$

that is, $Q = H$ means the pulse shape is omitted in the integral equation and $Q = U$ means it is included. The frequency correlation functions are defined as

$$R_Q(f,f') = \begin{cases} R_H(f,f'), & Q = H \\ C(f)R_H(f,f')C^*(f'), & Q = U \\ R_{\widetilde{H}}(f,f'), & Q = \widetilde{H} \\ C(f)R_{\widetilde{H}}(f,f')C^*(f'), & Q = \widetilde{U} \end{cases} \tag{3.4}$$

The KL expansion is defined as

$$u(t,\xi) = \sum_{i=0}^{\infty} x_{Q,i}(t) z_{Q,i}(\xi), \tag{3.5}$$

$$U(f,t) = \sum_{i=0}^{\infty} x_{Q,i}(t) Z_{Q,i}(f), \tag{3.6}$$

where $x_{Q,i}(t)$ is the ith KL expansion TSC and

$$Z_{Q,i}(f) = \begin{cases} \Phi_{H,i}(f)C(f), & Q = H \\ \Phi_{U,i}(f), & Q = U \\ \Phi_{\widetilde{H},i}(f)C(f), & Q = \widetilde{H} \\ \Phi_{\widetilde{U},i}(f), & Q = \widetilde{U} \end{cases} \tag{3.7}$$

These series are truncated to produce approximate decompositions with finite dimension as

$$\widehat{u}(t,\xi) = \sum_{i=0}^{J-1} x_{Q,i}(t) z_{Q,i}(\xi), \tag{3.8}$$

$$\widehat{U}(f,t) = \sum_{i=0}^{J-1} x_{Q,i}(t) Z_{Q,i}(f), \tag{3.9}$$

where J is the dimension of or number of terms in the decomposition. In practice the depth of truncation is chosen so that the resulting error of approximation in modelling the overall CIR has negligible efect on performance. Some of the results in this chapter and Chapter 5, quantify the effect on performance at the boundary of acceptable truncation depth. The TSCs are obtained as the inner products

$$x_{H,i}(t) = \int_{-W/2}^{W/2} H(f,t)\Phi^*_{H,i}(f)df, \tag{3.10}$$

$$x_{U,i}(t) = \int_{-W/2}^{W/2} U(f,t)\Phi^*_{U,i}(f)df, \tag{3.11}$$

$$x_{\widetilde{H},i}(t) = \int_{-W/2}^{W/2} H(f,t)\Phi^*_{\widetilde{H},i}(f)df, \tag{3.12}$$

$$x_{\widetilde{U},i}(t) = \int_{-W/2}^{W/2} U(f,t)\Phi^*_{\widetilde{U},i}(f)df. \tag{3.13}$$

The autocorrelations of the first two types of TSC are obtained using (2.16), (3.2), (3.10) and (3.11) as

$$E\left[x_{H,i}(t)x^*_{H,i'}(t')\right] = \lambda_{H,i}\delta_{ii'}\rho(t-t'), \tag{3.14}$$

$$E\left[x_{U,i}(t)x^*_{U,i'}(t')\right] = \lambda_{U,i}\delta_{ii'}\rho(t-t'), \tag{3.15}$$

that is, these TSCs are mutually uncorrelated. For the mismatched case, using (2.16), (3.2), (3.12) and (3.13),

$$E\left[x_{\widetilde{H},i}(t)x^*_{\widetilde{H},i'}(t')\right] = \int_{-W/2}^{W/2}\int_{-W/2}^{W/2} \Phi^*_{\widetilde{H},i}(f)R_H(f,f')\Phi_{\widetilde{H},i'}(f')df'df\rho(t-t'), \tag{3.16}$$

$$E\left[x_{\widetilde{U},i}(t)x^*_{\widetilde{U},i'}(t')\right] = \int_{-W/2}^{W/2}\int_{-W/2}^{W/2} \Phi^*_{\widetilde{U},i}(f)R_U(f,f')\Phi_{\widetilde{U},i'}(f')df'df\rho(t-t'), \tag{3.17}$$

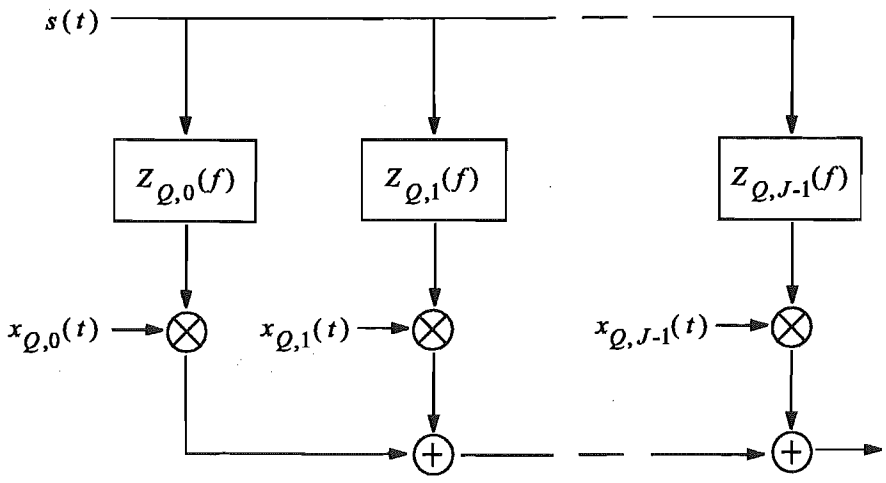

Figure 3.2: Structure for single spread KL expansion of the channel.

and in relation to the matched case

$$E\left[x_{H,i}(t)x^*_{\tilde{H},i'}(t')\right] = \lambda_{H,i}\int_{-W/2}^{W/2}\Phi^*_{H,i}(f)\Phi_{\tilde{H},i'}(f)df\rho(t-t'), \tag{3.18}$$

$$E\left[x_{U,i}(t)x^*_{\tilde{U},i'}(t')\right] = \lambda_{U,i}\int_{-W/2}^{W/2}\Phi^*_{U,i}(f)\Phi_{\tilde{U},i'}(f)df\rho(t-t'), \tag{3.19}$$

Figure 3.2 illustrates the structure implied by the single spread KL expansion.

3.2.1 Spheroidal Wave Functions

For the single spread KL expansion and a uniform delay profile the eigenfunctions for $Q = H$ are proportional to prolate spheroidal wave functions as defined in [82, 53, 54] which illustrate the finite dimensionality of bandlimited and essentially time limited signals. In the application considered in this thesis the channel transfer function is to be modelled and is assumed to be delay limited and essentially bandlimited. It is generally accepted that delay profiles encountered in practice are more likely to be exponential. However, both the uniform and exponential delay profiles are continuous over a certain range of

delay and both are delay limited to all intents and purposes. Thus a case can be made for using either the uniform or exponential delay profile for general aspects of design and analysis. For the examples in the following chapters the choice of delay profile is open and to some extent arbitrary.

A consequence of the link between the eigenfunctions for a uniform delay profile and spheroidal wave functions is that the eigenfunctions are orthonormalised Legendre polynomials as the channel becomes frequency non-selective or the delay spread tends towards zero. The set containing orthonormalised versions of the first J Legendre polynomials is a suitable fixed basis and can be used for moderate delay spreads since the Legendre polynomials and eigenfunctions have roughly the same shape. Another general property of the ith spheroidal wave function is that it has i roots over the finite frequency range of orthogonality.

The parameter c in [82] is here denoted c_s along with $\lambda_{s,i}$, T_s and W_s denoting corresponding parameters. The links between the quantities in this thesis and that paper, with W fixed at $1/T$, are defined by $T_s = 1/T$, $W_s = d_1 T/2$, $c_s = 2d_1/\pi$ and $\lambda_{s,i} = d_1 \lambda_{H,i}$, noting that time and frequency in [82] correspond to frequency and delay in this thesis.

The orthogonality of spheroidal wave functions over two ranges of frequency, one finite and one infinite, and their localisation in both time and frequency suggests application for systems with time limited as opposed to bandlimited formats. The general idea is to consider a time limited pulse which is to some extent localised in frequency such as a rectangular pulse. For modelling the channel the finite frequency range of orthogonality is defined so that a large proportion of the energy of the pulse amplitude spectrum is contained in that range. The infinite range of orthogonality is then utilised assuming

that the low energy of the pulse spectrum outside the finite range means that the overall representation can be of finite dimension. This approach is applicable for continuous phase modulation including minimum shift keying.

3.2.2 Numerical Evaluation

The eigen decomposition implied by the integral equation (3.2) is converted to a matrix equation and solved numerically using a method analogous to the discrete Fourier transform and representing sampling in frequency. The frequency spectrum is divided into an even number, N_f, of segments. The qth point in frequency is $f[q] = -W/2+(q-0.5)W/N_f$. Although slightly less accurate than Simpson's method as used in [22], this approach allows a function inner product to be directly calculated as a vector inner product.

In selecting N_f the consideration is the resulting accuracy of the significant eigenvalues and associated eigenfunctions. The objective is to avoid implicit aliasing in the time domain. When both eigenvalues and eigenfunctions are required then N_f is typically chosen so that the sample spacing is between $0.01/T$ and $0.005/T$. When eigenfunctions are not required N_f can be smaller. The number of significant eigenvalues is chosen so that the ratio of the maximum eigenvalue to the minimum eigenvalue is roughly 10^8. The eigen decomposition is performed with standard software routines. By comparison of computed eigenvalues with those in [82] for the uniform delay profile it is found that an accuracy of 4-5 significant figures is achieved with the numerical method. Any eigenvalues beyond the threshold are less accurate and unlikely to influence calculations since they represent low relative energies.

A more sophisticated numerical method is one involving Gaussian quadrature [75].

Gaussian quadrature is presented as the method of choice for solving Fredholm integral equations in [75]. The integral equation (3.2) considered in this chapter is of this type and homogeneous if $Q = H$.

Note that in the case of a two-ray delay profile there are two elements in the eigen decomposition which can be obtained analytically as the eigenvalues

$$\lambda_{H,0} = \frac{1}{2}(1 + \mathrm{sinc}(2WdT)),\ \lambda_{H,1} = \frac{1}{2}(1 - \mathrm{sinc}(2WdT)), \tag{3.20}$$

and eigenfunctions

$$\Phi_{H,0}(f) = \frac{\cos(2\pi f dT)}{\sqrt{\lambda_0}},\ \Phi_{H,1}(f) = \frac{\sin(2\pi f dT)}{\sqrt{\lambda_1}}. \tag{3.21}$$

3.3 Double Spread Karhunen-Loève Expansion

The double spread KL expansion is based on a decomposition when each transmitted pulse is considered in isolation. This section presents a frequency domain derivation which is closely related to the time domain approach in [43]. The lth received pulse is denoted $v_l(t)$ and is given by

$$v_l(t) = u(t, t - lT). \tag{3.22}$$

The $l = 0$ received pulse is given by

$$v_0(t) = c_T(\xi) \otimes h(t, \xi)\Big|_{\xi=t} \tag{3.23}$$

where $\otimes$ denotes convolution. This has Fourier transform given by

$$\begin{aligned} V_0(f) &= \int_{-\infty}^{\infty}\int_{-\infty}^{\infty} C_T(f')H(f',t)e^{-j2\pi(f-f')t}dtdf' \\ &= \int_{-\infty}^{\infty} C_T(f')G(f',f-f')df' \\ &= \int_{-f_D}^{f_D} C_T(f-\nu)G(f-\nu,\nu)d\nu \end{aligned} \tag{3.24}$$

where $C_T(f)$ is the transmitted pulse amplitude spectrum and $G(f,\nu)$ is the channel output Doppler spread function. The correlation of $G(f-\nu,\nu)$ is derived as

$$E\left[G(f-\nu,\nu)G^*(f'-\nu',\nu')\right] = R_H(f-\nu-(f'-\nu'))R_\rho(\nu)\delta(\nu-\nu'), \tag{3.25}$$

where R_ρ, the Doppler power spectral density, is the Fourier transform of ρ as in (2.14). There is a slight problem with notation here. It is assumed that it is consistent to write $R_H(f,f') = R_H(f-f')$. This is consistent with the three delay profiles defined in Chapter 2 and considered throughout the thesis and justified by the stationary property under the WSSUS assumption. This leads to a full definition for the correlation properties of V_0 which are defined by

$$\begin{aligned} R_V(f,f') &= E\left[V_0(f)V_0^*(f')\right] \\ &= R_H(f-f')\int_{-f_D}^{f_D} C_T(f-\nu)C_T^*(f'-\nu)R_\rho(\nu)d\nu \end{aligned} \tag{3.26}$$

Eigenvalues, $\{\gamma_i\}$, and eigenfunctions, $\{\Psi_i(f)\}$, are defined from the integral equation

$$\int_{-W_D/2}^{W_D/2} R_V(f,f')\Psi_i(f')df' = \gamma_i\Psi_i(f), \tag{3.27}$$

for $i \in \{0,1,\dots\}$ and where $W_D = W + 2f_DT$ is the bandwidth of the received pulse. Since the statistics are WSSUS the lth pulse can be modelled in the same way as the $l=0$ pulse. Thus the lth pulse is given by

$$v_l(t) = \sum_{i=0}^{\infty} x_{R,i,l}\psi_i(t-lT), \tag{3.28}$$

where $x_{R,i,l}$ is the TSC with

$$E\left[x_{R,i,l}x^*_{R,i',l}\right] = \gamma_i \delta_{ii'}. \tag{3.29}$$

The TSCs are zero mean, complex Gaussian random variables with correlation over the symbol index, l.

3.3.1 Numerical Evaluation

The integral in (3.26) can be evaluated using the transfer function of a root raised-cosine pulse shaping filter for C_T. This evaluation is somewhat tedious but comparatively straightforward. The results of the evaluation are not shown since they are piecewise continuous with many cases, over a number of intervals of frequency, and do not in and of themselves provide any insight. The integral equation (3.27) is again converted to a matrix equation by discretisation of the spectrum as in the case of the single spread KL decomposition, replacing W with W_D.

3.4 f-Power Series Expansion

The f-power series expansion is obtained via a Taylor series expansion [48] of the time varying channel transfer function, as [9]

$$H(f,t) = \sum_{i=0}^{\infty} \frac{1}{i!} H^{(i)}(0,t) f^i, \tag{3.30}$$

where $H^{(i)}(f,t)$ denotes the ith partial derivative of $H(f,t)$ with respect to f. This expansion can be written as

$$H(f,t) = \sum_{i=0}^{\infty} x_{S,i}(t)(j2\pi f)^i, \tag{3.31}$$

where $x_{S,i}(t)$ is the ith f-power series TSC given by

$$x_{S,i}(t) = \frac{1}{i!(j2\pi)^i} H^{(i)}(0,t) = \frac{1}{i!(j2\pi)^i} \sum_{n=0}^{\infty} x_{H,n}(t) \Phi_{H,n}^{(i)}(0), \tag{3.32}$$

in terms of the KL expansion TSCs. This definition of the TSC is based on [9] and on obtaining the derivative at $f = 0$ of a single spread KL expansion for the channel transfer function.

The f-power series expansion for the overall CIR is defined as

$$u(t,\xi) = \sum_{i=0}^{\infty} x_{S,i}(t) c^{(i)}(\xi), \tag{3.33}$$

$$U(f,t) = \sum_{i=0}^{\infty} x_{S,i}(t) (j2\pi f)^i C(f), \tag{3.34}$$

where $c^{(i)}(\xi)$ is the ith derivative of $c(\xi)$. The approximate decomposition with finite dimension is obtained by truncation of these series as

$$\widehat{u}(t,\xi) = \sum_{i=0}^{J-1} x_{S,i}(t) c^{(i)}(\xi), \tag{3.35}$$

$$\widehat{U}(f,t) = \sum_{i=0}^{J-1} x_{S,i}(t) (j2\pi f)^i C(f). \tag{3.36}$$

The covariances of the TSCs in terms of the KL expansion are derived from (3.32) and (3.14) as

$$E\left[x_{S,i}(t) x_{S,i'}^*(t')\right] = \frac{1}{i!i'!(j2\pi)^{i+i'}(-1)^{i'}} \sum_{n=0}^{\infty} \lambda_{H,n} \Phi_{H,n}^{(i)}(0) \Phi_{H,n}^{(i')*}(0) \rho(t-t'), \tag{3.37}$$

where $\Phi_{H,n}^{(i')*}(0)$ denotes $\left[\Phi_{H,n}^{(i')}(0)\right]^*$. In addition using (3.10),

$$E[x_{H,i}(t) x_{S,i'}^*(t')] = \frac{1}{i'!(-j2\pi)^{i'}} \lambda_{H,i} \Phi_{H,i}^{(i')*}(0) \rho(t-t'). \tag{3.38}$$

Derivatives of the eigenfunctions are required in (3.37) and (3.38). Rearranging and differentiating (3.2) gives

$$\Phi_{H,n}^{(i)}(f) = \frac{1}{\lambda_{H,n}} \int_{-W/2}^{W/2} R_H^{(i)}(f, f') \Phi_{H,n}(f') df', \tag{3.39}$$

where $R_H^{(i)}(f, f')$ denotes the ith partial derivative of $R_H(f, f')$ with respect to f. This allows evaluation of the eigenfunction derivatives numerically which is necessary for most delay profiles.

3.5 Mean Squared Error of Approximation

A measure of the approximation error for the truncated series expansions is the mean squared error of approximation defined as

$$\text{MSE} = \int_{-W/2}^{W/2} E\left[|U(f,t) - \widehat{U}(f,t)|^2\right] df, \tag{3.40}$$

where $\widehat{U}$ is the truncated series expansion. It has J terms indexed from 0 to $J-1$. For a matched KL expansion the MSE is given by

$$\text{MSE} = 1 - \sum_{i=0}^{J-1} \lambda_{Q,i} \int_{-W/2}^{W/2} |Z_{Q,i}(f)|^2 df, \tag{3.41}$$

where $Q \in \{H, U\}$. In the case $Q = U$ the expression is simply

$$\text{MSE} = 1 - \sum_{i=0}^{J-1} \lambda_{U,i}. \tag{3.42}$$

The mean squared error (MSE) of approximation is shown in Figure 3.3 for the two-ray channel delay profile and in Figure 3.4 for the uniform channel delay profile. The graphs illustrate the fact that a greater number of terms in the expansion and a smaller delay

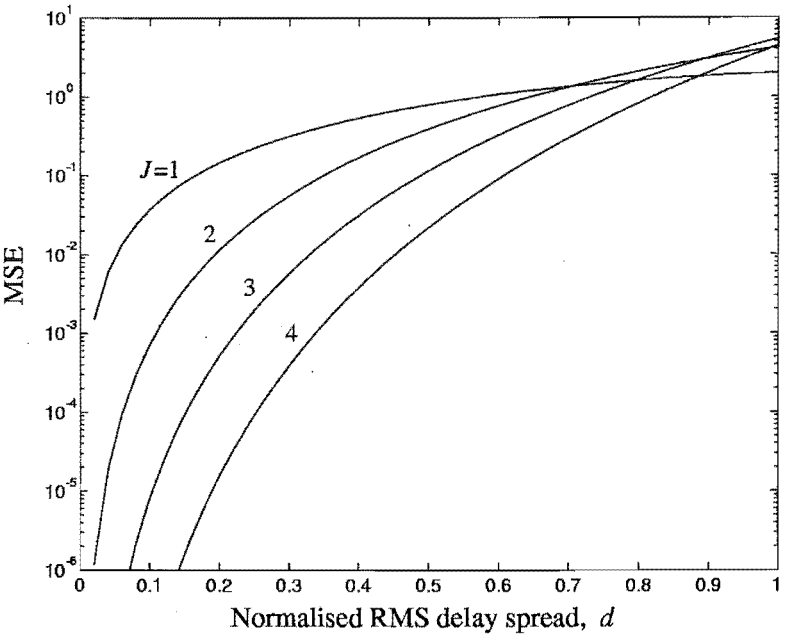

Figure 3.3: Mean squared error of approximation vs normalised RMS delay spread for two-ray delay profile and f-power series expansion.

spread both imply a smaller MSE, i.e. a better fit to the overall CIR. Figure 3.5 illustrates the fact that incorporating the pulse shape directly in the decomposition leads to a slightly more efficient representation. The crossover of the curves in Figure 3.3 for a two-ray delay profile with large d is counter intuitive but given that the eigen decomposition is available in closed form the calculation can be performed without numerical error and the effect confirmed.

The accuracy of the representation ultimately affects the performance of a receiver and this is investigated further in Chapter 5. The impact on the performance of MLSE when the receiver has a finite number of the terms in a decomposition is considered.

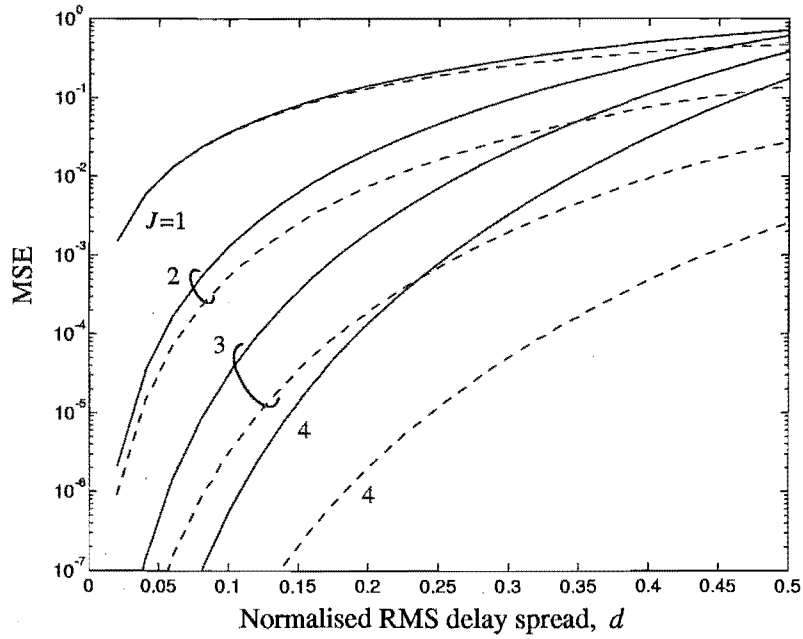

Figure 3.4: Mean squared error of approximation vs normalised RMS delay spread for uniform delay profile, f-power series (solid lines) and single spread KL (dashed lines) expansions.

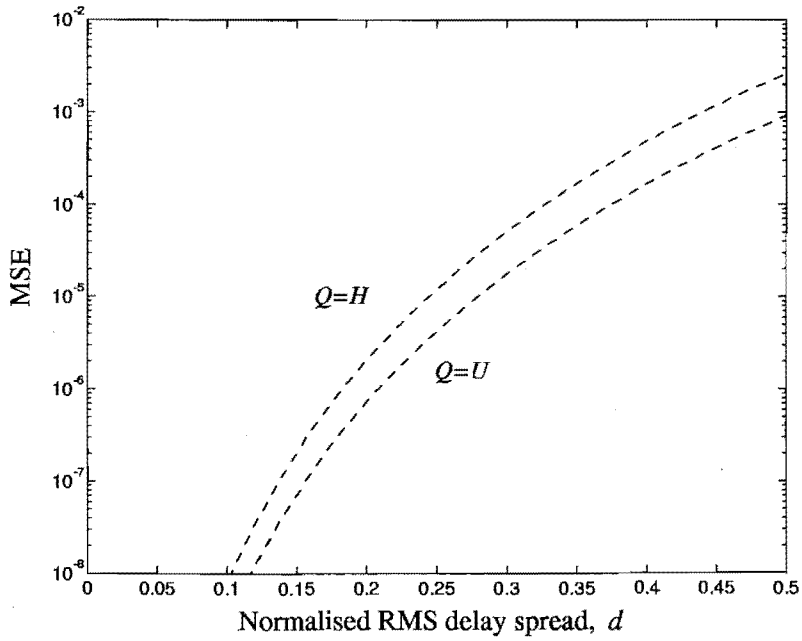

Figure 3.5: Mean squared error of approximation vs normalised RMS delay spread for uniform delay profile, single spread KL expansions for $Q = H$ and $Q = U$ with $J = 4$.

3.6 Summary

Three channel decompositions have been developed in this chapter. Where there is an original enhancement of the models this has been noted. All of the decompositions are applicable to the modelling of fast fading channels. It is clear from quantifying the mean squared error of approximation that the models are essentially finite dimensional with the dimension depending on the delay spread for a single spread KL expansion. This decomposition may have an underlying model that is mismatched to the channel with respect to its second order statistics. The shape of the eigenfunctions varies to some extent as the delay spread is increased. Orthonormalised Legendre polynomials are the limiting case for a uniform delay profile as the channel becomes frequency non-selective or d tends to zero. These functions still form an effective basis for channels with moderate delay spreads. The next four chapters illustrate applications of the channel decompositions.

Chapter 4

Pulse Shaping

Intersymbol interference (ISI) occurs during transmission over wireless channels as a result of fading and dispersion. A drive towards system bandwidth compression has resulted in a need for sophisticated equalisation to avoid degradation of the bit error rate [76]. Some approaches to equalisation were presented in Chapter 2 and it is generally accepted that equalisation is required to combat the effects of time dispersion. However, the use of bandwidth expansion combined with proper design can, under specific conditions produce a system with no significant ISI at the output of a receiver front-end filter. The approach dramatically lessens the need for, or complexity of, equalisation. Increasing the bandwidth of the filters typically leads to greater concentration in time and therefore less ISI. In addition, the ISI can be reduced further by ensuring that the pulse shape has low levels in the vicinity of the non-peak sampling points. This approach is particularly effective at low delay spreads with modest bandwidth expansion. Also associated with the approach are an extended range of validity for a slow fading assumption and increased stability and robustness of symbol timing recovery.

The f-power series is used in [56] to find the optimum bandlimited pulse shaping filters for a linearly frequency selective channel. The result is the sinc squared pulse which represents 100% excess bandwidth. In [59] the approach for the linearly frequency selective channel is extended to the case where two receiver filters are implemented in a binary DPSK system. The aim is to recover energy from the second term of the f-power series decomposition of the channel and to mitigate ISI through fixed ratio combining.

In this chapter it is shown that the original result for a linearly frequency selective channel can be extended to channels that have a polynomial transfer function with the penalty of further bandwidth expansion. It turns out that the appropriate pulse shaping filters are based on taking powers of an underlying Nyquist pulse.

Under certain circumstances there is an advantage in using orthogonal expansions to replace the f-power series expansion. Specifically, when the delay spread is sufficiently large there are efficiency gains in terms of the accuracy as a function of dimension as shown in Chapter 3 and explored further in Chapter 5. For slow fading dispersive channels the single spread KL expansion can be applied to the problem of pulse shaping with the aim of minimising the ratio of the mean peak-sample energy to mean residual ISI energy.

A performance evaluation for powers of sinc pulses is presented in this chapter, investigating the extent to which the need for equalisation can be lessened and the stability of timing recovery increased. The Gaussian distribution is employed to model the probability density function of the ISI. For the assessment of timing offset estimation the modified Cramér-Rao bound (MCRB) [68, 28] is used.

In [56] calculus of variations was employed to show that the sinc squared shaped pulse is the optimum bandlimited pulse shape for a slow fading, linearly frequency selective

channel. For a power series with two terms, representing the channel, the condition over $0 \leq f \leq 1/T$ for the transfer function of the optimum pulse shape, $C(f)$, reduces to an Euler equation. The optimum pulse is

$$C(f) = \begin{cases} T(1 - |f|T), & |f| \leq 1/T \\ 0, & \text{otherwise} \end{cases} \tag{4.1}$$

This is a sinc squared shaped pulse in the time domain. For a linearly dispersive channel ISI is completely eliminated.

4.1 Application of Channel Decomposition

In this section the idea of designing pulse shaping and receiver filters with the aid of channel decompositions is explored further. The f-power series and single spread KL expansions are employed. A generalisation of the sinc squared result follows. Powers of Nyquist shaped pulses eliminate ISI in slow fading channels that have a polynomial transfer function. This can be seen by examining the derivatives of the pulse shape. Assuming the channel transfer function is polynomial of order $K-1$, the f-power series expansion of (3.36) has $J = K$ terms. The overall filter is constructed as

$$c(t) = b^K(t), \tag{4.2}$$

where $b^K(t)$ denotes the Kth power of $b(t)$, a bandlimited Nyquist pulse shape. It follows, by application of the chain and product rules of differentiation, that $c^{(i)}(t)$ is zero at the non-peak sampling points for $i \in \{0, 1, \ldots, K-1\}$. Hence the overall CIR has the property $u(kT, (k-l)T) = 0$ for $k, l \in \mathbb{Z}$, $k \neq l$. That is, ISI is eliminated at the sampling points $t = kT$.

To justify the assertion in more detail it can be seen that $c(t)$ is a finite energy bandlimited signal with frequency spectrum

$$C(f) = \overset{K-1}{\underset{n=1}{\otimes}} B(f), \tag{4.3}$$

where the notation on the right hand side indicates the $(K-1)$-fold convolution of $B(f)$ with itself. Any finite energy bandlimited signal is continuously differentiable as many times as required and the ith derivative of $c(t)$ can be written as

$$c^{(i)}(t) = b^{K-i}(t)b_i(t), \tag{4.4}$$

where, for the first two cases, $b_0(t) = 1$, $b_1(t) = Kb^{(1)}(t)$. Thus

$$\begin{aligned} c^{(i+1)}(t) &= b^{K-(i+1)}(t)\left[(K-i)b_i(t) + b(t)b_i^{(1)}(t)\right] \\ &= b^{K-(i+1)}(t)b_{i+1}(t), \end{aligned} \tag{4.5}$$

that is, $b(t)$ is a factor of $c^{(i)}(t)$ provided $i \in \{0, \ldots, K-1\}$ and the result follows.

Since the transfer function of a generalised dispersive or frequency selective channel can be approximated as polynomial it follows that the use of powers of Nyquist shaped pulses implies reduced ISI in the receiver. Viewed another way, the pulses are resistant to ISI because they have decreasingly low levels near the non-peak sampling points as well as being increasingly localised in time. The drawback of the approach is that increasing K implies a greater bandwidth requirement. For powers of raised-cosine shaped pulses each increment in K implies an increase of $(1+\alpha)/T$ in the two-sided bandwidth where α, the rolloff factor, has range $0 \leq \alpha \leq 1$. The total two-sided bandwidth is $W = K(1+\alpha)/T$.

This result begs the question of whether it is possible to design other pulses for near ISI free transmission in dispersive channels. For example, scaling Nyquist pulses in time

gives increasingly narrow pulses. In what follows, optimised pulses are derived for a fixed bandwidth expansion factor using a KL decomposition of the slow fading dispersive channel. The single spread KL expansion can be employed in place of the f-power series for application to pulse shaping. QPSK is assumed with uncorrelated symbols so that

$$E\left[a_l a_{l'}^*\right] = E_s \delta_{ll'}. \tag{4.6}$$

A received sample, y_k, is defined as if there were no noise as

$$y_k = \sum_{l \in \mathbb{Z}} a_l u(kT, (k-l)T), \tag{4.7}$$

and an ideal sample with no ISI as

$$\hat{y}_k = a_k u(kT, 0). \tag{4.8}$$

The error is $e_k = y_k - \hat{y}_k$. The mean residual ISI energy, averaged over the data, is denoted σ_e^2 and given by

$$\sigma_e^2 = \sigma_r^2 - \sigma_s^2, \tag{4.9}$$

where

$$\sigma_r^2 = E_s \sum_{l \in \mathbb{Z}} |u(kT, (k-l)T)|^2, \tag{4.10}$$

$$\sigma_s^2 = E_s |u(kT, 0)|^2. \tag{4.11}$$

The mean residual ISI energy, averaged over the data and channel ensemble, is denoted σ_f^2 and given by

$$\sigma_f^2 = \sigma_t^2 - \sigma_u^2, \tag{4.12}$$

where

$$\sigma_t^2 = E\left[\sigma_r^2\right], \tag{4.13}$$

$$\sigma_u^2 = E\left[\sigma_s^2\right]. \tag{4.14}$$

Using Poisson's sum formula [46] it follows that

$$\sigma_t^2 = \frac{E_s}{T}\sum_{l\in\mathbb{Z}} R_H\left(\frac{l}{T}\right)\int_{-W/2}^{W/2} C(f)C^*\left(f-\frac{l}{T}\right)df, \tag{4.15}$$

$$\sigma_u^2 = E_s\int_{-W/2}^{W/2}\int_{-W/2}^{W/2} C(f)R_H(f-f')C^*(f')df'df. \tag{4.16}$$

There is the same misuse of notation for the argument of R_H as employed in Chapter 3.

The optimised pulse shape is obtained by maximising the ratio σ_u^2/σ_t^2 which is the mean peak sample energy to mean residual ISI energy ratio, denoted SIR. Expressing $C(f)$ in terms of the eigenfunctions in a single spread KL expansion gives

$$C(f) = \sum_{i=0}^{\infty} c_i\Phi_{H,i}(f), \tag{4.17}$$

where c_i is the ith coefficient of the optimised pulse shape. The coefficients are collected in vector form as

$$\mathbf{c} = (c_0, c_1, \ldots, c_{J-1})^\dagger, \tag{4.18}$$

where the dimension of the channel decomposition is assumed to be essentially limited to J and $\dagger$ denotes Hermitian transpose. It can be seen that the problem amounts to finding the coefficient vector $\mathbf{c}$ which maximises the quantity

$$\text{SIR} = \frac{\mathbf{c}^\dagger\mathbf{B}\mathbf{c}}{\mathbf{c}^\dagger\mathbf{C}\mathbf{c}}, \tag{4.19}$$

where

$$\mathbf{C} = \mathbf{A} - \mathbf{B}. \tag{4.20}$$

Substituting (4.17) into (4.15), (4.16) and using (3.2) in the case of (4.16) the elements of matrices $\mathbf{A}$ and $\mathbf{B}$ are given by

$$A_{ii'} = \frac{1}{T}\sum_{l\in\mathbb{Z}} R_H\left(\frac{l}{T}\right)\int_{-W/2}^{W/2} \Phi_{H,i}(f)\Phi^*_{H,i'}\left(f-\frac{l}{T}\right)df, \tag{4.21}$$

$$B_{ii'} = \lambda_{H,i}\delta_{ii'}. \tag{4.22}$$

The ratio (4.19) can be maximised under an assumption that the matrix $\mathbf{C}$ is strictly Hermitian positive definite. The Hermitian property of $\mathbf{C}$ is true by inspection of (4.21) and (4.22) and using the property

$$R_H(f-f') = R^*_H(f'-f), \tag{4.23}$$

which is the case for the delay profiles considered. This property is required in order that $\mathbf{C}$ be unitarily diagonalisable [2]. The strictly positive definite property of $\mathbf{C}$ is true by virtue of the fact that for the delay profiles considered with non-zero delay spread, the mean residual ISI energy, $\sigma_f^2 = \mathbf{c}^\dagger\mathbf{C}\mathbf{c}$, is positive unless $\mathbf{c} = \mathbf{0}$. This property is required in order that all of the eigenvalues of $\mathbf{C}$ be positive.

With the stated assumption there exists a diagonal matrix, $\mathbf{D}$, with positive real diagonal elements and a rotation matrix, $\mathbf{P}$, such that

$$\mathbf{C} = \mathbf{P}\mathbf{D}\mathbf{P}^\dagger. \tag{4.24}$$

Letting $\mathbf{E}^2 = \mathbf{D}$, $\mathbf{X} = \mathbf{E}\mathbf{P}^\dagger$, $\mathbf{Y} = \mathbf{X}^{-1}$ and $\mathbf{c} = A_c\mathbf{Y}\mathbf{x}$ the quantity to be maximised can be written as

$$\text{SIR} = \frac{\mathbf{x}^\dagger(\mathbf{Y}^\dagger\mathbf{B}\mathbf{Y})\mathbf{x}}{\mathbf{x}^\dagger\mathbf{x}}. \tag{4.25}$$

The solution $\mathbf{y}$ is the eigenvector of $\mathbf{Y}^\dagger\mathbf{B}\mathbf{Y}$ corresponding to the maximum eigenvalue and the optimum SIR is that eigenvalue [72]. The vector $\mathbf{c}$ can be multiplied by the constant A_c without altering the ratio (4.19). Defining a vector $\mathbf{g}$ with elements

$$g_i = \int_{-W/2}^{W/2} \Phi^*_{H,i}(f)df, \tag{4.26}$$

it follows that the desired solution is given by $\mathbf{c} = A_c\mathbf{Y}\mathbf{y}$ with

$$A_c = \frac{1}{\mathbf{g}^\dagger\mathbf{Y}\mathbf{y}}, \tag{4.27}$$

where the constant A_c is set to ensure that the overall pulse shape is consistent with unit energy for the transmitter pulse shape.

If it is required to support moderate to large delay spreads then one approach is to allow a small number, L, of symbols to contribute to ISI and minimise the residual ISI due to other symbols. The matrix $\mathbf{B}$ can be generalised with elements set as

$$B_{ii'} = \lambda_{H,i}\delta_{ii'} + \sum_{l=1}^{L}\int_{-W/2}^{W/2}\int_{-W/2}^{W/2} \Phi_{H,i}(f)R_H(f-f')e^{j2\pi(f-f')lT}\Phi^*_{H,i'}(f')df'df. \tag{4.28}$$

The envelope of the overall pulse shape is effectively Nyquist given sufficient bandwidth for the delay spread. However, there is a time shift resulting in the peak being moved away from $t = 0$. This must be taken into account in normalising $C(f)$ and splitting the overall filter between transmitter and receiver.

Additive noise is left out of the optimisation. The solutions apply in situations where ISI is potentially the dominant form of interference. Once the SIR has reached roughly

the level of the SNR further reductions in ISI do not lead to performance gains. The approach leads to overall pulse shapes which are near Nyquist given sufficient bandwidth expansion for the assumed delay spread.

A uniform delay profile is assumed in the performance evaluation to follow. This represents a worst case Rayleigh fading dispersive channel in the sense that the energy level of the channel at the maximum delay is the same as that at zero relative delay. In addition there is an analogy between the maximum frequency in the sampling theorem and the maximum delay in the dispersive channel. This is of interest from a theoretical perspective.

In practice the delay profile is typically exponential and often there is a non-zero mean or line-of-sight component. The approach described in this chapter, involving some bandwidth expansion, generally leads to more robust performance in a variety of dispersive environments.

4.2 Performance Evaluation

To illustrate the potential of powers of Nyquist shaped pulses the performance of a system employing them is evaluated. The system involves a slow fading dispersive channel. Powers of sinc shaped pulses are considered by way of example, i.e. the underlying pulse is defined as

$$b(t) = \text{sinc}(t/T). \tag{4.29}$$

Figure 4.1 shows the transfer functions of the filters corresponding to different values of exponent, K.

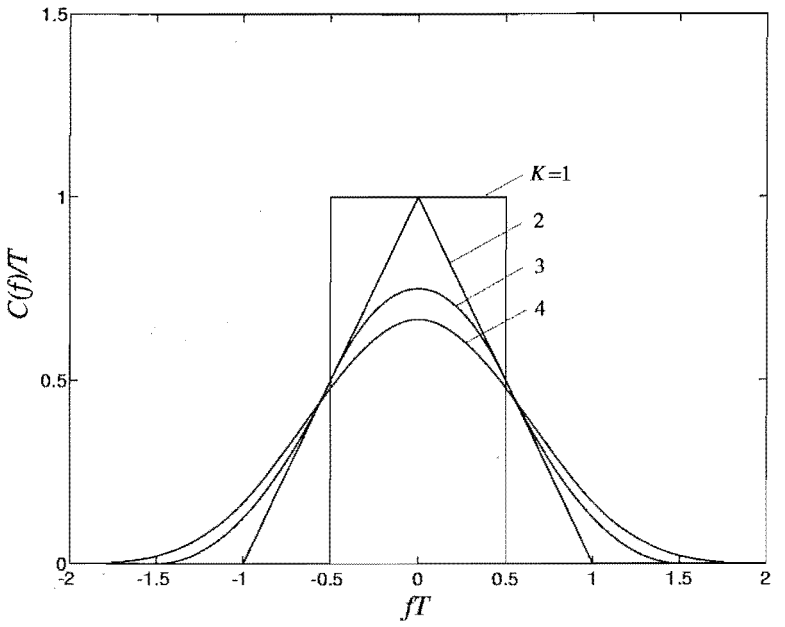

Figure 4.1: Transfer functions of power of sinc pulse shaping filters.

Concerning the optimisation procedure, it has been found that when the delay spread is low, $d_1 < 1$, accurate results are obtained using a basis of Legendre polynomials. This represents a fixed basis, independent of the delay spread. Matrices **A** and **B** are modified accordingly. Specifically, this requires substituting orthonormalised Legendre polynomials in place of the KL eigenfunctions in (4.17) and obtaining alternative forms of (4.21), (4.22) from (4.15), (4.16).

Assuming a Gaussian model of ISI and given a channel from the ensemble, the bit error rate (BER) for QPSK is upper bounded as [46]

$$\text{BER} < \exp\left(-\frac{1}{2}\frac{\sigma_s^2}{\sigma_e^2 + N_0}\right). \tag{4.30}$$

This assumes a coherent phase reference which is not always available. Differential encoding and detection may be one option to remove the need for estimating the channel and carrier phase.

The modified Cramér-Rao bound (MCRB) [68, 28] offers a method for quantifying the performance improvement in timing recovery that can be obtained using powers of Nyquist shaped pulses. The essence of the MCRB is to take an unbiased estimate, $\hat{\lambda}$, of a synchronisation parameter λ, i.e.

$$E\left[\hat{\lambda}\right] = \lambda, \tag{4.31}$$

and find a lower bound on the variance as

$$\mathrm{Var}\left[\lambda - \hat{\lambda}\right] \geq \mathrm{MCRB}(\lambda). \tag{4.32}$$

For BPSK timing recovery the MCRB for a timing offset τ is given by [68, 28]

$$\mathrm{MCRB}(\tau) = \frac{T^3}{8\pi^2 T_0 A_\tau E_b/N_0}, \tag{4.33}$$

where T_0 is the interval of the timing estimate and A_τ is given by

$$A_\tau = T^2 \int_{-W/2}^{W/2} f^2 C(f) df. \tag{4.34}$$

4.3 Numerical Results and Discussion

Figure 4.2 shows the eye diagram for the sinc pulse and Figure 4.3 for the 4th power of the sinc pulse. Values of σ_u^2 and σ_f^2, computed for the powers of sinc shaped pulses, are shown in table 4.1. This illustrates that the ISI is reduced for higher powers of the underlying sinc shaped pulse.

When the optimisation described above is implemented for a uniform delay profile with a bandwidth expansion factor of 4, the transfer functions of the overall pulse shapes are as shown in Figure 4.4.

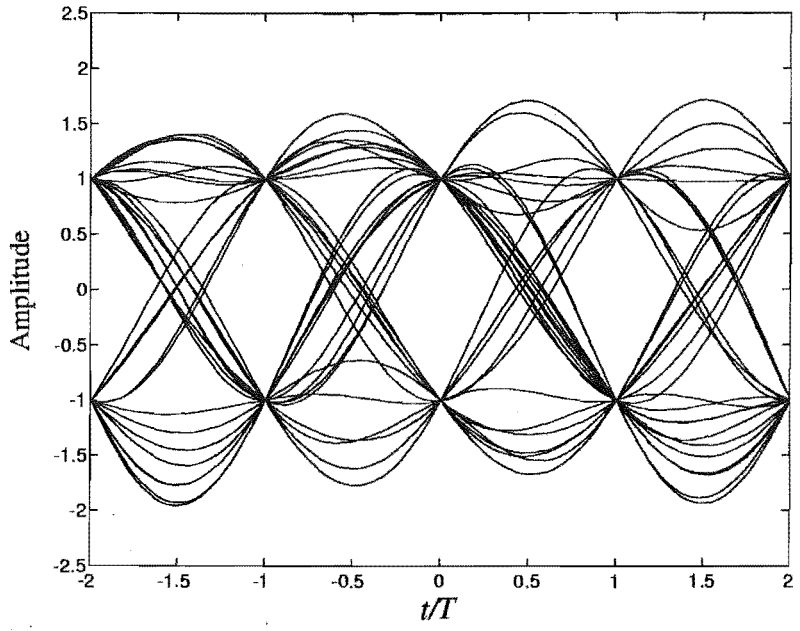

Figure 4.2: Eye diagram for the sinc pulse shape.

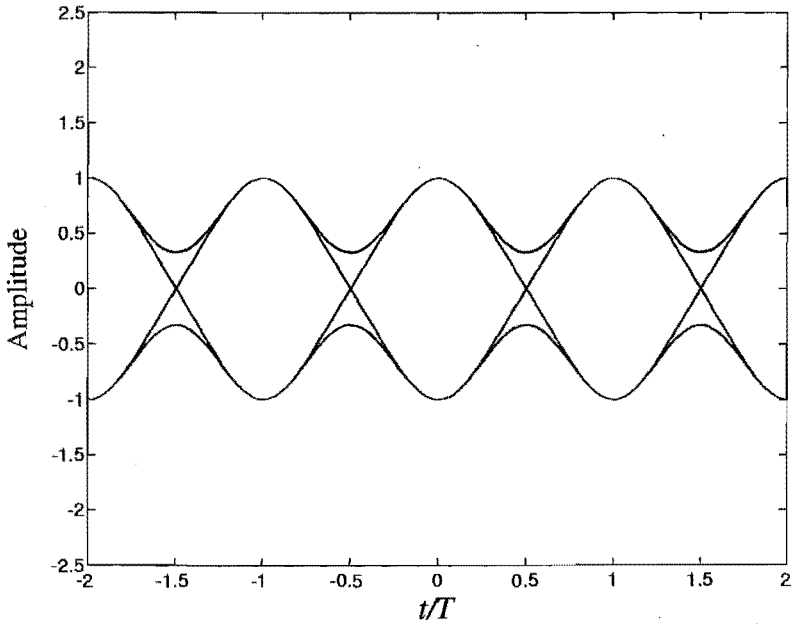

Figure 4.3: Eye diagram for 4th power of the sinc pulse shape.

Exponent, K	σ_u^2/E_s	σ_f^2/E_s	SIR (dB)
1	0.93	6.5×10^{-2}	12
2	0.88	1.9×10^{-3}	27
3	0.83	1.0×10^{-4}	39
4	0.78	6.8×10^{-6}	51

(a) $d_1 = 0.5$

Exponent, K	σ_u^2/E_s	σ_f^2/E_s	SIR (dB)
1	0.77	2.3×10^{-1}	5
2	0.63	3.3×10^{-2}	13
3	0.54	9.2×10^{-3}	18
4	0.48	2.9×10^{-3}	22

(b) $d_1 = 1$

Table 4.1: Residual ISI, σ_f^2 and σ_u^2 for Kth power of sinc shaped pulses with two values of d_1.

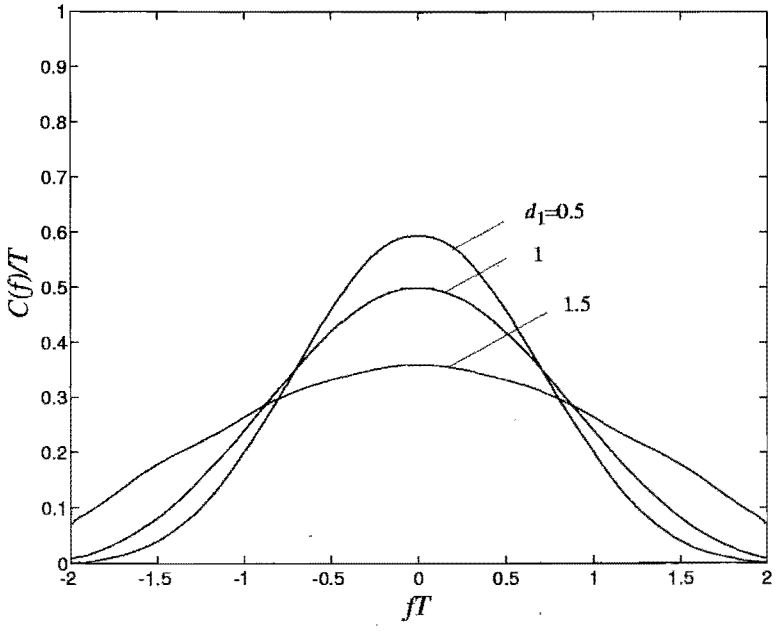

Figure 4.4: Transfer functions of optimised pulse shaping filters.

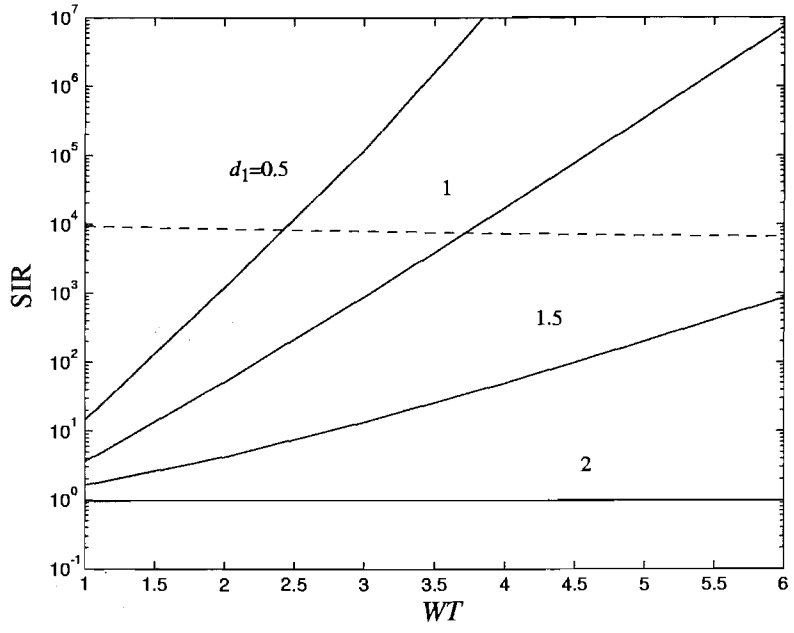

Figure 4.5: Signal to ISI ratio for optimised pulse shaping (solid lines) and average signal to noise ratio for $d_1 = 0.5$ with a nominal signal to noise ratio of 40dB (dashed line).

The optimisation process seeks to spread the transfer function out over the available spectrum to the point where the filters are unrealisable if the bandwidth expansion is insufficient for the given delay spread. However, if there is sufficient bandwidth expansion the resulting pulse has been found to be realisable and near Nyquist. In Figure 4.5 the SIR, which is the ratio of the mean peak-sample energy to mean residual ISI energy, is shown as a function of bandwidth expansion. The SIR in dB turns out to be a near linear function of the allocated bandwidth, W. If the total delay spread is less than $2T$ then ISI can be effectively eliminated. All results in this section are obtained with $N_f = 100WT$.

The SIR for powers of sinc pulses is similar to that for the optimised pulses. Figure 4.6 shows the transfer function of the optimised pulse for $d_1 = 0.5$ compared to that for the 4th power of sinc pulse and Figure 4.7 shows the SIR of optimised pulses and power of sinc pulses as a function of allocated bandwidth. A variation on the approach is to assume

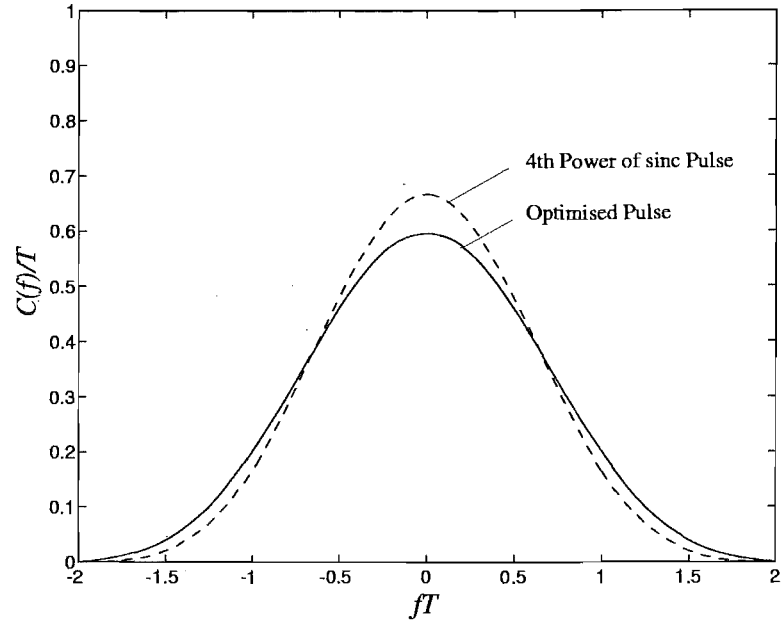

Figure 4.6: Transfer functions of optimised pulse shaping filter for $d_1 = 0.5$ and 4th power of sinc pulse.

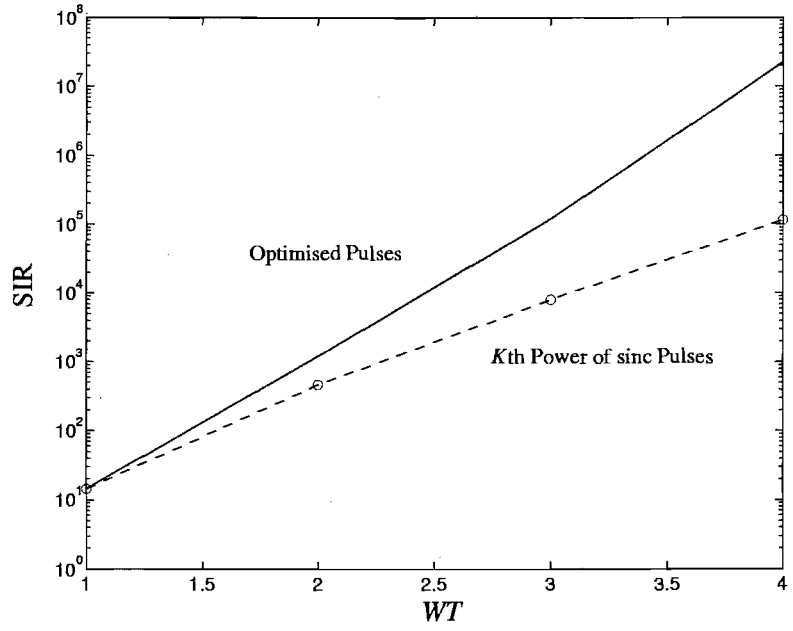

Figure 4.7: Signal to ISI ratio for optimised pulse shaping (solid line) and Kth power of sinc pulses (dashed line), $d_1 = 0.5$.

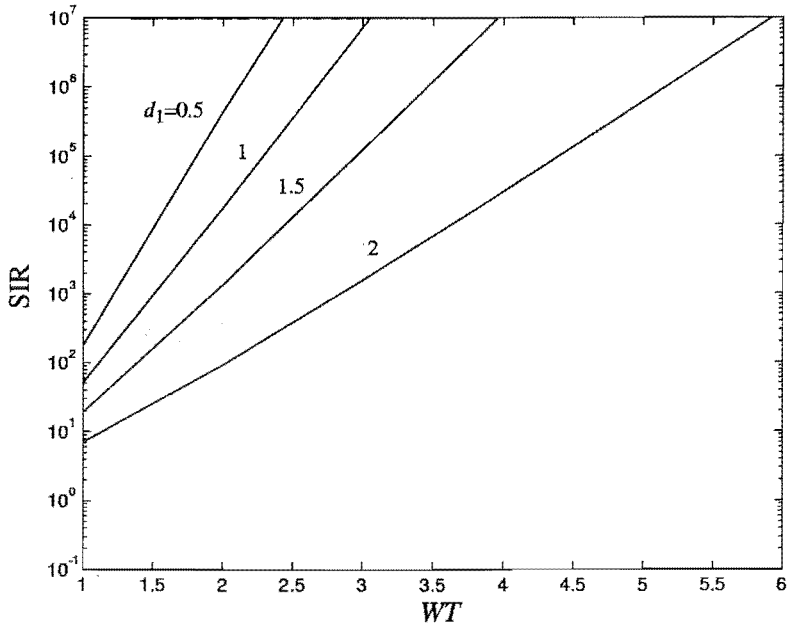

Figure 4.8: Signal to residual ISI ratio for optimised pulse shaping with one symbol of assumed ISI.

that there is a small number of symbols contributing to allowed ISI. If there is one symbol of allowed ISI then the SIR is shown in Figure 4.8. In practical terms this allows, for example, the Viterbi algorithm to be used for equalisation with fewer states than otherwise for the given delay spread. With 16-QAM a 16 state Viterbi algorithm is required and implemented with symbol spaced samples in the metric calculations. Ignoring symbol timing and carrier frequency offsets, and for the joint detection of a desired QPSK signal and two dominant co-channel interferers the approach allows suboptimal MLSE with 64 states.

Figure 4.9 illustrates the outage probability or bit error rate distribution for a bandwidth expansion factor of 4, with a delay spread of $d_1 = 1$, using QPSK and with $E_b/N_0 = 40$dB. The energy per bit, E_b, is related to the symbol energy as $E_s = 2E_b$. For this combination of bandwidth and delay spread there is a significant performance gain

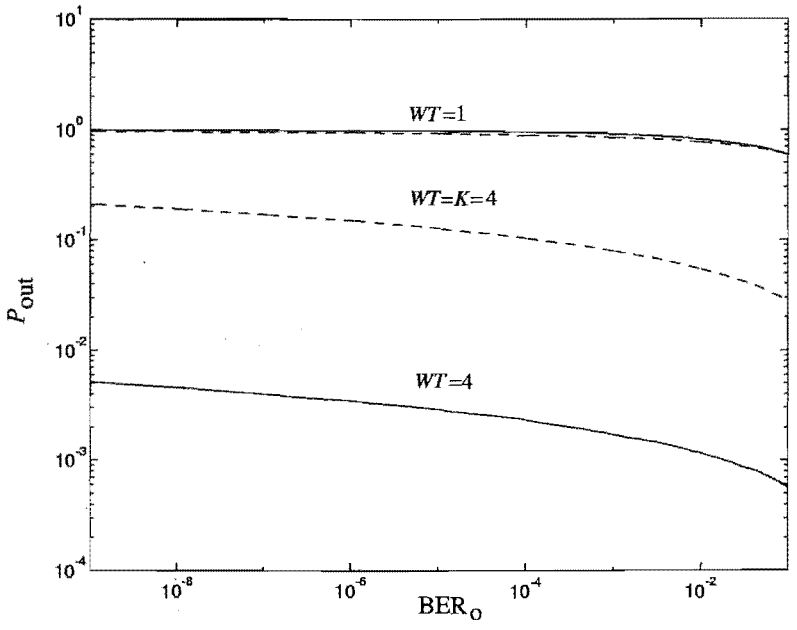

Figure 4.9: BER distribution of QPSK for optimised pulses (solid lines) and powers of sinc pulses (dashed lines) with $d_1 = 1$ and $E_b/N_0 = 40$dB.

using the optimised pulses without equalisation. The filters are close to realisable. In other words, the filters could be implemented with small changes or by a further small increase in the allocated bandwidth. The optimisation process maximises the ratio of mean energies rather than the mean of the energy ratio. The fact that σ_u^2 remains roughly constant with increasing bandwidth justifies the method to some extent, as does Figure 4.9 in which the bound on the BER is computed for at least 10^5 channels from the ensemble for each curve. The figure demonstrates the inherent immunity to ISI which results from the use of excess bandwidth and optimised pulse shaping. It emphasises the fact that for certain delay profiles the optimised pulses outperform the powers of sinc pulses. However both imply a lessening of the need for equalisation.

For the powers of sinc shaped pulses, $1/A_\tau$ in the MCRB for a timing offset estimate takes the values shown in table 4.2. This suggests that the final variance would be as

Exponent, K	Parameter, $1/A_\tau$
1	12
2	6
3	4
4	3

Table 4.2: Parameter $1/A_\tau$ in the modified Cramér-Rao bound on a timing offset estimate for powers of sinc pulses.

low as 25% of the initial variance in going from the first to the 4th power of the sinc shaped pulse. The parameter $1/A_\tau$ for powers of raised-cosine shaped pulses is shown in Figure 4.10. The results are relatively insensitive to rolloff, α, for $K \geq 2$ but $1/A_\tau$ decreases as K increases. The slope of the pulse shape decreases near the sampling points as K increases and this increases stability in timing recovery. The MCRB of a timing offset estimate is shown in Figure 4.11 for powers of sinc shaped pulses with a 20 symbol interval for estimation. At a given value of E_b/N_0 there are performance gains for higher powers of the underlying sinc shaped pulse. All results in this section are for BPSK.

Corresponding results relating to timing offset estimation for the optimised pulses can be obtained by numerical integration. Although not shown here the behaviour is similar to that for the powers of Nyquist pulses. A larger bandwidth leads to a smaller variance of the timing offset estimate for optimised pulses at a given delay spread. It would be worthwhile to investigate the effect on timing recovery of bandwidth expansion in the presence of dispersion.

It is also possible to overlap adjacent channels within an OFDM structure along the lines in [15] although the carrier frequency spacings need to be greater than $1/T$. In particular, the spacings are required to be sufficient to ensure that each band has at most

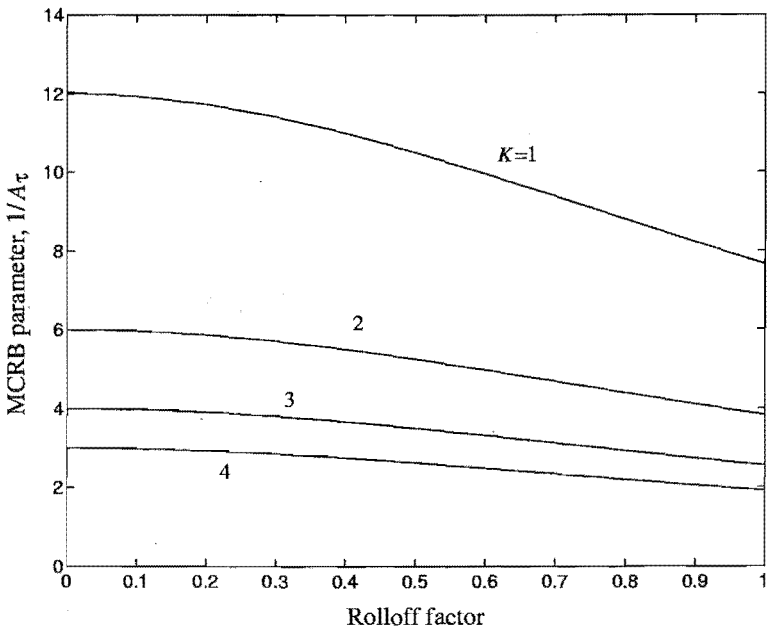

Figure 4.10: MCRB parameter, $1/A_\tau$, versus rolloff factor, α, for timing offset estimates with Kth power of raised-cosine pulses.

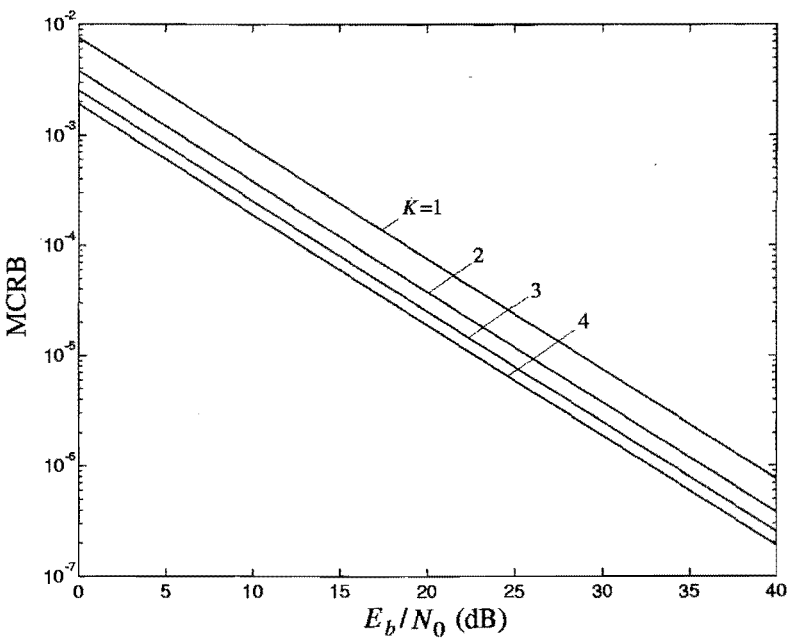

Figure 4.11: MCRB versus E_b/N_0 for the variance of timing offset estimates with Kth power of sinc pulses.

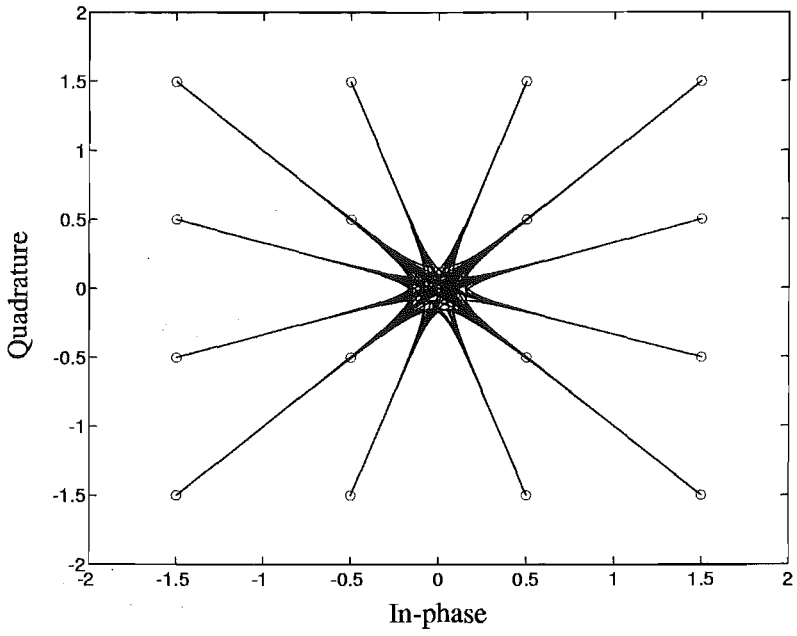

Figure 4.12: Amplitude-phase diagram of 16-QAM with an optimised pulse for $WT = 6$ and $d_1 = 0.25$.

one overlapping band on each side.

The results in this section are oriented towards BPSK and QPSK. Another line of development is to consider higher order modulation formats such as 16-QAM. Figure 4.12 shows the amplidtude and phase for 16-QAM with an optimised pulse. The pulse is optimised with $WT = 6$ and $d_1 = 0.25$ assumed. The optimisation leads to an amplitude-phase characteristic that is well contained. It may be possible to exploit this property to lessen the need for equalisation and to simplify other aspects of receiver design. Since 16-QAM is a modulation format of higher order than BPSK or QPSK there is some scope for using excess bandwidth without sacrificing throughput vs bandwidth efficiency.

Given pulse shaping as described in this chapter, differential encoding and synchronised OFDM at a transmitting base station the mobile receiver is extremely simple. The receiver functions required are demodulation and double filtering [59] and timing offset es-

timation. The second filter can be optimised using a similar method to the one described above for the overall pulse shape and taking $c_T(t)$ as given by the first optimisation. Specifically, it is necessary to take into account the desired odd symmetry of the transfer function of the second filter. The way to do this is to effectively replace the basis functions of the CIR with their Hilbert transforms.

Considering the mobile-to-base link, it is assumed that the receiving base station has antenna diversity and can perform a more complex set of functions. The transmitting mobile may then implement constant envelope modulation. There may be advantages in employing different formats on the base-to-mobile and mobile-to-base links to shift the complexity and power consumption away from the mobile unit and place more of the burden of both links at the base station.

4.4 Summary

The approach taken in this chapter is useful in situations involving dispersive channels where a system with low complexity is required. It may be possible to implement a wireless communication system without equalisation and the associated need for CSI estimation depending on the delay spread and the availability of excess bandwidth and explicit diversity. Taking a different line it may be possible to preserve bandwidth efficiency by allowing some bandwidth expansion in combination with the use of higher order modulation formats such as 16-QAM.

Chapter 5

Equalisation

For systems emloying traditional pulse shaping, equalisation is required, including the estimation of channel state information (CSI). CSI in this context refers to the instantaneous channel impluse response (CIR) or its Fourier transform, the channel transfer function. In the equalisation of a received signal there is the parallel task of estimating the CSI. For a slow fading channel this is typically done by sending a training sequence and then subsequently tracking the channel with a least mean square algorithm [77]. When using the Viterbi algorithm for MLSE with a fast fading channel, the CSI can be estimated by per-survivor processing [24, 78].

It is desirable to select a structure for modelling the CSI which simplifies the estimation process. The traditional approach is to store a time selective coefficient (TSC) for each tap in the overall CIR, which is modelled as a tapped delay line, and is the convolution of the transmitter pulse shape with the CIR. The number of TSCs is equal to the length of the overall CIR in symbols times the number of receiver samples per symbol. Typically, ten or more TSCs are required. An alternative approach is to use a channel decomposition, the

aim being to reduce the number of TSCs and thereby the complexity of CSI estimation. Results in [31] suggest that decompositions with as few as three TSCs can provide support for channels with reasonably large delay spreads.

5.1 Application of Channel Decomposition

Given that there are advantages in utilising channel decompositions for modelling CSI it is appropriate to investigate and quantify their applicability within the context of equalisation. This chapter studies this problem on the assumption that a receiver has perfect knowledge of a finite dimensional channel decomposition given a full channel specification. This is intended to illustrate that it is valid to truncate an expansion but that there are limits on the channel delay spread that can be supported with a finite number of TSCs. The result is a lower bound on the performance of adaptive receivers employing a decomposition with finite dimension.

The receiver evaluated in this chapter has approximate CSI in the sense that the first J terms of the decomposition are known and employed. The metric to be minimised for maximum likelihood sequence estimation (MLSE), as developed in Chapter 2, is given by

$$\sum_{k\in\mathbb{Z}} \left| y(kT_r) - \sum_{l\in\mathbb{Z}} \hat{a}_l \hat{u}(kT_r, (k-lr)T_r) \right|^2, \tag{5.1}$$

where $\hat{a}_l$ is an hypothesised symbol. Under the assumption of AWGN, this simple squared distance metric leads to the same performance as the optimum receiver structure described in [44] which is based on a time varying matched filter.

The above metric with a truncated f-power series expansion can be written as

$$\sum_{k\in\mathbb{Z}}\left|y(kT_r)-\sum_{i=0}^{J-1}x_{S,i}(kT_r)\left[\sum_{l\in\mathbb{Z}}\hat{a}_l c_T^{(i)}((k-lr)T_r)\right]\right|^2, \tag{5.2}$$

where $c_T^{(i)}(t)$ denotes the ith derivative of $c_T(t)$. In practice the range of l is assumed finite in the receiver and the quantity in square brackets can be precomputed. This leads to fewer computations per state in an implementation of the Viterbi algorithm. Similar precomputing is possible in the implementation of adaptive receivers when CSI is required to be estimated [58].

5.2 Performance Evaluation

The covariance matrices required in (2.55), repeated here as

$$\mathbf{R}_{\mathbf{xx}}=\left(\begin{array}{c|c|c}\mathbf{R}_{\mathbf{uu}} & \mathbf{R}_{\mathbf{u\hat{u}}} & \mathbf{0}\\ \hline \mathbf{R}_{\mathbf{\hat{u}u}} & \mathbf{R}_{\mathbf{\hat{u}\hat{u}}} & \mathbf{0}\\ \hline \mathbf{0} & \mathbf{0} & \mathbf{R}_{\mathbf{nn}}\end{array}\right), \tag{5.3}$$

are expressed as follows in the case of channel decompositions. The elements of the top left submatrix are given by

$$E\left[u_{k,k-lr}u^*_{k',k'-l'r}\right]=\sum_{i=0}^{\infty}\sum_{i'=0}^{\infty}z_{Q,i}((k-lr)T_r)E\left[x_{Q,i}(kT_r)x^*_{Q,i'}(k'T_r)\right]z^*_{Q,i'}((k'-l'r)T_r), \tag{5.4}$$

where $Q\in\{H,U\}$. The elements of the top middle submatrix, are given by

$$E\left[u_{k,k-lr}\hat{u}^*_{k',k'-l'r}\right]=\sum_{i=0}^{\infty}\sum_{i'=0}^{J-1}z_{Q,i}((k-lr)T_r)E\left[x_{Q,i}(kT_r)x^*_{\hat{Q},i'}(k'T_r)\right]z^*_{\hat{Q},i'}((k'-l'r)T_r), \tag{5.5}$$

for the KL expansion where $Q \in \{H, U\}$, $\widehat{Q} \in \{H, U, \widetilde{H}, \widetilde{U}\}$ and

$$E\left[u_{k,k-lr}\widehat{u}^*_{k',k'-l'r}\right] = \sum_{i=0}^{\infty}\sum_{i'=0}^{J-1} z_{Q,i}((k-lr)T_r)E\left[x_{Q,i}(kT_r)x^*_{S,i'}(k'T_r)\right] c_T^{(i')*}((k'-l'r)T_r), \tag{5.6}$$

for the f-power series expansion where $Q \in \{H, U\}$. In this section Q and $\widehat{Q}$ are used to distinguish between an exact channel model, for the purposes of analysis, and the receiver channel model, obtained by truncating a series model. The elements of the middle submatrix, are given by

$$E\left[\widehat{u}_{k,k-lr}\widehat{u}^*_{k',k'-l'r}\right] = \sum_{i=0}^{J-1}\sum_{i'=0}^{J-1} z_{\widehat{Q},i}((k-lr)T_r)E\left[x_{\widehat{Q},i}(kT_r)x^*_{\widehat{Q},i'}(k'T_r)\right] z^*_{\widehat{Q},i'}((k'-l'r)T_r), \tag{5.7}$$

for the KL expansion where $\widehat{Q} \in \{H, U, \widetilde{H}, \widetilde{U}\}$ and

$$E\left[\widehat{u}_{k,k-lr}\widehat{u}^*_{k',k'-l'r}\right] = \sum_{i=0}^{J-1}\sum_{i'=0}^{J-1} c_T^{(i)}((k-lr)T_r)E\left[x_{S,i}(kT_r)x^*_{S,i'}(k'T_r)\right] c_T^{(i')*}((k'-l'r)T_r), \tag{5.8}$$

for the f-power series expansion.

A simplified form of the error event method described in Chapter 2 is used to analyse the performance of the MLSE receiver assuming BPSK and that all sequences, indexed by x, of length $2L-1$ symbols are equally likely. An approximate expression for the probability of bit error is given by

$$p(e) \approx \frac{1}{2^{2L-1}} \sum_{x=1}^{2^{2L-1}} P(\mathbf{a}^x \rightarrow \hat{\mathbf{a}}^x), \tag{5.9}$$

where $P(\mathbf{a}^x \rightarrow \hat{\mathbf{a}}^x)$ is the pairwise probability of error. The expression is derived under the assumption of a single symbol error event at $l = 0$. Thus the hypothesised symbols

are given by

$$\hat{a}_l^x = \begin{cases} -a_l^x, & l = 0 \\ a_l^x, & l \neq 0 \end{cases} \tag{5.10}$$

The expression (5.9) represents a lower bound on $p(e)$ assuming there is no error floor. When there is an error floor, that is the effects of mismatch begin to dominate, there is no guarantee that the expression is a lower bound. Hence the expression is described as approximate rather than a lower bound. Equation (5.9) is merely a form of (2.57), simplified under the stated assumptions. A union bound may be obtained by considering error sequences of length longer than one symbol. In that case (2.57) is an upper bound. $P(\mathbf{a}^x \rightarrow \hat{\mathbf{a}}^x)$ is a complex Gaussian quadratic form as defined by (2.52).

5.3 Numerical Results and Discussion

The performance of the MLSE receiver with channel decomposition is quantified in this section with BPSK the assumed modulation format. Extensions to higher level modulation formats are straightforward but significantly more computationally intensive. For most of the results in this section the number of samples per symbol is set to $r = 2$ and the length of the overall CIR and its approximation is set to $L = 3$. A root raised-cosine pulse shape with 50% excess bandwidth is used throughout this section.

Figure 5.1 shows a lower bound on the probability of error versus E_b/N_0 for a fixed RMS delay spread, $d = 0.3$, a fade rate of $f_D T = 0$ and a uniform delay profile. This fade rate represents a static channel. As the number of terms, J, increases the error floor is lowered. E_b is the bit energy and the single spread KL expansion is the channel

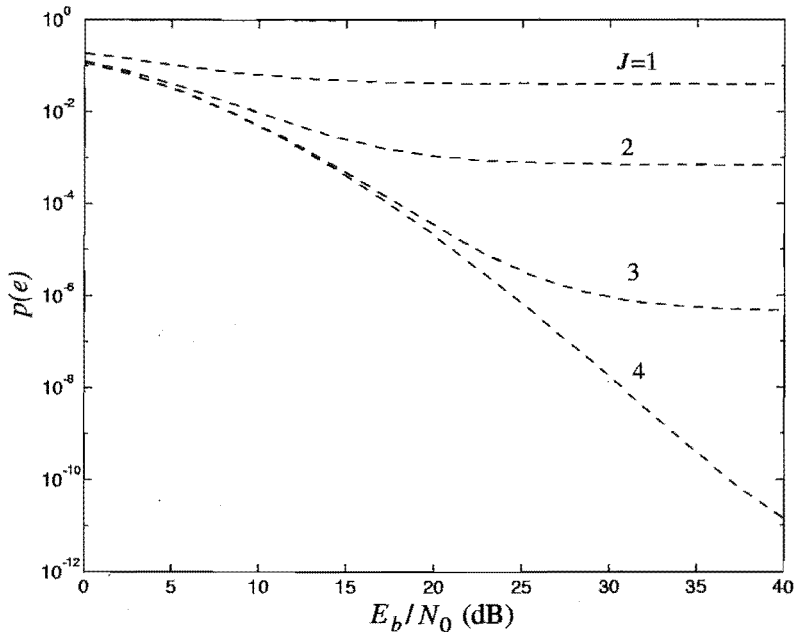

Figure 5.1: Lower bound on probability of error vs E_b/N_0 for uniform delay profile and J-term single spread KL expansion.

decomposition for this graph.

Figure 5.2 compares analysis and simulation results for the bit error rate as a function of d and J for the receiver with BPSK, $f_D T = 0.1$, $r = 3$, $L = 5$ and a 16 state Viterbi algorithm. Each point in the simulation represents 500 accumulated bit errors. A fixed transmitter sequence, $\sqrt{E_b}\{\ldots, 0, 1, 0, 1, 0, \ldots\}$, and single symbol error event are assumed. The use of a fixed sequence removes the need for computationally intensive averaging and allows further simplification in the computation of both analysis and simulation results. The fading processes are implemented as in [85]. Windowing of the filters is not required since the fade rate is high and many complex Gaussian samples are used. Multirate filtering is employed as well as library routines documented in [11] for random number generation. It appears that the analysis curves are less accurate given error floors and for high delay spreads when there is no error floor. The KL expansion

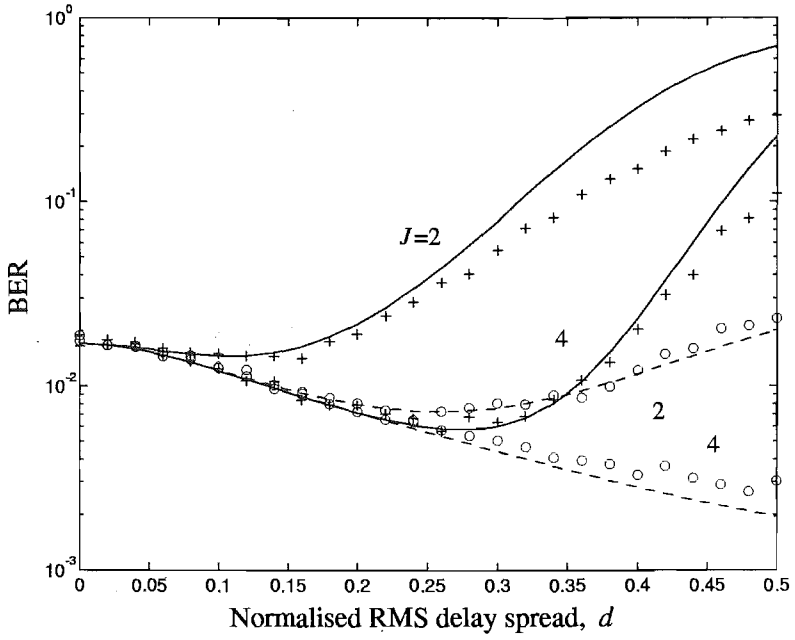

Figure 5.2: Bit error rate vs normalised RMS delay spread for uniform delay profile, f-power series expansion (analysis-solid lines, simulation-pluses) and KL expansion (analysis-dashed lines, simulation-circles), $E_b/N_0 = 10$dB, $f_DT = 0.1$.

provides greater delay spread support than the f-power series for a fixed number of terms.

It is of interest to further quantify the effect of varying the delay spread. Figures 5.3 and 5.4 show a comparison between the f-power series and KL expansions for the uniform and exponential delay profiles. These graphs again illustrate that the KL expansion provides greater delay spread support. For $J = 4$ terms there is a significant advantage in using the KL expansion at higher delay spreads. The graphs demonstrate the effect of implicit delay diversity which is seen in the decrease of the probability of error as the delay spread increases. Using more terms means that the receiver can support higher delay spreads without an error floor. Above a certain delay spread an error floor appears.

Figure 5.5 shows the effect of model mismatch in the case of the KL expansion for $J = 4$ terms. The receiver employs orthonormalised versions of the first J Legendre polynomials.

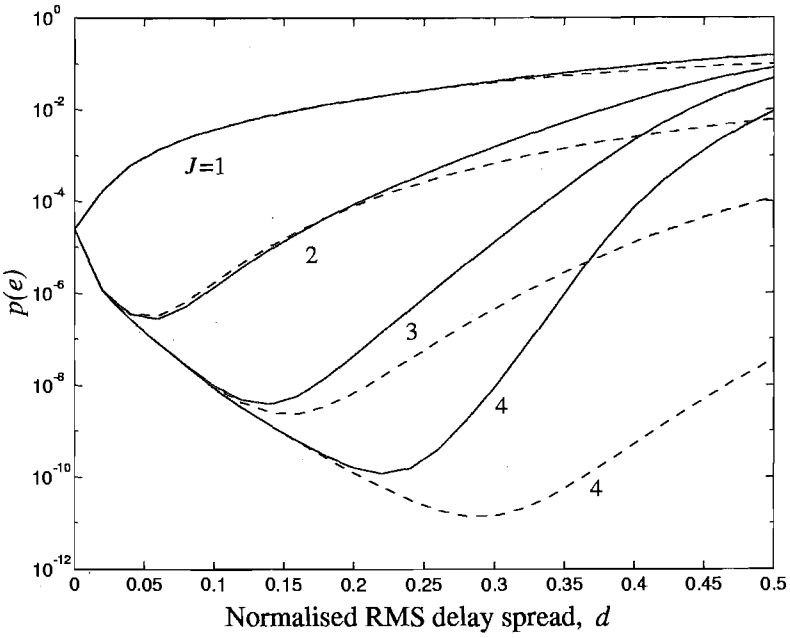

Figure 5.3: Lower bound on probability of error vs normalised RMS delay spread for uniform delay profile, f-power series (solid lines) and KL (dashed lines) expansions, $E_b/N_0 = 40$dB.

The cases of the f-power series and KL expansions are also shown. The graph suggests that mismatch is not a fundamental problem. In the case of the uniform delay profile there is no appreciable loss in performance due to mismatch; for the exponential delay profile there is an advantage in having some knowledge of the channel statistics. A mean delay mismatch between models has a more significant effect on the performance of the receiver than a RMS delay spread mismatch. This is highlighted here since the one-sided exponential delay profile implies a non-zero mean delay.

For Figures 5.3 and 5.5, $N_f = 150$ is used for discretisation of the spectrum; for Figure 5.2, $N_f = 300$ is used since the received samples in the simulation are computed with a longer overall CIR, $L = 61$ symbols.

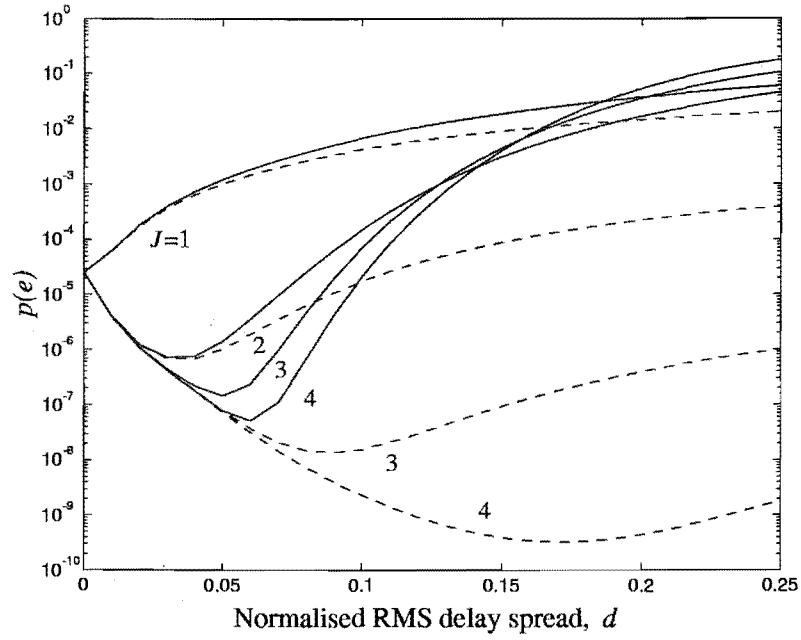

Figure 5.4: Lower bound on probability of error vs normalised RMS delay spread for exponential delay profile, f-power series (solid lines) and KL (dashed lines) expansions, $E_b/N_0 = 40$dB.

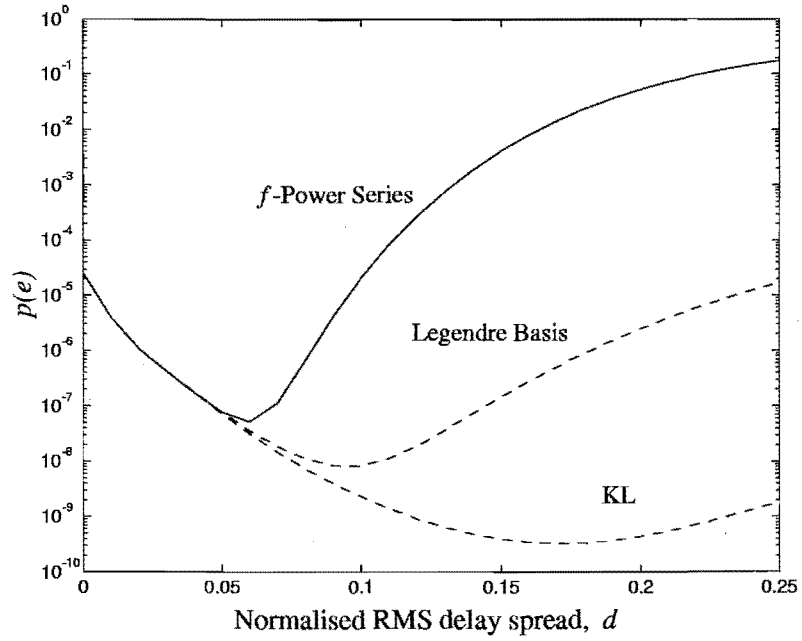

Figure 5.5: Lower bound on probability of error vs normalised RMS delay spread for exponential delay profile, f-power series (solid lines), Legendre basis and KL (dashed lines) expansions, $E_b/N_0 = 40$dB, $J = 4$.

5.4 Summary

The essentially delay limited property of fading dispersive channels encountered in practice enables a representation known in this thesis as a channel decomposition. In the estimation of CSI for equalisation a decomposition offers an underlying structure derived with some basic knowledge of the statistics of the channel.

It is seen that the mismatch arising from truncating the various expansions leads to a limit on the performance of MLSE for equalisation. Specifically, the receiver supports dispersion up to a certain delay spread which depends on the dimension of the decomposition. This effect is illustrated by both simulation and analysis results. The results are approximate lower bounds on the performance of adaptive MLSE receivers.

Chapter 6

Matched Filter Bounds

The matched filter bound (MFB) is an analytical tool for assessing the optimum performance of a wireless receiver. The method assumes transmission of an isolated pulse so that there is no need to consider intersymbol interference (ISI). The result is a lower bound on the probability of bit error that can be achieved with equalisation. MFBs are considered in [65, 22] for slow fading, dispersive channels characterised by the delay profile.

This chapter extends the concept of the matched filter bound to a generalised fading dispersive channel. There is no slow fading assumption. As in [22] the calculations are based on a Karhunen-Loève (KL) expansion of the received pulse spectrum. The transmitter is a standard linear modulator and sends an isolated pulse $c_T(t)$. The modulation format is assumed to be quaternary phase shift keying (QPSK). Explicit uncorrelated receiver space diversity is considered.

6.1 Application of Channel Decomposition

The transmitted signal has a complex baseband representation defined as

$$s_T(t) = a_0 c_T(t), \tag{6.1}$$

where a_0 is the symbol to be detected. A double spread KL expansion of the received pulse is considered. Under specific assumptions on the channel the probability of bit error is sought. In [22] the distribution of the probability of bit error and the average probability of bit error are found analytically for a slow fading dispersive channel.

The basic idea presented in this chapter is that the double spread KL expansion is applicable for calculation of matched filter bounds in time varying channels in the same way that the single spread KL expansion is applicable in slow fading channels where the ensemble is considered.

6.2 Performance Evaluation

The probability of bit error for coherent BPSK and QPSK, conditioned on a scale factor z, is denoted $p(e \mid z)$ and is given by

$$p(e \mid z) = \frac{1}{2}\text{erfc}\left(\sqrt{z\frac{E_b}{N_0}}\right). \tag{6.2}$$

Each diversity thread has a separate matched filter and the scale factor, z, is given by

$$z = \sum_{m=1}^{M} \int_{-W_D/2}^{W_D/2} |V_{m,0}(f)|^2 df, \tag{6.3}$$

where W_D is the two-sided bandwidth of the $\{V_{m,0}\}$ given by $W_D = W + 2f_D$. The pulse $v_{m,0}(t)$ is received on the mth diversity thread where M is the number of diversity threads.

The bit energy to noise ratio is scaled by z since the variance of the sample of a noise free, received and matched filtered signal is proportional to z^2 and the variance of a sample due to matched filtered noise is proportional to z. In this thesis the fading dispersive channel response is assumed to have zero mean for all delays. Rayleigh fading is considered and the channel is modelled as completely random. In practice there is often a deterministic, line-of-sight or near line-of-sight component which leads to lower bit error rates.

A uniform channel delay profile is considered here. With this assumption for frequency correlation it follows that, on each diversity thread, there are no eigenvalues with multiplicity greater than unity [82]. Considering all threads, the multiplicity of each eigenvalue is M, the number of threads. The first few eigenvalues are significant and subsequent eigenvalues decrease rapidly towards zero and so the number of eigenvalues can be assumed to be a finite number J. Machine accuracy and computational complexity place a practical upper limit on J. Using the orthonormality of the eigenfunctions the scale factor z is obtained as

$$z = \sum_{m=1}^{M} \sum_{i=0}^{J-1} |x_{R,m,i,0}|^2. \tag{6.4}$$

where $x_{R,m,i,0}$ is the $\{m,i\}$th TSC in a double spread KL expansion of the $l = 0$ received pulse. The probability density function (pdf) of z is denoted $p_z(z)$. It has a characteristic function, $P_\zeta(\zeta)$, given by

$$P_\zeta(\zeta) = \prod_{i=0}^{J-1} (1 - j\zeta\gamma_i)^{-M}. \tag{6.5}$$

The pdf is obtained from an inverse integral transform as

$$p_z(z) = \frac{1}{2\pi} \int_{-\infty}^{\infty} P_\zeta(\zeta) \exp(-j\zeta z) d\zeta, \tag{6.6}$$

which is evaluated using residue calculus [48]. The residues depend on M because multiplicity of eigenvalues leads to multiplicity of poles in (6.5).

The pdf is derived as

$$p_z(z) = \sum_{m=1}^{M} \sum_{i=0}^{J-1} Y_{m,i} \frac{z^{m-1} e^{-z/\gamma_i}}{\gamma_i^m (m-1)!}, \tag{6.7}$$

where

$$Y_{m,i} = \frac{1}{(-j\gamma_i)^{M-m}(M-m)!} \left[\frac{d^{M-m}}{d\zeta^{M-m}} \left\{ \prod_{\substack{p=0 \\ p \neq i}}^{J-1} (1 - j\zeta\gamma_p)^{-M} \right\} \right]_{\zeta=-j/\gamma_i}. \tag{6.8}$$

Based on the derivation in [22], the average probability of bit error is given by

$$p(e) = \int_0^\infty p(e \mid z) p_z(z) dz. \tag{6.9}$$

Using the result [81]

$$\frac{1}{2}\text{erfc}\left(\sqrt{z\frac{E_b}{N_0}}\right) = \frac{1}{\pi}\int_0^{\pi/2} \exp\left(-\frac{z}{\sin^2\theta}\frac{E_b}{N_0}\right) d\theta, \tag{6.10}$$

and

$$\frac{1}{\pi}\int_0^{\pi/2} \frac{d\theta}{\left(\frac{E_b}{N_0 \sin^2\theta} + \frac{1}{\gamma_i}\right)^m} = \frac{\gamma_i^m}{2}\left(1 - \sum_{l=0}^{m-1} \beta_l\left(\gamma_i \frac{E_b}{N_0}\right)\right), \tag{6.11}$$

where

$$\beta_l(x) = \frac{(2l)!}{2^{2l}(l!)^2}\sqrt{\frac{x}{(x+1)^{2l+1}}}, \tag{6.12}$$

the $p(e)$ can be derived as

$$p(e) = \frac{1}{2}\sum_{m=1}^{M}\sum_{i=0}^{J-1} Y_{m,i}\left(1 - \sum_{l=0}^{m-1}\beta_l\left(\gamma_i\frac{E_b}{N_0}\right)\right), \tag{6.13}$$

The result (6.11) is stated but left unproven. The analysis and final result are the same as in [22] except for the structure of the KL expansion and the statistical properties of the

noise including the consequent dependence of the results on the transmitter pulse shape. In [22] the results are made independent of the pulse shape through the use of whitening matched filters. The noise PSD is assumed to be an arbitrary function of frequency. In this thesis a constant, two-sided noise PSD of $N_0/2$ is assumed.

6.3 Numerical Results and Discussion

In this subsection some representative results are presented, initially for a root raised-cosine pulse with 50% excess bandwidth, i.e. a rolloff factor, $\alpha = 0.5$. The time selective correlation function, ρ, is as defined in (2.14) for isotropic scattering and a uniform channel delay profile is considered. The system is assumed to have a coherent phase reference. The sole source of inaccuracy in the results is the numerical evaluation of the received pulse eigensystem. The number of frequency divisions is set to $N_f = 50$. No variations have been found in the following results that are attibutable to using larger N_f.

Figure 6.1 shows the matched filter bound on the probability of bit error vs E_b/N_0. A lowering of the curve occurs for higher delay spreads or fade rates. This effect is due to implicit delay or Doppler diversity. Implicit diversity is most effective when there is no explicit diversity, that is, the receiver has a single thread. Although not shown in the graph, the performance of a one thread receiver given large delay spread or fade rate is potentially better than a two thread one with small delay spread and fade rate. For $M = 4$, it can be seen that the effect of implicit diversity is diminished with respect to the effect for no explicit diversity, $M = 1$. In slow fading the results are similar to those in [22]. Discrepancies can be attributed to the different underlying structure of the systems,

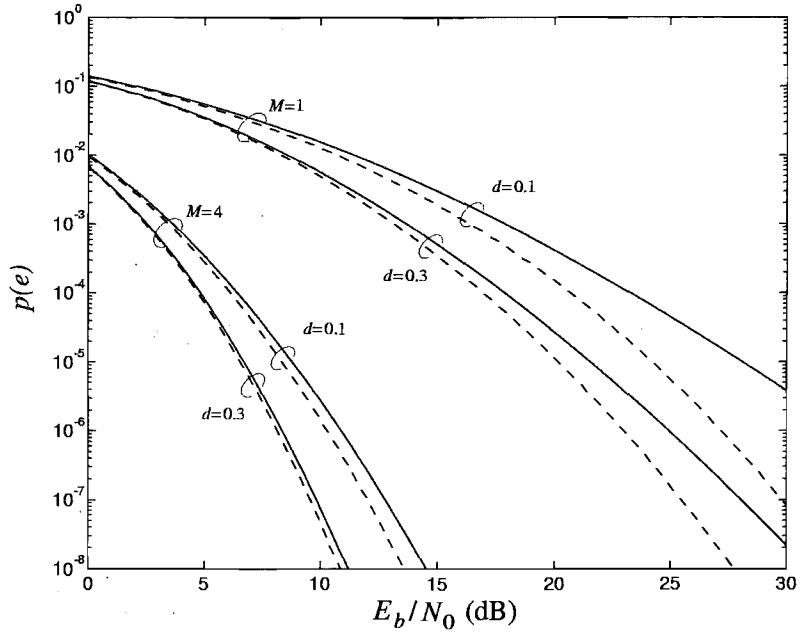

Figure 6.1: Probability of bit error, $p(e)$, vs E_b/N_0 for a uniform delay profile with pulse rolloff factor, $\alpha = 0.5$, two values of M, two values of d and two values of fade rate ($f_D T = 0$-solid lines and $f_D T = 0.1$-dashed lines).

including the definition of the noise PSD, or to the fact that a uniform delay profile is assumed.

Figure 6.2 shows a contour plot of the matched filter bound on probability of bit error as a function of normalised RMS delay spread, d, and fade rate, $f_D T$, for $M = 1$ and $E_b/N_0 = 30$dB. The contours are lines of constant probability of bit error. Figure 6.3 illustrates the effect of the rolloff factor, α, of the pulse shape. Both graphs show the effect of implicit diversity. There is significant improvement in the achievable probability of bit error as d and $f_D T$ increase. For the ranges of d and $f_D T$ considered the rolloff factor has minimal impact on the effect of delay diversity in slow fading but significant impact on the ability of a system to exploit Doppler diversity. There are greater performance gains as a result of Doppler diversity if the pulse shape is more spread out in time, i.e.

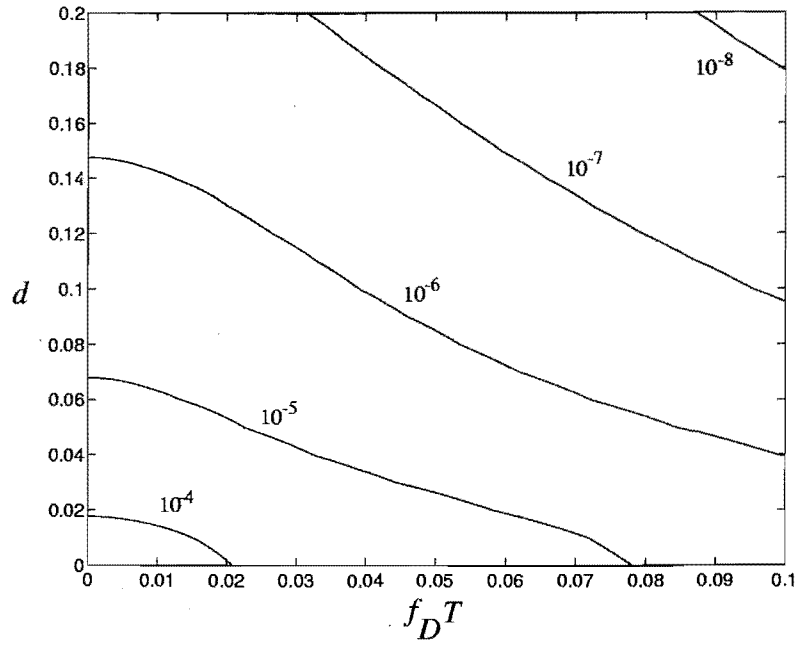

Figure 6.2: Contour plot of the probability of bit error, $p(e)$, as a function of normalised RMS delay spread, d, and fade rate, $f_D T$, with pulse rolloff factor, $\alpha = 0.5$, $M = 1$ and $E_b/N_0 = 30$dB.

has a smaller rolloff factor. On the other hand, a larger rolloff can extend the range of validity for a slow fading assumption.

Figure 6.4 shows that the probability of bit error for an ideal AWGN channel (no fading) provides a lower bound on the performance in slow fading dispersive channels. Figure 6.5 shows the same for flat fading channels. In this last figure alternative definitions are used for the pulse shape and time selective correlation function. Specifically,

$$c_T(t) = \text{sinc}(t/T)/\sqrt{T}, \tag{6.14}$$

and

$$\rho(t - t') = \text{sinc}(2f_D(t - t')). \tag{6.15}$$

This model is similar to the one used so far but it implies a pulse shape which can be expected to lead to greater implicit Doppler diversity effect as well as offering a simpler

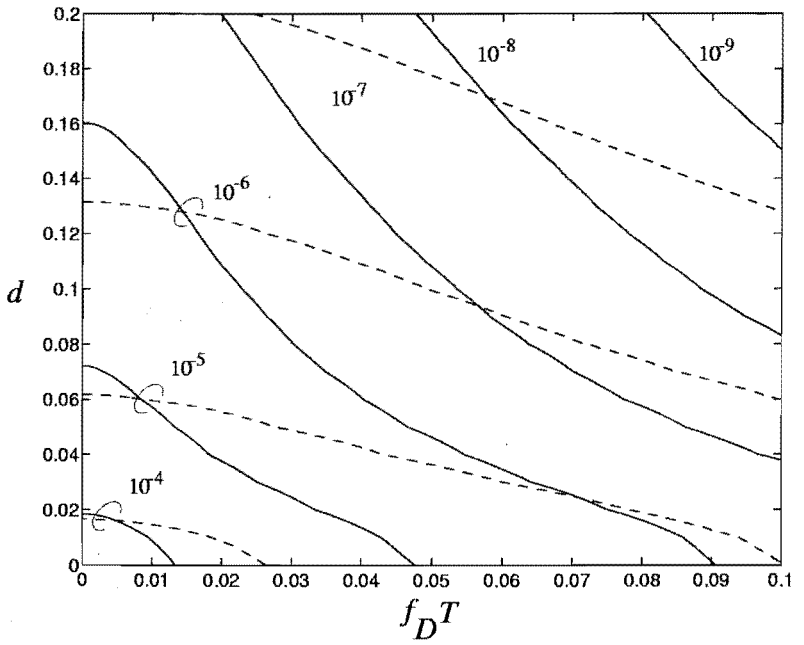

Figure 6.3: Contour plot of the probability of bit error, $p(e)$, as a function of normalised RMS delay spread, d, fade rate, $f_D T$ and pulse rolloff factor ($\alpha = 0.2$-solid lines and $\alpha = 0.8$-dashed lines), with $M = 1$ and $E_b/N_0 = 30$dB.

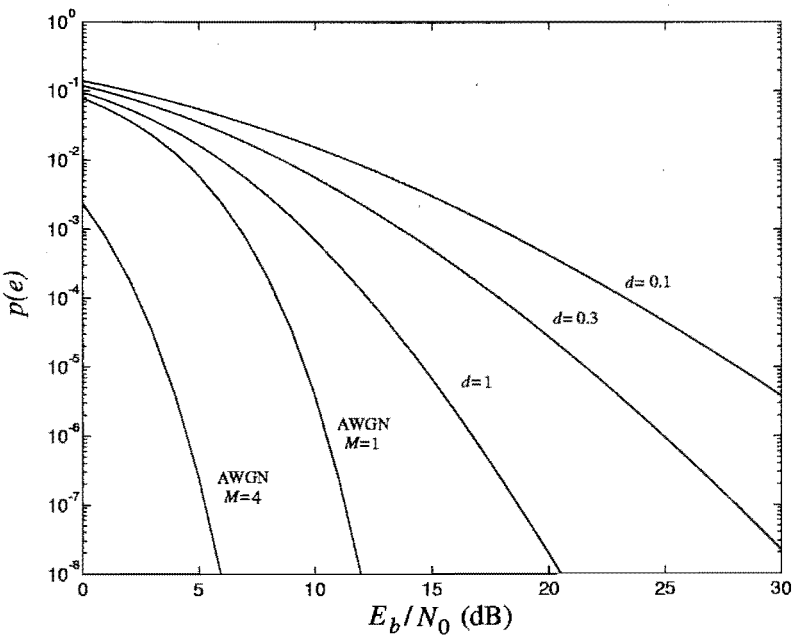

Figure 6.4: Probability of bit error, $p(e)$, vs E_b/N_0 for a uniform delay PSD with pulse rolloff factor, $\alpha = 0.5$, various values of d, $f_D T = 0$, $M = 1$, and for ideal AWGN channel with $M = 1$ and $M = 4$.

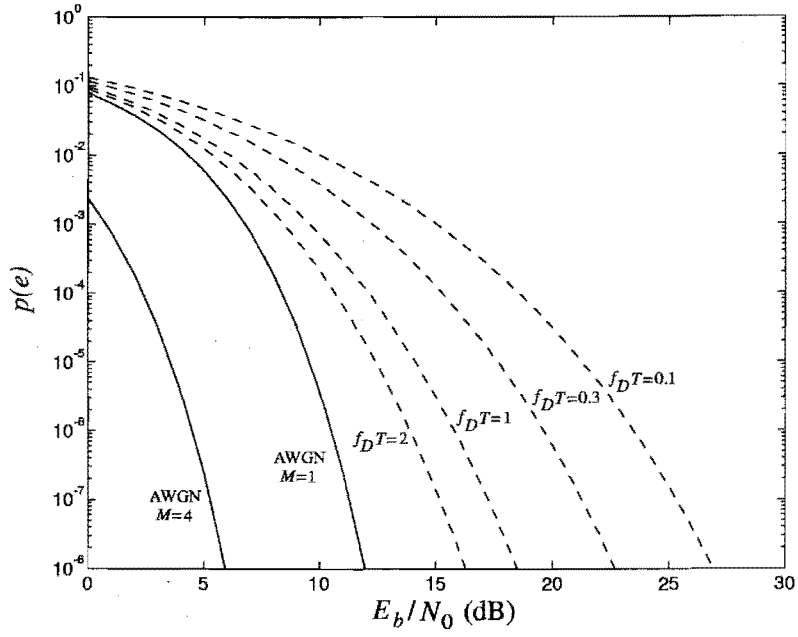

Figure 6.5: Probability of bit error, $p(e)$, vs E_b/N_0 for a flat fading channel, sinc time selective correlation function, with pulse rolloff factor, $\alpha = 0$, various values of f_DT, $d = 0$, $M = 1$, and for ideal AWGN channel with $M = 1$ and $M = 4$.

evaluation of the integral in (3.26). As d and/or f_DT increase the channel response becomes less correlated in frequency and/or time. The figures show that more of the energy can be recovered and quantify the implicit diversity effects in relation to the AWGN channel.

6.4 Summary

It has been demonstrated that the matched filter bound can be calculated without the assumption of slow fading. For faster fading the effect of implicit Doppler diversity becomes apparent. The effect of implicit delay and Doppler diversity is diminished when there is explicit diversity but for a fixed number of threads the exploitation of implicit diversity yields some improvement in performance. In fast fading a smaller transmitter

pulse rolloff factor offers the potential for a lower bit error rate.

Chapter 7

Channel Capacity

This chapter is concerned with the definition and determination of capacity for fading dispersive channels. It turns out that the channel decompositions considered up to this point are applicable. The capacities of discrete time AWGN channels, input power constrained and bandlimited AWGN channels and time invariant dispersive channels with AWGN are well known. The result for dispersive channels [41] relies on a system being able to distribute energy over compactly supported regions of the frequency spectrum.

The linear modulation formats considered in previous chapters represent an imposed structure which limits options for the remaining aspects of the design of communication systems. In what follows quantities relevant to the capacity of fading dispersive channels are determined with some basic assumptions about the structure of the communication system. The approach is based on the assumption of ideal CSI at the receiver. The consideration of ISI is avoided by taking a similar approach to the previous chapter on the determination of matched filter bounds, that is, an isolated pulse is assumed. In practice, equalisation of the channel and decoding of the transmitted signal are jointly

performed with, for example, a soft decision Viterbi algorithm.

Explicit diversity is also of interest. If transmitter space or frequency diversity is available then it is feasible to distribute energy and code separately over each diversity thread. In the final analysis it is likely that code design with combined equalisation and decoding can lead to full utilisation of any form of diversity. In [40] the idea of using multiple antennas at both the transmitter and receiver is considered in the context of slow, flat, Rayleigh fading. Using the Bell Labs Layered space-time (BLAST) architecture a lower bound on capacity is obtained.

To follow are definitions of entropy and information and results on the capacity of various channels. These are well established results originating from the work of Shannon and described in detail in [41]. The probability densities and joint probability density of two random variables, x and y, are denoted $p(x)$, $p(y)$ and $p(x,y)$. The conditional probabilities are then given by

$$p(x|y) = \frac{p(x,y)}{p(y)}, \tag{7.1}$$

$$p(y|x) = \frac{p(x,y)}{p(x)}. \tag{7.2}$$

Various quantities relating to information can be defined. The mutual information between x and y is the information provided about the event x given the event y defined as

$$I_m(x;y) = \log\left(\frac{p(x|y)}{p(x)}\right), \tag{7.3}$$

and the average mutual information is defined as

$$H_m(X;Y) = \sum_x \sum_y p(x,y) \log\left(\frac{p(x|y)}{p(x)}\right). \tag{7.4}$$

The self information of event x is defined as

$$I_c(x) = -\log(p(x)), \tag{7.5}$$

and the entropy of the ensemble as

$$H_c(X) = -\sum_x p(x)\log(p(x)). \tag{7.6}$$

The joint information of x and y is given by

$$I_c(x,y) = -\log(p(x,y)), \tag{7.7}$$

and the average by

$$H_c(X,Y) = -\sum_x \sum_y p(x,y)\log(p(x,y)). \tag{7.8}$$

The conditional self information is defined as

$$I_c(x|y) = -\log(p(x|y)), \tag{7.9}$$

and the average as

$$H_c(X|Y) = -\sum_x \sum_y p(x,y)\log(p(x|y)). \tag{7.10}$$

Several results follow for the mutual information as

$$I_m(x;y) = I_c(x) - I_c(x|y), \tag{7.11}$$

or in terms of averages

$$H_m(X;Y) = H_c(X) - H_c(X|Y). \tag{7.12}$$

The self information, $I_c(x)$, is the *a priori* information required to specify x and the conditional self information, $I_c(x|y)$, is the uncertainty in x given y. Self information is always non-negative. Furthermore

$$I_m(x;y) = I_c(x) + I_c(y) - I_c(x,y), \tag{7.13}$$

or in terms of averages

$$H_m(X;Y) = H_c(X) + H_c(Y) - H_c(X,Y), \tag{7.14}$$

For continuous density functions the summations are replaced with integrations. An intuitive understanding of entropy can be gained by considering the use of letters in english language. For the letter 'e' which occurs frequently in english usage, the probability of an occurence, $p(\text{'}e\text{'})$, is large and the contribution to entropy, $-p(\text{'}e\text{'})\log(p(\text{'}e\text{'}))$, is small. In an efficient representation, the cost of this letter is smaller than for other letters which occur less frequently.

Given a discrete time AWGN channel with input x, additive noise z and output y the capacity is the maximum over the input density function of the average mutual information between y and x which is given by and simplified as

$$\begin{aligned} H_m(Y;X) &= H_c(Y) - H_c(Y|X) \\ &= H_c(Y) - H_c(Z) \end{aligned} \tag{7.15}$$

The variables x and y have been reversed so that y is the output. Reversal is valid by symmetry regardless of the underlying model. The last equation indicates that the average mutual information is dependent on the input density function through $H_c(Y)$ but not $H_c(Y|X)$. To verify this it is seen that since x and z are uncorrelated,

$$p_{Y|X}(y|x) = p_Z(y-x), \tag{7.16}$$

and

$$\begin{aligned} H_c(Y|X) &= -\int_{-\infty}^{\infty}\int_{-\infty}^{\infty} p_X(x)p_Z(y-x)\log(p_Z(y-x))dydx \\ &= -\int_{-\infty}^{\infty} p_X(x)\int_{-\infty}^{\infty} p_Z(z)\log(p_Z(z))dzdx \\ &= H_c(Z) \end{aligned} \tag{7.17}$$

Assuming an average energy constrained input, that is

$$E\left[x^2\right] = E_c, \tag{7.18}$$

and AWGN with mean zero and variance

$$E\left[z^2\right] = \sigma^2, \tag{7.19}$$

it can be shown by calculus of variations [41] that the maximising output density function is Gaussian giving the density function as

$$p_Y(y) = \frac{1}{\sqrt{2\pi(E_c+\sigma^2)}}\exp\left(-\frac{y^2}{2(E_c+\sigma^2)}\right). \tag{7.20}$$

The optimum input density function is therefore Gaussian. The capacity is given by

$$C = \frac{1}{2T}\log\left(1+\frac{E_c}{\sigma^2}\right). \tag{7.21}$$

where the units of C are natural units per second (for the natural logarithm). Given N parallel discrete time memoryless AWGN channels where the nth channel has input x_n, with energy E_{cn}, noise variance σ_n^2 and

$$\sum_{n=1}^{N} E[x_n^2] = E_c, \tag{7.22}$$

it follows that the capacity is [41]

$$C = \frac{1}{2T}\sum_{n=1}^{N}\log\left(1+\frac{E_{cn}}{\sigma_n^2}\right) \tag{7.23}$$

where

$$E_{cn} = \begin{cases} B - \sigma_n^2 & \sigma_n^2 < B \\ 0 & \sigma_n^2 > B \end{cases} \tag{7.24}$$

and B chosen so that

$$\sum_{n=1}^{N} E_{cn} = E_c. \tag{7.25}$$

A famous expression due to Shannon for the capacity of an input power constrained and bandlimited AWGN channel is given by [41]

$$C = \frac{W}{2} \log \left(1 + \frac{2S}{N_0 W} \right), \tag{7.26}$$

where S is the input power constraint, $N_0/2$ is the two-sided noise PSD and W is the two-sided bandwidth.

When the channel is other than simple AWGN and, specifically, slow fading dispersive, it is necessary to take the transfer function of the channel into account. Given an input power constraint S, a channel with transfer function $H(f)$ and additive noise with power spectral density $N(f)$ the capacity is given by [41]

$$C = \frac{1}{2} \int_{f: \frac{N(f)}{|H(f)|^2} \leq B} \log \left[\frac{|H(f)|^2 B}{N(f)} \right] df, \tag{7.27}$$

where B is defined from

$$S = \int_{f: \frac{N(f)}{|H(f)|^2} \leq B} \left[B - \frac{N(f)}{|H(f)|^2} \right] df. \tag{7.28}$$

The result has a water pouring analogy if the function $N(f)/|H(f)|^2$ is viewed as the bottom of a container to be filled. Regions of f where the function is low are filled and

the final level at which pouring stops is the constant B. The notation for the limits of integration describe compactly supported regions of frequency where the given inequality holds.

7.1 Application of Channel Decomposition

The last result requires energy to be distributed over compactly supported regions of frequency. Whether this is achievable in practice is unclear. Certainly it can be said that the underlying structure of typical transmitters and receivers has some influence on the capacity of the overall communication system. It seems intuitive that the benefits of diversity be reflected in system capacity. The remainder of this chapter investigates this largely open question.

In the last chapter matched filter bounds on the probability of error were found by considering the transmission and reception of an isolated pulse and ignoring the effect of ISI. A similar approach is taken in this chapter for calculating capacity.

7.2 Performance Evaluation

It is assumed that the input density function is Gaussian and that the signal to noise ratio is denoted SNR where AWGN is assumed. The joint average mutual information is calculated by explicitly assuming an isolated pulse and without attempting to make any conclusion about whether it is the achievable capacity of the channel. This mirrors the approach taken in the last chapter on matched filter bounds. It is motivated by the observation that the matched filter bound is a tight lower bound on probability of bit

error at high signal to noise ratio.

It is assumed that there is a single input with a zero mean, complex Gaussian density function, modulated onto an isolated pulse. There are MJ filters matched to the components of the channel decomposition which has TSCs, $x_{R,m,i,0}$, in a double spread KL decomposition of the overall CIR. The joint average mutual information (AMI) over the filter outputs, conditioned on the input and channel, is derived using a multiple complex variable form of (7.15) as

$$v = g(z) = \frac{1}{2}\log\left(1 + z\text{SNR}\right), \tag{7.29}$$

where the units of v are natural units (nats) and the scale factor is given by

$$z = \sum_{m=1}^{M}\sum_{i=0}^{J-1} |x_{R,m,i,0}|^2. \tag{7.30}$$

as in (6.4). In the case of slow, flat, Rayleigh fading such that $J = 1$, it follows that z is a chi-squared random variable with $2M$ degrees of freedom. Equation (7.29) closely resembles the corresponding equation in [40] for one transmitting antenna.

The cumulative distribution of the joint AMI is given by

$$F(v_0) = P(v \leq v_0) = \int_0^{z_0} p_z(z)dz, \tag{7.31}$$

where $p_z(z)$ is the same as in (6.7), $v_0 = g(z_0)$ from (7.29) and

$$z_0 = h(v_0) = \frac{e^{2v_0} - 1}{\text{SNR}}. \tag{7.32}$$

The cumulative distribution is the integral of a Gamma distribution [50] and is derived as

$$F(v_0) = \sum_{m=1}^{M}\sum_{i=0}^{J-1} Y_{m,i}\left(1 - \sum_{l=0}^{m-1}\left(\frac{h(v_0)}{\gamma_i}\right)^l \frac{e^{-h(v_0)/\gamma_i}}{l!}\right), \tag{7.33}$$

where $Y_{m,i}$ is defined by (6.8). The probability density function of the joint AMI is then given by

$$\begin{aligned} p_v(v) &= F'(v) \\ &= p_z(h(v))h'(v) \end{aligned} \tag{7.34}$$

since v is a monotonic increasing function of z. For example with $M = 1$ the density function is derived as

$$p_v(v) = \frac{2e^{2v}}{\mathrm{SNR}} \sum_{i=0}^{J-1} \frac{\gamma_i^{J-2} \exp\left(-\dfrac{e^{2v}-1}{\gamma_i \mathrm{SNR}}\right)}{\prod\limits_{\substack{i'=0 \\ i' \neq i}}^{J-1} (\gamma_i - \gamma_{i'})}. \tag{7.35}$$

A more general derivation requires a sequence of inputs to be considered. If these are assumed to be zero mean, complex Gaussian with arbitrary correlation then the approach may lead to conclusions about capacity and how to design codes. A relevant issue is interleaving which is beneficial in slow fading [84].

7.3 Numerical Results and Discussion

Assuming slow fading, a two-ray delay profile and using (7.34) the density function of joint AMI is shown in Figure 7.1 for two values of one-sided delay spread and two values for the number of diversity threads. The effect of greater implicit diversity is to sharpen the density function, that is reduce the variance, of the joint AMI. Receiver space diversity increases the joint AMI. All of the conclusions of the last chapter on matched filter bounds have a corresponding interpretation in terms of joint AMI. Further results can include the effects of fast fading and pulse shaping. An interpretation of the joint AMI as capacity is

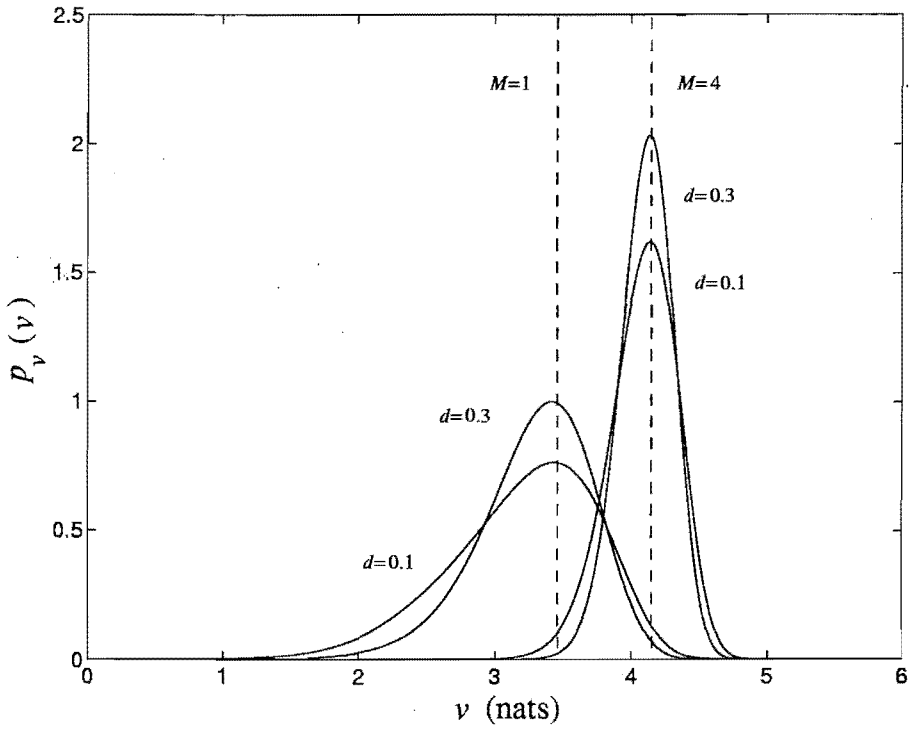

Figure 7.1: Joint AMI density function for a two-ray delay profile, SNR = 30dB, with two values of d and two values of M and corresponding vertical dashed lines for discrete time AWGN cases.

less convincing in fast fading since joint AMI varies from symbol to symbol rather than remaining constant over many symbol spacings as in slow fading.

7.4 Summary

Long standing results in information theory have been summarised in this chapter. A start has been made on the definition and determination of fading dispersive channel capacity using channel decompositions. The effects of diversity on joint AMI are considered assuming that an isolated pulse is transmitted. Implicit diversity tends to lower the variance of the joint AMI whereas explicit uncorrelated space diversity shifts the mean upwards. Explicit transmitter space or frequency diversity presents the option of distributing energy over multiple threads.

In the limit, with interleaving and appropriate coding, the capacity of a fading dispersive channel is a constant rather than a random variable. The impact of transmitter, channel or receiver diversity is to lessen the range of variation of available capacity.

Chapter 8

Conclusion

The major contributions of this thesis are the definition and application of fading dispersive channel decompositions. In the area of pulse shaping it is shown that with bandwidth expansion and appropriate design, ISI can be driven towards zero provided that the total delay spread is less than twice the symbol spacing. There is a tradeoff between bandwidth, the number of symbols in a constellation and the need for equalisation.

It is also shown that for bandlimited modulation formats and essentially delay and Doppler frequency limited channels it is possible to obtain a decomposition with finite dimension and symbol spaced coefficients. This offers a structure for the representation of channels allowing the calculation of matched filter bounds and the potential for new adaptive equaliser formulations.

Additional material includes a study of the precision of MLSE with approximate CSI in the form of a finite dimensional channel decomposition. This illustrates that for higher delay spreads it is necessary to increase model dimension. It is also advantageous to use orthogonal expansions such as one involving Legendre polynomials over non-orthogonal

ones such as the f-power series. Furthermore if there is some knowledge of channel second order statistics and timing offsets then greater efficiencies associated with modelling can be obtained. This is illustrated by results obtained with a one-sided exponential channel delay profile.

Applications of channel decompositions to the determination of matched filter bounds and joint average mutual information are considered. The results illustrate the effects of diversity in wireless systems operation.

8.1 Future Work

It is proposed that work be undertaken to:

1. design and build a system to assess the merits of bandwidth expansion for linear modulation;

2. formalise the mathematics of the decompositions of delay and Doppler frequency limited channels looking in particular at dimensionality;

3. investigate the application of the channel decompositions to the determination of channel capacity and to the design of adaptive receivers.

To investigate the use of bandwidth expansion the objective would be to take full advantage of the interference suppression to keep the complexity of the receiver as low as possible. It would be worthwhile to include consideration of dominant co-channel interference (CCI), as defined in Chapter 2.

The dimensionality of time varying linear channels is essentially limited by virtue of the fact that the overall CIR is bandlimited and essentially time limited. A more rigorous proof may be obtained, taking a similar line to the development in [82], yielding a statement about the approximate number of orthogonal signals required to form a basis for the overall CIR.

The f-power series is utilised in the implementation of adaptive receivers [58] based on the Viterbi algorithm and Kalman filtering to track channel variations. The single and double spread Karhunen-Loève (KL) expansions are applicable in a similar way.

Bibliography

[1] M. Abramowitz and I. A. Stegun, *Handbook of Mathematical Functions*, Dover Publications, Inc., New York, 1972.

[2] H. Anton, *Elementary Linear Algebra*, John Wiley and Sons, New York, 2nd edition, 1984.

[3] E. Arthurs and H. Dym, "On the optimum detection of digital signals in the presence of white Gaussian noise - a geometric interpretation and a study of three basic data transmission systems," *IEEE Transactions on Communication Systems*, 10:336–372, December 1962.

[4] N. J. Baas and D. P. Taylor, "Bandwidth expansion for robust, low complexity communication over fading dispersive channels," *Revised for IEEE Transactions on Communications*, April 2000.

[5] N. J. Baas and D. P. Taylor, "Decomposition of a fading dispersive channel - effects of mismatch on the performance of MLSE," *IEEE Transactions on Communications*, 48:1467–1470, September 2000.

[6] N. J. Baas and D. P. Taylor, "Matched filter bounds for wireless communication over Rayleigh fading dispersive channels," *Revised for IEEE Transactions on Communications*, December 2000.

[7] I. Bar-David and R. Krishnamoorthy, "Delay spread profiles and receiver performance in a dense multipath environment," *Presented at University of Canterbury*, 1996.

[8] E. Bejjani, J. C. Belfiore and P. Leclair, "Coherent detection for transmission over severely time and frequency dispersive multipath fading channels," In *Proceedings 1995 IEEE International Symposium on Information Theory*, page 212, 1995.

[9] P. A. Bello, "Characterization of randomly time-variant linear channels," *IEEE Transactions on Communications Systems*, 11:360–393, December 1960.

[10] A. Beutelspacher, *Cryptology*, Mathematical Society of America, Washington, 1994.

[11] B. W. Brown and J. Lovato, *RANLIB.C Library of C Routines for Random Number Generation*, Department of Biomathematics, University of Texas, Houston, Texas, 1994.

[12] J. K. Cavers, "On the validity of slow and moderate fading models for matched filter detection of Rayleigh fading signals," *Canadian Journal of Electrical and Computer Engineering*, 17:183–189, 1992.

[13] J. K. Cavers, "Pilot symbol assisted modulation and differential detection in fading and delay spread," *IEEE Transactions on Communications*, 43:2206–2212, July 1995.

[14] J. K. Cavers and P. Ho, "Analysis of the error performance of trellis-coded modulations in Rayleigh fading channels," *IEEE Transactions on Communications*, 40:74–83, January 1992.

[15] R. W. Chang, "Orthogonal signals for data transmission," *Bell Systems Technical Journal*, 45:1775–1796, December 1966.

[16] J. C-I. Chuang, "The effects of time delay spread on portable radio communications with digital modulation," *IEEE Journal on Selected Areas in Communications*, 5:879–889, June 1987.

[17] K. M. Chugg and A. Polydoros, "MLSE for an unknown channel - part I: Optimality considerations," *IEEE Transactions on Communications*, 44:836–846, July 1996.

[18] K. M. Chugg and A. Polydoros, "MLSE for an unknown channel - part II: Tracking performance," *IEEE Transactions on Communications*, 44:949–958, August 1996.

[19] C. K. Chui, *Wavelet Analysis and its Applications Volume 1: An Introduction to Wavelets*, Academic Press, Inc., 1992.

[20] M. V. Clark, *Diversity and Equalization in Digital Cellular Radio*, PhD thesis, University of Canterbury, New Zealand, May 1992.

[21] M. V. Clark, L. Greenstein, W. K. Kennedy and M. Shafi, "Optimum linear diversity receivers for mobile communications," *IEEE Transactions on Vehicular Technology*, 43:47–56, February 1994.

[22] M. V. Clark, L. J. Greenstein, W. K. Kennedy and M. Shafi, "Matched filter bounds for diversity combining receivers in digital mobile radio," *IEEE Transactions on Vehicular Technology*, 41:356–362, November 1992.

[23] M. V. Clark, L. J. Greenstein, W. K. Kennedy and M. Shafi, "MMSE diversity combining for wide-band digital cellular radio," *IEEE Transactions on Communications*, 40:1128–1135, June 1992.

[24] Q. Dai and E. Shwedyk, "Detection of bandlimited signals over frequency selective Rayleigh fading channels," *IEEE Transactions on Communications*, 42:941–950, February 1994.

[25] W. C. Dam, "An adaptive maximum likelihood receiver for Rayleigh fading channels, Master's thesis, McMaster University, Hamilton Ontario, Canada, 1990.

[26] W. C. Dam and D. P. Taylor, "An adaptive maximum likelihood receiver for correlated Rayleigh-fading channels," *IEEE Transactions on Communications*, 42:2684–2692, September 1994.

[27] A. N. D'Andrea, F. Guglielmi and A. Spalvieri, "Design of transmit and receive digital filters for data communications," *IEEE Transactions on Communications*, 42:357–359, February 1994.

[28] A. N. D'Andrea, U. Mengali and R. Reggiannini, "The modified Cramer-Rao bound and its application to synchronization problems," *IEEE Transactions on Communications*, 42:1391–1399, February 1994.

[29] I. Daubechies, *Ten Lectures on Wavelets*, Society for Industrial and Applied Mathematics, Philadelphia, 1992.

[30] W. B. Davenport and W. L. Root, *An Introduction to the Theory of Random Signals and Noise*, McGraw-Hill, New York, 1st edition, 1958.

[31] G. Deng, J. K. Cavers and P. Ho, "A reduced dimensionality propagation model for frequency selective Rayleigh fading channels," In *ICC*, pages 1158–1162, 1995.

[32] G. Dickson and A.Lloyd, *Open Systems Interconnection: Computer Communications Standards and GOSIP Explained*, Prentice-Hall, London, 1991.

[33] S. N. Diggavi and A. Paulraj, "Performance of multisensor adaptive MLSE in fading channels," In *IEEE 47th Vehicular Technology Conference*, volume 3, pages 2148–2152, May 1997.

[34] S. N. Diggavi, A. Paulraj and A. Singh, "Signal detection for time-varying vector channels," In *29th Asilomar Conference on Signals, Systems and Computers*, volume 1, pages 152–156, 1996.

[35] S. A. Fechtel, "A novel approach to modeling and efficient simulation of frequency selective fading radio channels," *IEEE Journal on Selected Areas in Communications*, 11:422–431, April 1993.

[36] S. A. Fechtel and H. Meyr, "A new method of evaluating the matched filter bound for uncoded and trellis-coded transmission over frequency-selective fading diversity channels," In *GLOBECOM*, volume 2, pages 905–909, 1992.

[37] C. Flammer, *Spheroidal Wave Functions*, Stanford University Press, California, 1957.

[38] G. D. Forney, "Maximum likelihood sequence estimation of digital sequences in the presence of intersymbol interference," *IEEE Transactions on Information Theory*, 18:363–378, May 1972.

[39] G. D. Forney, "The Viterbi algorithm," *Proceedings of the IEEE*, 61:268–278, March 1973.

[40] G. J. Foschini, "Layered space-time architecture for wireless communication in a fading environment when using multi-element antennas," *Bell Labs Technical Journal*, Autumn:41–59, 1996.

[41] R. G. Gallager, *Information Theory and Reliable Communication*, John Wiley and Sons, New York, 1968.

[42] W. A. Gardner, "Exploitation of spectral redundancy in cyclostationary signals," *IEEE Signal Processing Magazine*, 8:14–36, April 1991.

[43] B. D. Hart, *MLSE Diversity Receiver Structures*, PhD thesis, University of Canterbury, New Zealand, October 1996.

[44] B. D. Hart and D. P. Taylor, "Extended MLSE diversity receiver for the time- and frequency- selective channel," *IEEE Transactions on Communications*, 45:322–333, March 1997.

[45] S. Haykin, *Digital Communications*, John Wiley and Sons, New York, 1st edition, 1988.

[46] S. Haykin, *Communications Systems*, John Wiley and Sons, New York, 3rd edition, 1994.

[47] M. G. Hebley, W. K. Kennedy and D. P. Taylor, "The performance of a space diversity receiver with finite-length fractionally-spaced equalisers with frequency selective rayleigh fading and co-channel interference," In *GLOBECOM*, pages 90–94, 1994.

[48] F. B. Hildebrand, *Advanced Calculus for Applications*, Prentice-Hall, New Jersey, 2nd edition, 1976.

[49] W. Hirt and J. L. Massey, "Capacity of the discrete-time Gaussian channel with intersymbol interference," *IEEE Transactions on Information Theory*, 34:380–387, May 1988.

[50] R. Y. Hogg and E. A. Tanis, *Probability and Statistical Inference*, Macmillan Publishing, New York, 1977.

[51] W. C. Jakes, *Microwave Mobile Communications*, IEEE Press (re-issue), 1994.

[52] T. I. Laasko, L. P. Sabel, A. Yardim and G. D. Cain, "Optimal receive filters for the suppression of ISI and adjacent channel interference," *Electronics Letters*, 32(15):1346–1347, July 1996.

[53] H. J. Landau and H. O. Pollak, "Prolate spheroidal wave functions, Fourier analysis and uncertainty - II," *Bell Systems Technical Journal*, 40:65–84, January 1961.

[54] H. J. Landau and H. O. Pollak, "Prolate spheroidal wave functions, Fourier analysis and uncertainty - III: The dimension of the space of essentially time- and band-limited signals," *Bell Systems Technical Journal*, pages 1295–1336, July 1962.

[55] W. C. Y. Lee, *Mobile Communications Engineering*, McGraw-Hill, New York, 1982.

[56] W. S. Leon, U. Mengali and D. P. Taylor, "Equalization of linearly frequency selective fading channels," *IEEE Transactions on Communications*, 45:1501–1503, December 1997.

[57] W. S. Leon and D. P. Taylor, "An adaptive receiver for the time- and frequency-selective fading channel," *IEEE Transactions on Communications*, 45:1548–1555, December 1997.

[58] W. S. Leon and D. P. Taylor, "MLSE receiver for the dispersive Rayleigh fading channel," In *ICC*, pages 1513–1517, 1997.

[59] W. S. Leon and D. P. Taylor, "DPSK receiver with implicit diversity gain for the linear frequency-selective Rayleigh fading channel," *Conf. Rec. WCNC'99, New Orleans, LA*, pages 510–514, September 1999.

[60] J-P. Linnartz, *Narrowband Land-Mobile Radio Networks*, Artech-House, London, 1993.

[61] J. N. Livingston and C.-C. Tung, "Bandwidth efficient PAM signalling using wavelets," *IEEE Transactions on Communications*, 44:1629–1631, December 1996.

[62] J. H. Lodge and M. L. Moher, "Maximum likelihood sequence estimation of cpm signals transmitted over Rayleigh flat-fading channels," *IEEE Transactions on Communications*, 38:787–794, June 1990.

[63] R. W. Lucky, J. Salz and E. J. Weldon, *Principles of Data Communications*, McGraw Hill, New York, 1968.

[64] H. Lui, G. Xu, L. Tong and T. Kailath, "Recent developments in blind channel equalization: From cyclostationarity to subspaces," *Elsevier Signal Processing*, 50:83–99, 1996.

[65] J. E. Mazo, "Exact matched filter bound for two-beam Rayleigh fading," *IEEE Transactions on Communications*, 39:1027–1030, July 1991.

[66] P. J. McLane, "A residual intersymbol interference error bound for truncated-state Viterbi detectors," *IEEE Transactions on Information Theory*, IT-26:548–553, September 1980.

[67] M. Médard and A. J. Goldsmith, "Capacity of time-varying channels with channel side information at the sender and receiver," In *ICC Miniconference on Theory*, pages 16–20, 1999.

[68] U. Mengali, *Lecture Notes on Synchronization*, Dipartimento di Ingegneria dell'Informazione, Pisa, September 1993.

[69] U. Mengali, "Notes on power series models for time and frequency selective channels," *University of Canterbury*, July 1994.

[70] K. Metzger, "On the probability density of intersymbol interference," *IEEE Transactions on Communications*, COM-35:396–402, April 1987.

[71] P. Monsen, "Feedback equalization for fading dispersive channels," *IEEE Transactions on Information Theory*, January 1971.

[72] B. Noble and J. W. Daniel, *Applied Linear Algebra*, Prentice Hall, New Jersey, 3rd edition, 1988.

[73] H. Nyquist, "Certain topics in telegraph transmission theory," *Transactions of the AIEE*, 47:617–644, February 1928.

[74] B. R. Petersen and D. D. Falconer, "Exploiting cyclostationary subscriber-loop interference by equalization," In *GLOBECOM*, volume 2, pages 1156–1160, December 1990.

[75] W. H. Press, S. A. Teukolsky, W. T. Vetterling and B. P. Flannery, *Numerical Recipes in C*, Cambridge University Press, Cambridge, 2nd edition, 1992.

[76] J. G. Proakis, *Digital Communications*, McGraw-Hill, New York, 2nd edition, 1989.

[77] S. Qureshi, "Adaptive equalization," *Proceedings of the IEEE*, 73:1349–1387, September 1985.

[78] R. Raheli, A. Polydorus and C.-K. Tzou, "Per-survivor processing: A general approach to MLSE in uncertain environments," *IEEE Transactions on Communications*, 43:354–364, February 1995.

[79] M. E. Rollins and S. J. Simmons, "Simplified per-survivor Kalman processing in fast frequency-selective fading channels," *IEEE Transactions on Communications*, 45:544–553, May 1997.

[80] M. Schwartz, *Telecommunication Networks: Protocols, Modeling and Analysis*, Addison-Wesley, Reading, MA, 1987.

[81] M. K. Simon and D. Divsalar, "Some new twists to problems involving the Gaussian probability integral," *IEEE Transactions on Communications*, 46:200–210, February 1998.

[82] D. Slepian and H. O. Pollak, "Prolate spheroidal wave functions, Fourier analysis and uncertainty - I," *Bell Systems Technical Journal*, 40:43–63, January 1961.

[83] G. Ungerboeck, "Adaptive maximum likelihood receiver for carrier modulated data transmission systems," *IEEE Transactions on Communications*, 22:624–636, May 1974.

[84] R. van Nobelen, *Coding for the Rayleigh Fading Channel*, PhD thesis, University of Canterbury, New Zealand, January 1996.

[85] D. Verdin and T. C. Tozer, "Generating a fading process for the simulation of land-mobile radio communications," *Electronics Letters*, 29(23):2011–2012, November 1993.

[86] M. Visintin, "Karhunen-Loève expansion of a fast Rayleigh fading process," *Electronics Letters*, 32(18):1712–1713, August 1996.

[87] G. M. Vitetta, D. P. Taylor and U. Mengali, "Double filtering receivers for PSK signals transmitted over Rayleigh frequency flat fading channels," *IEEE Transactions on Communications*, 44:686–695, June 1996.

[88] S. B. Weinstein and P. M. Ebert, "Data transmission by frequency-division multiplexing using the discrete Fourier transform," *IEEE Transactions on Communication Technology*, COM-19:628–634, October 1971.

[89] M. V. Wickerhauser, *Adapted Wavelet Analysis from Theory to Software*, A.K. Peters, Wellesley, Mass., 1994.

[90] G. W. Wornell, "Emerging applications of multirate signal processing and wavelets in communications," *Proceedings of the IEEE*, 84:586–603, April 1996.

[91] J. M. Wozencraft and I. M. Jacobs, *Principles of Communication Engineering*, Wiley, New York, 1965.

[92] D. Wulich, "Reduction of peak to mean ratio of multicarrier modulation using cyclic coding," *Electronics Letters*, 32(5):432–433, February 1996.